COLOR DIFFERENCES ON THE LUNAR SURFACE

Thesis by
Thomas Bard McCord

Submitted January 12,1968

In Partial Fulfillment of the Requirements
For the Degree of
Doctor of Philosophy

California Institute of Technology
Pasadena, California
1968

(Submitted January 12, 1968)

ACKNOWLEDGMENTS

I wish to thank Dr. Bruce C. Murray for suggesting the lunar relative color problem and for many helpful and stimulating discussions. His patience and encouragements contributed significantly to the success of this study. Mr. James Westphal, a willing and stimulating partner in countless conversations and debugging sessions offered many helpful suggestions during the instrument design part of this program; without his help the author would have been deprived of a singular education in some of the subtleties of astronomical instrumentation. Mr. Sol Giles arrived on the scene at a particularly dark period during the instrument construction portion of the project and devoted his entire talents and energies (which are considerable) to constructing a dependable instrument.

Dr. John Adams of the Jet Propulsion Laboratory is to be thanked for several helpful conversations and for unselfishly allowing me to use his laboratory results before their publication. Mr. Robert Younkin, also of JPL, made possible the final interpretation of my measurements by allowing me to use his absolute lunar spectral measurements before publication. Mr. George Levchuk of Caltech contributed to the literature search reported in this dissertation by translating much of the Russian literature. Mr. John Dolan of Spectro Laboratory, Sylmar, California, provided, free of charge, the second set of interference filters used in the observational part of this study.

Special acknowledgment is due my wife, Carol, who was able to continue her own career while laboring for me as typist, draftsman, telescope night assistant and in other secretarial capacities far beyond the call of duty.

The author was supported by a National Aeronautic and Space Administration Traineeship for the duration of this investigation. Much of the research cost was supported by NASA Grant NSA 56-60.

ABSTRACT

Both a detailed literature survey and a new observational study were performed to determine and extend the knowledge of spectral reflectivity differences (color differences) on the lunar surface in the extended visible wavelength region. A survey of the extensive and disorganized literature revealed few positively known facts and indicated the need for an accurate, multi-passband observational study of a number of lunar areas of differing morphology. A 21-filter (0.4μ- 0.8μ), double beam photoelectric photometer was designed and constructed to observe differentially 83 lunar areas, some many times, to an accuracy of 0.1% to 0.3%. Some results were the discovery of: (1) many color variations up to 10% with some to about 60%, (2) a dependence of relative color on phase angle but no temporally varying luminescence, (3) broadband absorption features on spectral reflectivity curves and possibly some less broad, low amplitude (0.2% - 0.5%) humps, (4) a dependence of spectral curve shape on lunar morphology and, (5) no universal dependence of color on brightness, although some mare areas show this tendency. These results indicate that color differences are caused mainly by compositional differences and that the shapes of the spectral reflectivity curves give some indications of

the rock and mineral composition of the lunar surface.

TABLE OF CONTENTS

APPENDICES

INTRODUCTION

Need and Purpose

A principal means of studying the surface of the Moon and planets has been to observe and measure the solar radiation reflected by these surfaces. This will remain an important method, even in this age of space probes, for such observation can be best made using more convenient and relatively inexpensive ground-based, remote sensing techniques. Direct measurements and samples obtained using space vehicles will be important for calibrating Earth-based measurements. The wavelength region of interest ranges from about 0.3μ to 2.6μ and is restricted at either extreme by the opacity of the Earth's atmosphere and the energy distribution of solar radiation. In addition, thermal radiation emitted by the planetary body may become important at the long wavelength extremes of this spectral region. The wavelength interval is observed in two parts, the ultra violet and extended visible region of 0.3μ to 0.8μ and the near infrared region of 0.8μ to 2.6μ. This dichotomy has arisen primarily because two basically different types of radiation detectors are required. The reflected light observed is analysed relative to direct solar radiation for its intensity at one wavelength interval (albedo), the variation of intensity with wavelength (color) and plane polarization. The study discussed in this dissertation is concerned with wavelength dependence of light (color) reflected from different places on the lunar surface in the extended visible spectral region.

The variation of reflectivity with wavelength is an important property because changes of this property across a surface often indicate compositional changes or at least age and textural differences in the properties of the reflecting material. To detect and map these changes would be extremely important for any geologic mapping program, and of course a geological map of the lunar surface is an essential tool in unraveling the history of the surface of the Moon.

Aside from the importance of spectral reflectivity variations as a geologic mapping tool, they may give direct information on the composition and age of the lunar surface. All minerals have characteristic reflectivity spectra, and, although there are many complications, it may be possible in some cases to determine directly the general composition of certain lunar areas from ground based color measurements. In addition, the simple variations of color with morphology should tell something of the age and general structure without the necessity of producing a complete map and/or identifying composition.

A complete review of the existing data, of which there is a large and disorganized body is presented first. Conclusions drawn by this author give some idea of the state of knowledge in this subject. The results of an extensive observational study to obtain measurements to a few tenths of one per cent of the relative reflectivity of many areas of the lunar surface in the spectral region 0.4μ to 0.8μ is the principal focus of this work. These data are presented in Chapter III along with the conclusions drawn from them. A comparison of the new measurements with earlier data is made.

Finally, the useful color data available (mostly new) are interpreted in terms of lunar structure, age and especially composition.

Definitions

The color of a reflecting object is determined by its reflectivity as a function of wavelength and the spectral energy distribution of the source light. In this study the primary interest was mainly in the spectral reflectivity differences (color differences) across the lunar surface rather than the absolute color of any one part of the surface. The most convenient way to express differential color is by using a twicenormalized quantity which will be called differential or relative reflectivity. This quantity is derived in the following way.

Consider two regions of the lunar surface with reflectivity $r_a(\lambda)$ and $r_b(\lambda)$ as shown at the top of Figure 1. Since the absolute reflectivity is not of interest in this study it can be eliminated by dividing each reflectivity function by its value at some wavelength, say 0.56μ. In effect a reflectivity of 1 is assigned to all lunar regions at some standard wavelength. Two new quantities are defined

$$R_a(\lambda) = \frac{r_a(\lambda)}{r_a(.56)} \qquad R_b(\lambda) = \frac{r_b(\lambda)}{r_b(.56)}$$

This procedure is especially helpful for lunar measurements because large differential changes in albedo occur with lunar phase.

If only the reflectivity differences from place to place are of interest, another normalization can be made, this time to a standard area on the lunar surface, say area <u>b</u>, to which all other areas can be

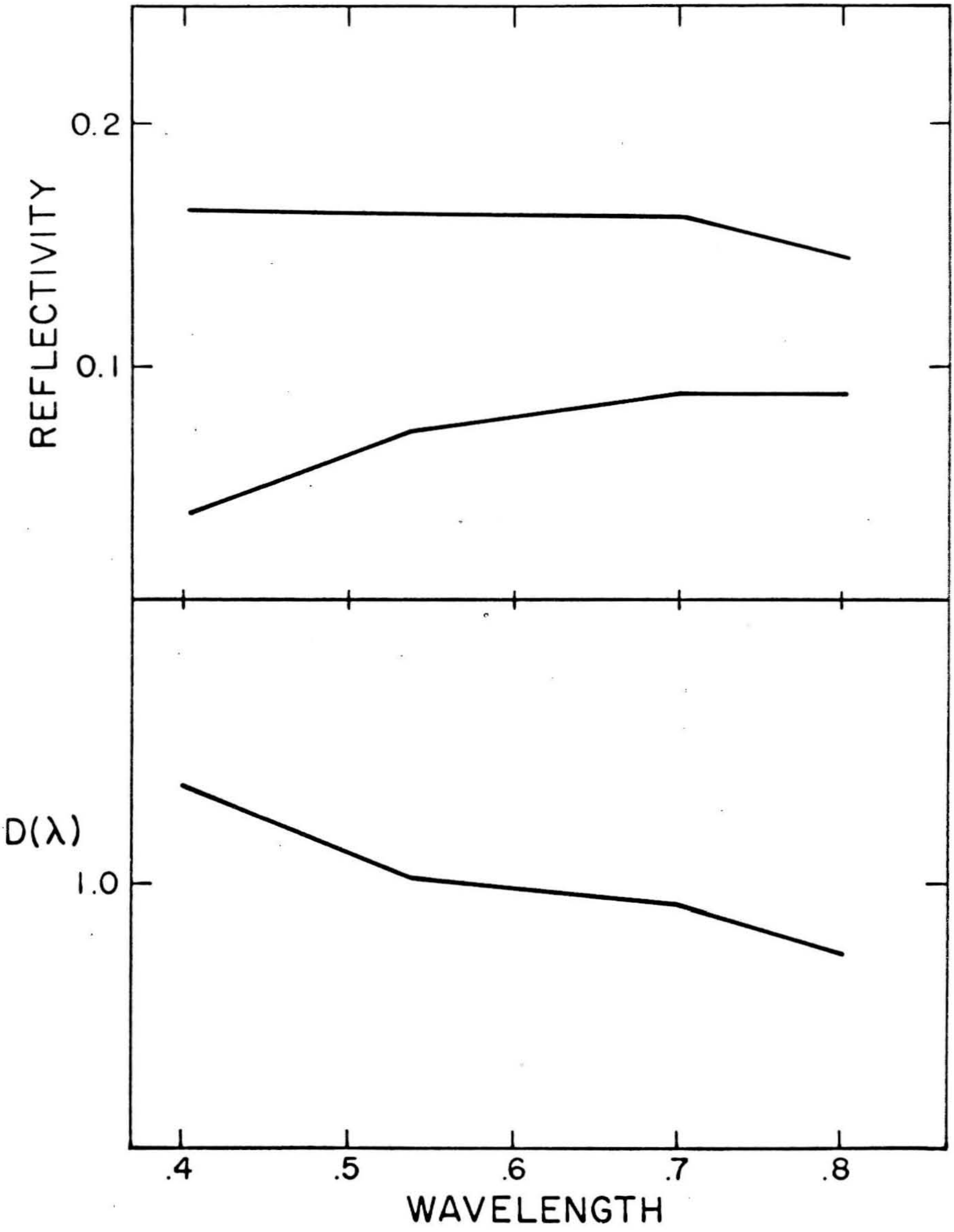

Figure 1

referred. This defines a relative reflectivity D

$$D(\lambda) = \frac{R_a(\lambda)}{R_b(\lambda)} = \frac{\dfrac{r_a(\lambda)}{r_a(.56)}}{\dfrac{r_b(\lambda)}{r_b(.56)}} = \frac{\dfrac{r_a(\lambda)}{r_b(\lambda)}}{\dfrac{r_a(.56)}{r_b(.56)}}$$

The second normalization is valuable because relative reflectivity can be more easily and accurately measured than absolute reflectivity. To obtain the absolute reflectivity for all regions for which only relative reflectivities have been measured, it is necessary to determine the absolute reflectivity for only the standard area.

For the particular example shown at the top of Figure 1, $D(\lambda)$ would appear as at the bottom of the same figure.

The result could be described by stating that region a is generally bluer than region b, i.e. region a reflects more short wavelength radiation and less long wavelength radiation relative to that which it reflects at 0.56 μ. This parameter best describes reflectivity differences on the lunar surface.

The quantities $R(\lambda)$ and $D(\lambda)$ are often modified for reasons of history and convenience. To maintain a constant proportionality scale, the logarithm of R (λ) and D (λ) is often plotted. Thus, a 1% variation corresponds to a constant increment of the new unit no matter what the absolute value.

Historically, units of stellar magnitude have been used. In this case R_a (λ) becomes a "color index" (CI).

$$CI (\lambda) = -2.5 \log \frac{R_a (\lambda)}{R_a (\lambda_0)}$$

Frequently the term color index refers to specific wavelengths, usually approximately .43 μ and .55 μ . In this case it is called a standard color index. Also in the stellar magnitude units, D (λ) becomes a "color excess" (CE).

$$CE (\lambda) = -2.5 \log \frac{R_a (\lambda)}{R_b (\lambda)}$$

Again, a special meaning may be implied; the wavelengths are those of the color index while the standard region is the sun itself.

The stellar magnitude system has a practical advantage in that for small reflectivity differences ($<$ 10% to 20%) the quantity CE can be read directly as a percentage difference in reflectivity. Thus a color excess of 0.025 magnitude would mean a difference in normalized reflectivity of about 2.5%.

A quantity sometimes used in the earlier literature is color temperature. A black body with a certain temperature radiates with a well defined spectral energy distribution. The energy distribution curve can be determined by specifying the slope of the curve in a specific wavelength interval. If another object, such as a part of the lunar surface, exhibits a spectral energy distribution curve having the same slope in the same wavelength interval, it is said to have a color temperature equal to that of the black body. The color temperature of reflecting bodies has no physical significance.

To present observational color data and to analyse those data, it is convenient to express the relative reflectivity in analytic form. Let the brightness B_i of a lunar region be of the form

$$B_i = A_i (\lambda_o, \alpha) \, p_i (\lambda, \alpha_o) \, q_i (\lambda, \alpha)$$

where $A_i (\lambda_o, \alpha)$ is the brightness of lunar region <u>i</u> at a specific wavelength λ_o and phase angle α, $p_i (\lambda, \alpha_o)$ is the wavelength dependence of the brightness as measured at $\alpha = 0$, and $q_i (\lambda, \alpha)$ is the phase dependence of the brightness for wavelengths other than λ_o. Also $p_i(\lambda_o, \alpha_o) = q_i(\lambda_o, \alpha) = 1$.

Using this form for B_i, the relative brightness of two lunar regions becomes

$$RB_i = \frac{B_i}{B_o} = \frac{A_i(\lambda_o \alpha)}{A_o(\lambda_o, \alpha)} \frac{P_i(\lambda, \alpha_o)}{P_o(\lambda, \alpha_o)} \frac{q_i(\lambda, \alpha)}{q_o(\lambda, \alpha)}$$

To express the relative reflectivity a second normalization, this time to a specific wavelength, is performed. The result

$$D(\lambda, \alpha) = \frac{\cancel{\frac{A_i(\lambda_o, \alpha)}{A_o(\lambda_o, \alpha)}} \frac{P_i(\lambda, \alpha_o)}{P_o(\lambda, \alpha_o)} \frac{q_i(\lambda, \alpha)}{q_o(\lambda, \alpha)}}{\cancel{\frac{A_i(\lambda_o, \alpha)}{A_o(\lambda_o, \alpha)}} \cancelto{=1}{\frac{P_i(\lambda_o, \alpha_o)}{P_i(\lambda_o, \alpha_o)}} \cancelto{=1}{\frac{q_i(\lambda_o, \alpha_o)}{q_o(\lambda_o, \alpha)}}}$$

$$D(\lambda, \alpha) = \frac{P_i(\lambda, \alpha_o)}{P_o(\lambda, \alpha_o)} \frac{q_i(\lambda, \alpha)}{q_o(\lambda, \alpha)}$$

expresses the relative reflectivity between two lunar regions and is the quantity of primary concern throughout this study.

II. LITERATURE REVIEW

Introduction

Investigations of spectral reflectivity differences across the lunar surface have been carried out by a large number of researchers throughout this century using at least seven different methods. Because of the lack of any previously published effort to relate systematically these works and because of the possible value of such a large body of data, a detailed discussion of the literature is presented in Appendix I. Works are mentioned according to the method of measurement because the method has direct bearing on the form, reliability and value of the data. Also given is a discussion of each of the observational methods which are: both qualitative and quantitative visual observations, photographic imagery, photographic spectrophotometry and spectrometry and photoelectric spectrophotometry and spectrometry.

In this chapter the properties of lunar color differences that were revealed or suggested by the existing data are listed and discussed. Conclusions were drawn by the present author after studying the data.

Properties of Lunar Relative Color Suggested by Existing Data

From the large body of data described in Appendix I, it should be possible to draw some tentative conclusions concerning lunar color differences. In addition, the need and nature of any additional observational studies should be evident. In this section the data are discussed with this in mind.

The existence of color differences

The most basic question that can be asked is, are there measurable color contrasts on the lunar surface or is the surface spectrally homogeneous? For a qualitative answer the imagery data are the most helpful. In all of the photographic imagery studies reported, color features were found. These features were the same when similar regions of the lunar surface were observed. The relative redness of Mare Serenitatis compared to the color of Mare Tranquillitatis, the blue area in Mare Imbrium to the south and astronautical east of Sinus Iridum, and the decreased reflectivity in the blue of the area west of Aristarchus, known as Wood's Spot, are among the most prominent color features that appear in all imagery data regardless of the technique used.

More quantitative evidence of color differences is plentiful. For the color contrast between Mare Serenitatis and Mare Tranquillitatis, for example, photoelectric work yielded values such as 5.4% (Van den Bergh, 1962), 5.8% (Gehrels, et.al., 1964), 4.6% (Coyne, 1965) for the wavelength regions 4500 to 5600 Å. Also, photographic spectroscopy data obtained by Barabashov, et. al., (1959) and Teifel (1960b) indicated a 6% color difference. Using visual comparison methods, Radlova (1941) found a 5% color contrast in this same spectral region. Keenan (1931) found a difference of 10% for a larger spectral interval (3300 to 7400 Å) using photographic photometry. In addition, Keenan (1931) found Wood's Spot to be 20% brighter at 7400 Å than at 3300 Å when compared to surrounding regions. Additional evidence confirming these and other color contrasts is abundant. There are contradictions in the literature concerning some features, but major color features, such as those mentioned above, seem well established by work using many different observational techniques.

Magnitude and range of lunar color contrasts

The magnitude of lunar color contrasts seems to depend on the size of the spectral interval considered. The spectral region in which many measurements have been made was approximately 0.44 μ to 0.55 μ . The maximum color contrasts in this region seemed to be about 8% to 10% as reported in more recent, and probably more accurate, two-color photoelectric studies (Van den Bergh, 1962; Wildey and Pohn, 1964; Gehrels, et. al., 1964; Coyne, 1965). However, earlier workers reported differences up to 20% to 25% (Barabashov, et. al., 1959; Teifel, 1961; Kozlova and Glagolevskii, 1961; Radlova, 1941). A few authors reported very small color contrasts or none at all (Murray and Liu, 1961; Sharanov, 1955). The different results may depend in part on which lunar regions were studied. The magnitude of the spectral contrasts reported seemed to increase somewhat as the spectral range increased. For the region 4000 Å to 6300 Å contrasts with a maximum of 10% to 25% were reported (Barabashov, 1924; Polozhentzeve, 1958; Teifel, 1960a). Color differences seemed to increase less rapidly as the spectral range was increased further. For example, Barabashov and Chekirda (1954) reported 15% to 20% differences from 3650 Å to 8400 Å while Evsiukov (1966) found 25% for 3700 Å to 10,000 Å. Keenan (1931) described color differences that were commonly 10% to 15% with some up to 20% for the spectral region 3300 Å to 7400 Å.

From the existing data, it appears that the range of color differences present on the lunar surface depends both on the spectral range used and the areas of the lunar surface observed. For the 4300 Å to 5500 Å region, maximum differences seem to be about 10% with a continuous distribution below this maximum, but some higher values were reported. As the spectral range is expanded, the contrasts appear to increase but not in proportion to the increase in the spectral range. As the spectral range is expanded to 8000 Å and beyond, the little evidence available suggests a less rapid further increase in the magnitude of the color differences.

The shape of the relative reflectivity curve

Determination of the shape of the relative reflectivity curve requires measurements made at several wavelengths over an extended spectral range. This requirement restricts the useful data to those obtained by the methods of spectroscopy and multi-filter photometry.

Wilsing and Scheiner (1921) were the first to obtain this type of information. A plot of their data, as reworked by Sharanov (1956), revealed relative absorption features of about 10% near 5000 Å and 5500 Å.

Keenan's (1931) measurements between 3300 Å and 7400 Å showed some reflectivity curves with absorption features near 4000 Å with an amplitude of 10% to 20%.

A plot of the measurements by Barabashov and Chekirda (1954) (not given in the original paper) showed general monotonic spectral curves with some features of about 800 Å width centered near 4300 Å, as well as some other irregularities with amplitudes of up to 10% and greater. These authors (1955) also studied the rays of some craters and found non-monotonic spectral curves.

A comparison was made by the present author of data obtained by Keenan and by Barabashov and Chekirda at common lunar regions. The spectral features presented by Keenan did not correlate with those found by the other authors.

The spectral curves obtained by Yezerskii and Fedorets (1956) again showed some spectral features that are similar but not identical at several lunar regions. These features appeared near 4900 Å, 5200 Å and 5900 Å and had an amplitude of about 15%.

Spectral curves by Sergeeve (1959) showed obvious spectral features of nearly 20%.

Coyne (1962, 1963) found humps of about 15% in the spectral curves for some lunar regions. These humps seemed to be temporally varying and he attributed them to luminescence on the lunar surface.

Petrova (1966) obtained spectral curves with humps of about 6% to 8% that he also attributed to lunar luminescence.

However, several authors have reported no irregularities above experimental error in reflectivity curves they measured. These included Teifel (1960a), Barabashov, Yezerskii, and Fedorets (1959), Vigroux (1956), Polozhentzeve (1958) and Murray and Lui (1961). Some lunar regions measured by these authors were also observed by other workers who reported spectral irregularities.

In summary, some authors found the relative spectral reflectivity curves for at least some lunar areas to contain humps, which could be interpreted as absorption or emission features. The amplitude of these features was as much as 20% of the "continuum" and their reported spectral positions varied. Other authors found no spectral features but recorded only smoothly varying reflectivity differences. The possibility of a time dependent phenomenon has been suggested. It appears that the question of the shape of the differential reflectivity curves has not been answered.

Time dependence of spectral contrasts

Discovery and description of the time dependence of lunar color contrasts is of obvious importance to data gathering studies and especially to mapping programs. To use the data described in Appendix I, one might compile all existing data for similar lunar regions and look for time variations greater than experimental error.

This is impractical because the data have been gathered in a disorganized way and few lunar areas have been measured by more than a few observers. Furthermore, past observers tended to make observations only in a limited range of phase angles. A wide variety of observational methods were used, making unreliable a comparison to the level of accuracy required to remove doubt of the existence of temporal variations. Therefore, the useful data are limited to those studies directed toward the detection of temporal variations.

There exists the possibility of at least two kinds of time dependent effects, an actual phase effect in reflectivity and effects such as luminescent emission. Qualitative studies have suggested that a phase effect exists. Miethe and Seegert (1911) mentioned that colors were more pronounced at full moon, especially when comparing Mare Tranquillitatis with Mare Serenitatis. They also reported that color differences were almost invisible at lunar sunrise. Wright (1929) mentioned one color feature that appeared more prominent at quarter phase than at full moon. This seemed to conflict with the earlier report. Scott (1964; personal communication, 1967) reported that regional color differences "on some nights are far more difficult to record than on others" and that the terminator area is often "brown" which this author interprets as meaning a lack of color contrasts.

Quantitative investigations have provided no evidence for a differential phase effect. Polozhentzeva (1958) detected no phase dependent change in differential color above about 2%. Teifel (1961) also noticed no dependence of color on lunar phase angle. Wildey and Pohn (1964) measured the standard color index of a number of lunar features as a function of phase and although they did not analyze the data for a color-phase dependence, the present author did. Figure 2 shows a general reddening of all lunar areas measured as phase angle increases, as has been reported by Gehrels, et. al., (1964), but no differential effect was evident above the considerable scatter of the data. Note that Wildey and Pohn's measurements (data points in Figure 2) do not follow the reddening law given by Gehrels, et. al. (line in Figure 2). Wildey and Pohn observed mostly craters and Gehrels et. al. did not. This discrepency in the magnitude of the general rate of reddening with phase could be considered weak evidence for a differential phase effect.

Coyne (1965) was the first to specifically seek a differential color-phase effect. He measured thirty-six lunar areas at phase angles from -19°to 75° using the two color B-V system and found no phase

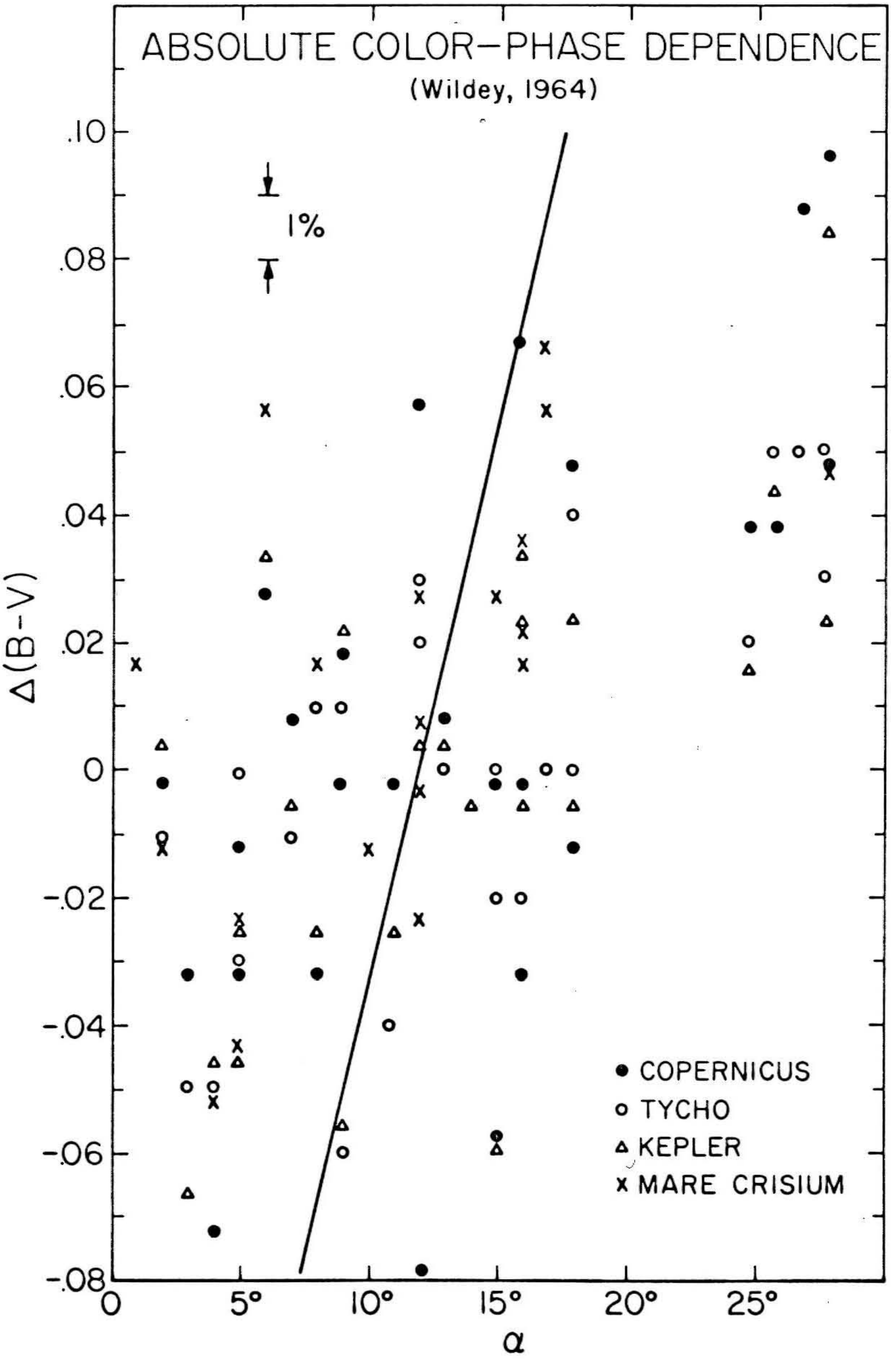
ABSOLUTE COLOR-PHASE DEPENDENCE
(Wildey, 1964)
1%
Δ(B-V)
.10
.08
.06
.04
.02
0
-.02
-.04
-.06
-.08
0
5°
10°
15°
20°
25°
α
● COPERNICUS
○ TYCHO
△ KEPLER
x MARE CRISIUM

Figure 2

dependence greater than about 0.5%.

Quantitative evidence from these last three studies would seem to rule out the presence of a differential color-phase dependence greater than about 1%to 2% in the spectral range considered.

Existence of nonperiodic or randomly occurring changes in differential color, such as those that would be caused by luminescent emission, is difficult to detect or recognize. Many measurements and a confident knowledge of all instrumental effects on the consistency of the measurements are required. Even so there have been reports of temporal broad band emission features appearing on the reflectivity curves for some lunar areas. This phenomenon is commonly called lunar luminescence and a body of literature (e.g. Ney et. al. 1966; McCord, 1967) on this subject has developed.

Coyne (1962, 1963) obtained relative spectral curves that contained humps which he interpreted as being due to luminescence. The luminescence bands were reported to be on the average about 500 Å wide with an amplitude from approximately 3% to 18% above the otherwise smooth comparative spectral reflectivity curve. He noted three distinct groups of bands centered at approximately 5050 Å, 5200 Å, and 6100 Å. These results were compared to Dubois' work (1959) on luminescence using the line depth method (measuring the filling-in of reflected Frauenhofer lines by background radiation) and general agreement was found. Coyne concluded that the existence of a broad band emission on the lunar surface was well established and that those studying lunar color must recognize this complication.

Gehrels, et. al., (1964) also mentioned the detection of luminescence using both filter photometry and polarimetry.

Petrova (1966) noted humps on relative spectral curves in two spectral regions (5305 Å and 6680 Å) with a width of about 300 Å in the green and 100 Å in the red. The amplitude of the humps was approximately 10% of the continuum. He interpreted the humps as being caused by emission excited by solar irradiation of the lunar surface,

Existence of lunar luminescence would explain the irregularities in the spectral curves obtained by several workers and described in the following part of this chapter. However, some workers have presented smooth spectral curves which showed no trace of luminescence.

The conclusions suggested by the existing data concerning the time dependence of lunar color are first, the systematic change of differential color with lunar phase does not exceed 2% and is probably much less. Secondly, there is some evidence for a broad-band emission phenomenon on the lunar surface that is time dependent but some contradictory data exist, keeping the question open for futher study.

Size and shape of color regions and their boundary sharpness

After discussing the properties of the color differences, it is appropriate to consider the relation of color contrasts to the lunar surface.

The imagery method yielded the most useful data to answer this question, for it provided two- dimensional spatial coverage and presented the data in a form allowing easy interpretation. It was shown in the first part of this chapter that the imagery data were in general agreement with quantitative measurements; thus they can be used with some confidence.

At a glance it can be seen that much color detail exists on the lunar surface. There are general regional features such as the color difference between the northeast and southwest parts of Mare Imbrium. However, within some of these regions there are many color details, especially in Mare Tranquillitatis. The shapes of these color regions are irregular and the color boundaries appear very sharp, less than a kilometer in width.

The conclusion is that although there are large-scale regional differences the color contrast detail is extremely complicated and has sharp boundaries.

Dependence of color on morphology

For the purpose of this study it is useful to catagorize lunar morphology into three groups; (1) mountains and upland or continental regions, (2) maria, and (3) bright craters. These groups are defined by albedo and surface texture. To show how they differ in color might help to determine their geologic distinctness and their relation to the basic structure of the lunar surface.

The imagery data are not very useful for determining the dependence of color on morphology because of the large albedo differences between morphologic features. The photographic process is linear over only a small range of densities and, considering the relatively small spectral reflectivity differences to be detected between areas of large albedo differences, the imagery method does not always give reliable results.

The quantitative photographic methods are also subject to systematic errors due to the large albedo variations, as has been discussed by Teifel (1960b). However, with the proper precaution most authors believe the effects can be minimized.

By the method of visual comparison, Radlova (1941) found continents to be redder on the average than maria, with the maria showing larger color variations. Sharanov (1962) agreed with these results and found that bright craters were redder than the continents, but that the range of color variations was about the same for bright craters as for continents.

Using photographic spectrophotometry, Radlova (1943) found that the ranges of color indexes for the three morphologic groups overlapped. However, on the average, she found maria regions to be bluer than uplands and bright craters, while upland regions were reddest. Barabashov and Chekirda (1954) presented averaged spectral data for the three morphologic groups which showed that no simple color groupings existed.

Photographic spectroscopy was applied to the problem by Teifel (1960a). He measured relative spectral curves to show that the curve gradients for mare regions were the lowest of the three groups, while the gradients for bright craters were the highest. (A high gradient indicates relative redness.) By examining the gradients of the spectral curves in two spectral intervals 3900-5000 Å (G_1) and 5100-6200 Å (G_2), he found continents differed from maria by having a considerably higher value of G_2, but the values for G_1 were similar. Bright craters showed the widest range of overall gradients while maria showed the smallest variations.

Polozhentzeva (1958) and Sergeeva (1959) reported that bright craters and mountains were redder than maria, with some exceptions. Coyne (1962, 1963) found that color contrasts are much greater when comparing uplands to maria than within the maria.

To summarize, the three morphologic groups do not seem to form three distinct color groups, although on the average bright craters are reported to be redder than continental regions, which are in turn redder than the maria. There is some uncertainty as to which group exhibits the largest variations in color, although the general body of data indicates that the maria are the least homogeneous of the three groups.

Dependence of color on albedo

A simple relation between the color of the lunar region and its albedo at, say, $.55\mu$ has been reported by almost all the investigators who have investigated this question. Wilsing and Scheiner (1921) and Rosenberg (1921) were early workers reporting a general reddening with an increase in albedo. Radlova (1941, 1943) found that, although the darker lunar regions exhibited a wide range of colors, the brighter regions were characterized exclusively by "reddish tints". The crater Aristarchus was found to be an exception to this rule. Barabashov, et. al. (1959) and Sharonov (1962) confirmed Radlova's findings.

Coyne (1962, 1963) and Evsiukov (1966) also noticed a basically redder color in brighter areas, but Wildey and Pohn (1964) reported only a very slight tendency for reddening with brightness. This latter work included mostly bright craters and this selection may be significant.

Teifel has studied the reddening effect in some detail He reported a dependence between color and brightness and noted that continents or upland regions have the least clearly marked relation, a result also pointed out by Adams (1967) and shown in his Figure 1.

In the most comprehensive study (1960b) of the reddening effect, Teifel found a linear relation between color and brightness for each lunar region studied, but this linear relation, characterized by a gradient $\Gamma = {}^{\Delta CE}/_{\Delta \log. (I_{0.55})}$, was different for different lunar regions. No clear cut connection between morphology or average color and the value of the gradient Γ was noted.

Teifel reported that, although there was a considerable range of colors for fairly dark regions, very dark regions showed only a blue color. In a later study Teifel (1960c) confirmed his previous results.

Van den Bergh (1962) investigated photoelectrically the color-brightness relation in a small dark region north of Schroter. He scanned across the region measuring both color and relative brightness. The results showed a clear dependence of color on brightness with darker areas being bluer.

This large body of data strongly supports the existence of a reddening law. It appears that the reddening tendency is stronger in some areas of the maria than in others, and darker areas have a wider range of color than lighter areas. The reddening law seems to hold more strongly in the maria than in the uplands or for bright craters.

Conclusions

A large body of data exists concerning differential spectral reflectivity variations on the lunar surface. In this chapter (and in detail in Appendix I) the data were organized and presented and the basic properties of lunar color differences themselves as well as their relation to the lunar surface were discussed. The conclusions reached by this author after studying these data are as follows: (1) there can be little doubt that measurable color differences do exist on the lunar surface. (2) The magnitude of these color features varies with spectral interval and lunar region, but variations to 10% are probably not unusual with 15% to 20% color differences occurring in some places. (3) The shape of the relative reflectivity curves, i.e., the spectral dependence of relative reflectivity, is not accurately determined. Some authors showed strong absorption or emission features while others presented smooth curves that showed only a monotonous change of reflectivity with wavelength. This problem is very important to a geologic and compositional study of the Moon and should be investigated further. (4) The existence of a dependence of relative color on lunar phase seems to be ruled out, at least to the 1% level. (5) The presence of a non-periodic time dependence of lunar color such as that due to luminescence is not well established. Several authors presented data that are said to show this effect, but the chance for systematic error and the lack of continuous quantitative data showing the history of an event cause this author to question these results. More careful and accurate studies directed specifically toward the detection of this effect are needed to establish positively its existence. All future observers should be aware of the possible existence of both a phase effect and a luminescence phenomenon. (6) Color features on the lunar surface are present in intricate detail, usually with very sharp boundaries. The imagery method must be used to fully demonstrate this fact. (7) It is not well established that a clear cut dependence of color on morphology exists. Upland regions appear to be redder on the average than mare regions but some mare regions are as red or redder than the uplands. (8) A reddening law is found by all authors who studied this effect. The slope of the linear dependence of color on brightness appears to vary with the lunar region studied. There is some evidence to suggest that the law does not hold in upland regions or for bright craters. This appears to be a complex phenomenon and more study is needed to completely define the effect. The strong possibility of systematic error affecting photographic results should be kept in mind by future investigators.

III. OBSERVATIONS

Introduction

In the previous chapter of this work a survey of the literature was presented, and the conclusions this author reached after studying the large body of data were listed. It appeared that color differences exist on the lunar surface and that these differences are probably on the order of 10% in at least a few lunar regions. Beyond this not much has been definitely established.

The major problem has been the accuracy of the observations. To define accurately a 10% phenomenon and to use that phenomenon to determine properties of the lunar surface requires at least 1% accuracy. Few studies of lunar differential reflectivity have actually approached that accuracy. Those that have, generally the most recent studies, have been imcomplete in both spectral and areal coverage. The most accurate studies have been two or three color, broad-band investigations that have contributed little to the knowledge of the shape of the spectral reflectivity curves for various areas on the lunar surface.

To provide the required information, an observation program was designed that would meet these primary requirements. (1) Measurement accuracy should be on the order of 1% of the magnitude of the phenomena (i.e. 0.1% of absolute intensity). (2) Spectral coverage should be complete enough to detect and define any spectral features that could reasonably be expected to exist in the extended visible wavelength region. (3) Areal coverage of the study should be great enough to include all types of terrain so that truly representative spectral curves can be presented.

In addition the observations must be continued over a period of time so that any commonly occurring time dependent effects would be detected.

During a period of about one year (1967) a differential narrow band filter photometric observational program was carried out by the author to determine to an accuracy on the order of 0.1%, the reflectivity curve for 83 lunar regions with respect to a standard region in Mare Serenitatis ($\lambda = -21\overset{\circ}{.}4$, $\phi = +18\overset{\circ}{.}7$). The spectral region from 0.4 to 0.8 microns was covered, by using interference filters. The 24-inch telescope located on Mt. Wilson, was used to make the majority of the observations, although the 60-inch reflector, also on Mt. Wilson, was used to obtain some high resolution measurements and as a check for systematic instrumental errors.

To routinely achieve the required measurement accuracy it was necessary to devise new observational techniques and design a new instrument. This instrument and its use have been described in detail in another paper (McCord, 1968; see Appendix II). Thus, only a general discussion is given here.

Instrumentation and Method

The object of this study was to measure the intensity of various lunar areas at many different wavelengths throughout the extended visible spectral region and compare each of these lunar areas to a standard lunar area. The method used in the past to accomplish this type of differential measurement was to observe an unknown object at one wavelength and then move the telescope so that the standard object could be measured. Two problems arose when this method was utilized: (1) a significant amount of time was spent shifting the telescope position and realining the object on the entrance aperture of the photometer. (2) Sky conditions are rarely such that significant changes in transparency do not occur during the time required to reposition the telescope, especially when an accuracy better than 1% is required.

The obvious solution was to measure both objects simultaneously, thus assuring that they were observed under as nearly the same atmospheric conditions as possible. A two-beam, photoelectric filter photometer was designed and built to allow simultaneous measurement of any two astronomical sources within the telescope field of view. In addition, the optics of the photometer (Figure 1, Appendix II) were designed so that the two objects are both imaged in focus, alternately at high frequency, on the same aperture regardless of the relative position of the two objects in the sky. This allows the use of the same aperture-filter-detector system for both beams. A strobe system enables the observer to view continuously either or both fields and to make a photographic record of the localities under observation.

The data system contained two channels—one for each beam. The signal emitted by the photomultiplier tube detector alternated between the two beams. Signals from the two beams were separated at the detector output and fed to their respective data-system channel. The data system was of the analogue type, consisting of a.c. amplifiers and synchronous demodulators which presented an amplified d.c. signal to a digital voltmeter and papertape punch system. A chart record of the signal from both channels was also kept as a monitor.

The raw data consisted of intensity measurements of each object made through the various filters. These data were punched on papertape for computer processing.

The two sets of interference filters used had the characteristics listed in Table 1. Set A was used for most observations; set B was used primarily as a check for systematic errors. Effective wavelengths of the filters were computed considering the spectral distribution of the energy from the Moon incident on the photocathode and the spectral response of the photomultiplier. An ITT FW-130 (S-20) photomultiplier was used throughout this study.

The method of observation was to place a lunar area of interest in one beam of the photometer and a standard lunar area in the other beam. The filters, mounted in a rotating wheel, were placed, one at a time, behind the entrance aperture of the photometer while digital samples were taken of the output signal of both channels. The two beams were alternately imaged on the detector at 30 Hz; the longest time constant in the data system was 0.15 seconds. Digitization rate was 2 $\sec^{-1}$ in each channel or 4 $\sec^{-1}$ total. Ten samples were taken of each channel before passing to another filter. This gave an effective sample time of about 1.5 seconds, which, as far as instrument stability and atmospheric and shot noise were concerned, was enough to determine the relative

FILTER CHARACTERISTICS

SET #1

λ_e(Å)	$\Delta\lambda$(Å)	T (%)
4032	130	27
4224	200	66
4422	190	60
4612	190	60
4800	190	60
5040	240	58
5210	200	73
5403	150	65
5600	170	56
5782	230	55
6030	210	68
6180	200	65
6380	200	61
6637	220	71
6814	210	63
6976	240	54
7204	230	69
7413	190	65
7610	160	64
7790	200	65
7990	220	67

SET #2

λ_e(Å)	$\Delta\lambda$(Å)	T (%)
4032	130	27
4224	200	66
4355	90	67
4550	100	61
4955	90	70
5150	80	77
5340	80	70
5555	80	70
5755	70	70
6130	80	72
6342	80	78
6550	80	80
6760	90	64
7155	90	67
7350	80	85
7750	80	68
7965	80	84
8150	80	78

The effective wavelengths have been calculated considering the spectral characteristics of the following:

1. solar energy distribution
2. average lunar reflectivity
3. terrestrial atmospheric transmission (1 atm)
4. telescope optics (aluminum mirrors)
5. filter transmission
6. photocathode sensitivity

Table 1

intensity in each beam to 0.1%, even in thin overcast skies. The major source of error at this accuracy level was small telescope positioning errors (guiding errors) which allowed the image of the lunar areas to move slightly on the entrance aperture of the photometer. To reduce this error, the entire set of twenty-one filters was run three times.

The two beams use different mirrors in the photometer, raising the possibility of color or polarization effects due to differences in the mirror reflectivities. To eliminate this effect, after a run was completed with, say, object 1 in beam 1, etc., the photometer was rotated 180° and a run was made with object 2 in beam 1, etc. These two runs were later averaged to eliminate any differential effect due to the photometer mirrors. These effects were found, in general, to be small ($< 1\%$) when the mirrors were surfaced carefully and kept clean. As an added check for otherwise undetected systematic errors a triangulation check was run on several areas, several times during the program. That is, three spots (A,B,C) all easy to guide on, were chosen at different distances from each other on the lunar surface. Spot A versus spot B and spot C versus spot B were measured. Then spot A versus spot C could be calculated. The results were checked against an actual measurement of spot A versus spot C. The results were always consistent within the error assigned to each spectral curve, as discussed later.

Data Presentation

During 1967 the instrument and the observation techniques were developed and the lunar color measurements were made. Lunar regions observed are listed in Table 2 along with their selenographic coordinates. These regions are indicated on the full moon mosaic (Figure 3). Table 2 provides the universal date and time of observation and the approximate ($\pm 1^\circ$) geocentric phase angle.

The entrance aperture used corresponded to a 10 arc second diameter circular spot projected on the sky. This corresponds to an area about 18 km in diameter on the lunar surface at the subearth point.

The data were reduced by computer from the punched paper tapes, with spot checks made using the strip chart record. The results were plots of the relative reflectivity (ratios) of one lunar area to several standard areas normalized at 0.52μ. All areas were then reduced to the final standard, Mare Serenitatis 2.

Relative reflectivity, D (λ , α), is the function discussed in the introduction of this work

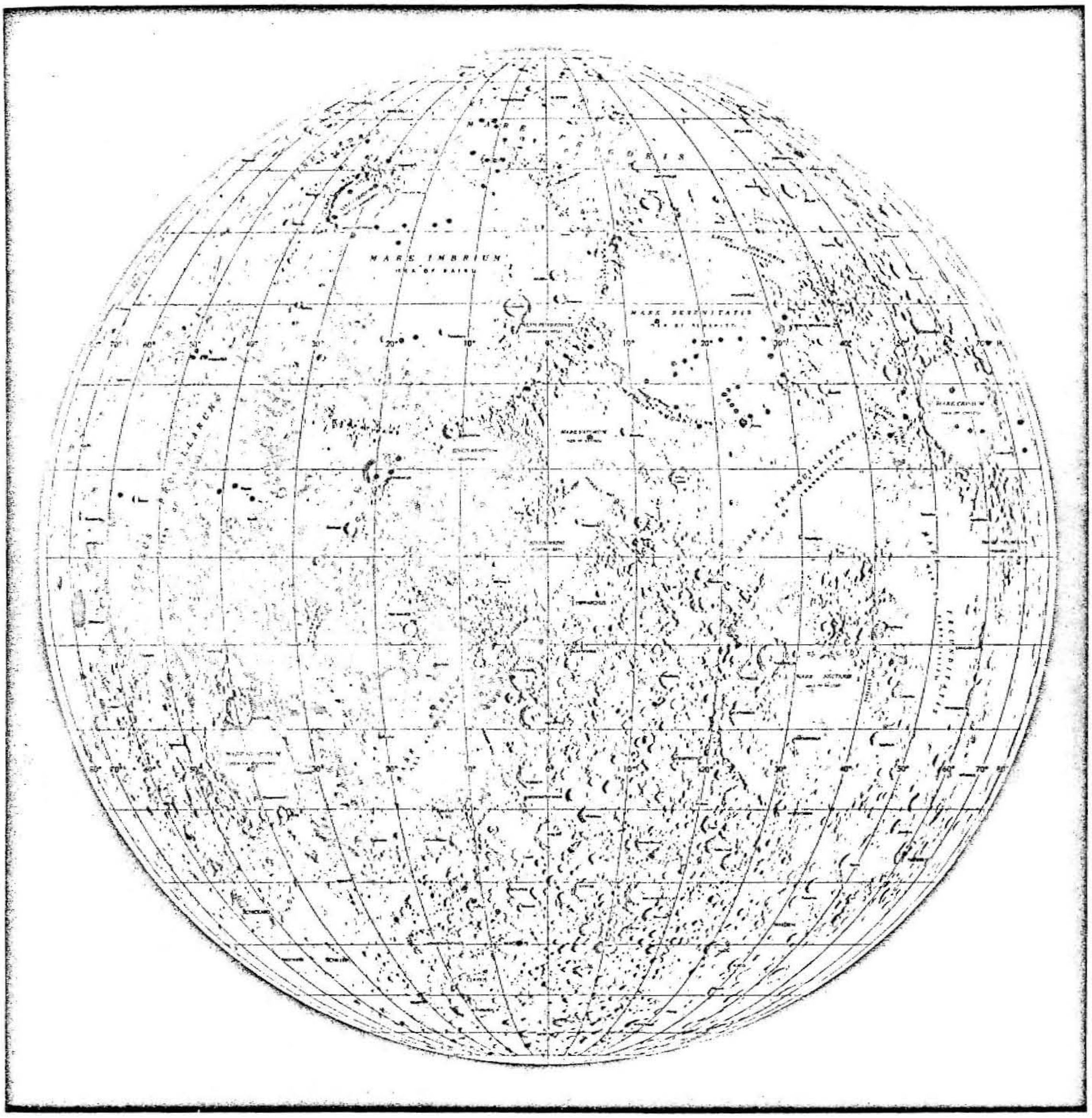
MARE FRIGORIS
MARE IMBRIUM
MARE SERENITATIS
MARE TRANQUILLITATIS
MARE CRISIUM
OCEANUS PROCELLARUM
70°
60°
50°
40°
30°
20°
10°
0°
10°
20°
30°
40°
50°
60°
70°

Figure 3

NAME	λ	ϕ	DATE (UT)	TIME (UT)	α
Areas relative to Mare Serenitatis (λ = 21.4, ϕ = 18.7)					
Alphonsus 2	4.2	-13.5	09/23/67	1100	52
Apennines 1	2.3	19.4	10/13/67	0600	-56
Bessel Ray N	-18.3	23.2	06/25/67	1040	41
Le Monnier	-30.2	26.3	06/24/67	1045	29
Mare Crisium 1	-61.5	14.6	10/17/67	0600	-12
			10/18/67	0620	-2
Mare Crisium 2	-54.6	14.7	10/17/67	0650	-12
			10/18/67	0540	-2
Mare Crisium 3	-59.7	14.8	10/11/67	2850	-81
			10/12/67	0250	-69
			11/15/67	0450	-20
Mare Crisium 4	-57.1	18.8	10/17/67	0750	-12
			10/18/67	0500	-2
Mare Frigoris	12.0	59.2	10/20/67	0840	20
Mare Frigoris 3	13.2	59.1	10/13/67		-57
Mare Imbrium 3	17.2	41.1	09/15/67	0430	-38
Mare Imbrium 4	14.5	41.7	09/15/67	0500	-38
Mare Imbrium 5	21.8	38.7	09/15/67	0550	-40
			09/16/67	0510	-28
Mare Imbrium 6	21.1	40.7	09/15/67	0620	-39
			09/16/67	0340	-28
Mare Imbrium 7	21.9	38.6	11/18/67	1210	15
Mare Nubium 1	13.6	-19.0	10/14/67	0620	-43
			10/19/67	0950	10
			10/22/67	0930	43
			11/18/67	0610	12
Mare Nubium 2	13.7	-17.0	10/14/67	0710	-45
			10/19/67	1040	10
Mare Seren 5	-24.2	19.6	06/24/67	1120	30
Mare Seren 6	-27.8	25.5	10/14/67	0400	-44
			10/15/67	0400	-34
Mare Seren 7	-25.0	25.0	10/14/67	0430	-45
Mare Seren 8	-22.2	25.2	06/25/67	1050	40
			10/15/67	0435	-35
Mare Seren 9	-16.5	22.8	06/25/67	1100	41
Mare Seren 10	-15.2	22.2	06/26/67	1100	52
Mare Seren 11	-11.8	20.3	06/26/67	1130	52
Mare Seren 13	-14.2	27.3	09/14/67	0310	-52
Mare Seren 14	-29.6	20.7	06/24/67	1140	30
			10/14/67	0310	-45
Mare Tranq 1	**-22.6**	**16.9**	09/11/67	0330	-89
			09/17/67	0330	-16
			10/11/67	0320	-82
			10/11/67	0400	-82
			10/12/67	0410	-70
			10/13/67	0230	-58
			10/14/67	0230	-45
			10/15/67	0240	-35
			10/17/67	0430	-12
			10/18/67	0340	-2
			10/19/67	0330	9
			10/19/67	0740	10
			10/20/67	0510	20
			10/21/67	0515	31
			11/15/67	0415	-20
			11/18/67	0525	12
Mare Tranq 3	-26.6	16.4	06/24/67	0900	28
			10/15/67	0315	-34
Mare Tranq 4	-24.7	15.5	11/18/67	0400	12
Mare Vaporum 1	-5.0	13.7	09/13/67	0520	-62
Palus Somni	-43.0	14.1	10/12/67	0330	-69
			10/17/67	1040	-13
			10/19/67	0510	8
Plato B	-13.1	53.3	10/19/67	1300	13
			10/20/67	0710	20
Plinius	-23.5	15.4	11/18/67	0430	12
Proclus	-47.0	16.1	10/17/67	1130	-10
			10/18/67	0420	-2
			10/19/67	0400	9
			10/19/67	0430	9
Sinus Iridum 1	34.3	42.2	10/19/67	0620	9
			10/21/67	0640	30
			10/22/67	0640	41
			11/15/67	0530	-30
			11/16/67	0310	-10
Sinus Iridum 3	29.9	46.8	09/15/67	0750	-38
Sinus Iridum 4	34.0	45.9	09/15/67	0830	-38
Upland 1	8.2	55.2	10/13/67	0410	-58
			10/20/67	0800	21
			11/18/67	1100	-14
Upland 5	-5.4	24.2	09/23/67	0920	51
Upland 6	-18.4	14.5	09/17/67	0440	-18
			09/23/67	0830	50
Upland 7	-31.2	27.8	06/24/67	1000	28
			06/25/67	0700	37
			10/12/67	0545	-75
Upland 10	30.2	51.0	10/19/67	0700	10
			10/20/67	0630	20
			10/21/67	0730	30
			10/22/67	0740	42
Upland 12	-74.5	12.7	10/13/67	0330	-58
Upland 13	-68.4	29.0	10/18/67	0700	-1.5
Upland South	-12.5	-16.7	10/14/67	0750	-45
			10/19/67	1120	11
			11/18/67	0515	12

NAME	λ	ϕ	DATE (UT)	TIME (UT)	α
Areas relative to Copernicus 3 (λ = 18.1, ϕ = 9.5)					
Copernicus 4	17.3	11.3	09/17/67	1000	-14
Copernicus 5	15.1	6.1	09/17/67	1020	-14
Areas relative to Le Monnier (λ = -30.1, ϕ = 26.3)					
Plato C	-11.2	51.5	06.20.67	0620	-25
Plato E	-8.0	51.6	09/26/67	0900	-45
Mare Seren 15	-28.0	23.8	10/25/66	0400	-60
Sinus Iridum	34.2	42.2	11/27/66		-15
Areas relative to Mare Crisium 1 (λ = -13.6, ϕ = -19.0)					
Palus Somni	43.0	14.1	11/21/66	0300	-80
Areas relative to Mare Nubium 1 (λ = 13.6, ϕ = -19.0)					
Tycho	10.6	-42.7	10/21/67	0845	31
			10/22/67	0900	43
			10/24/67	0915	65
			11/18/67	0715	12
Areas relative to Mare Serenitatis 3-A (λ = -21.9, ϕ = 17.0)					
Mare Tranq	-22.6	16.9	06/26/67	1115	52
Areas relative to Mare Seren 4 (λ = -21.8, ϕ = 17.9)					
Mare Tranq 2	-22.3	17.3	05/25/67	1050	22
Areas relative to Menelaus N.W. (λ = -15.2, ϕ = 17.2)					
Copernicus 1	20.8	10.6	05/28/67	1210	61
Le Monnier	-30.1	26.3	09/25/67	0300	-75
			09/26/67	0530	-55
Mare Frigoris 2	17.0	59.3	02/21/67	0420	-44
Mare Seren 12	-18.1	25.6	09/12/67	0410	-75
Palus Somni	43.0	14.1	05/23/67	0940	-88
Sinus Iridum 1	34.3	42.2	04/26/67	0830	25
Sinus Roris 1	-40.0	-56.0	05/27/67	1240	63
Areas relative to Plato C (λ = 11.2, ϕ = 51.5)					
Mare Seren 1	-15.5	21.1	02/24/67	0600	-7
			02/26/67	0830	23
Plato W	9.3	51.5	05/26/67	1000	35
Sinus Iridum 1	34.3	42.2	04/26/67	1000	27
			05/23/67	0610	-8
Upland 9	9.0	49.5	05/26/67	1115	36
Areas relative to Sinus Iridum 1 (λ = 34.3, ϕ = 42.2)					
Aristarchus 1	49.8	24.1	09/16/67	0900	-26
Aristarchus 2	49.1	25.0	09/16/67	0920	-26
			09/22/67	1000	41
			10/15/67	0730	-34
Aristarchus 3	47.5	23.8	09/22/67	1300	42
Copernicus 2	20.0	9.2	10/24/67	1200	67
Copernicus 3	18.1	9.5	09/17/67	0900	-15
Mare Imbrium S.	18.5	25.2	09/24/67	1100	63
			09/25/67	0940	73
			11/18/67	0900	13
Copernicus 7	8.4	5.0	09/24/67	1200	64
			11/18/67	1020	14
Copernicus Ray 1	16.7	25.8	11/18/67	0930	13
Kepler 1	35.9	6.6	09/16/67	0650	-26
Kepler 2	39.9	7.7	09/16/67	0800	-26
			09/17/67	0710	-16
			09/18/67	0950	-5
			09/22/67	1100	41
			09/24/67	0900	63
			09/25/67	0900	74
			09/26/67	1115	85
			10/15/67	0645	-33
			10/19/67	0900	10
			10/21/67	0600	32
Kepler 3	38.3	8.0	09/22/67	1100	41
Mare Imbrium 2	29.7	39.8	05/23/67	0715	-8
Mare Imbrium N	10.9	47.2	01/29/67	0800	42
Oceanus Procellarum 1	58.0	7.4	09/24/67	0950	63
Wood 1	51.4	29.5	09/26/67	1000	-26
Areas relative to Tycho 1 (λ = 10.6, ϕ = -42.7)					
Ptolemeaus 1	0.9	-9.8	09/18/67	0700	-5
			09/20/67	0710	29
Tycho 2	7.1	-44.0	09/18/67	0400	-5
Tycho 3	12.9	-40.0	09/19/67	0830	-5
			10/24/67	0900	66
Tycho 4	5.0	-29.6	09/18/67	0510	-5
			10/24/67	0940	66
Tycho 5	26.9	45.8	09/18/67	0540	-5
			10/24/67	1030	66

Table 2

(Chapter 1). A third order polynomial was least-squares fitted to each D (λ , α) plot to better demonstrate the shape of the function and to allow more accurate quantatative comparisons of different lunar areas. The most useful and non-redundant data are presented in Appendix III.

The accuracy of these measurements can be determined in several ways. The standard deviation of a single ratio measurement (ten samples of each beam through a filter) was almost always between 0.1% and 0.2%. Thus instrumental and atmospheric random noise were not important. Checks, such as those noted above, indicated that no systematic error greater than about 0.1% occurred as a result of either of these error sources. However, when measurements were made over the spectral range and repeated three times, the standard deviation varied from less than 0.1% to about 0.5% and at times exceeded 1%. These variations were due to guiding errors. An extremely small change in the position of the lunar image on the entrance aperture causes large errors when albedo and color variations exist in the lunar area observed. Measurements of upland areas and especially of the bright craters were not as accurate as those of areas having a relatively uniform albedo. Even so, the overall average standard deviation of the deviation of measured points from the smooth polynomial curves fit through them for all lunar areas observed was approximately 0.2% to 0.3%. Measurements made at the same exact lunar areas repeated to this accuracy, and averages of several runs produced the expected decrease in the standard deviations.

Another problem was small-scale spatial color irregularities that caused measurements at some lunar areas to show systematic differences from run to run if positioning was not accurately performed. The exact position of the entrance aperture on the lunar image was photographed during each run. Thus it was possible to diagnose this problem when it occurred.

The results of this observational program are probably best discussed under a format similar to that used in the conclusion section of the literature survey (Chapter II).

1. Color differences on the lunar surface were found. There is no room for doubt that differences in spectral reflectivity occur on the lunar surface.

2. The magnitude of the spectral reflectivity variations, as measured from the standard area, were most frequently under 5%, but differences of 10% occurred often. At particular areas, color variations

ranged above 20%. The maximum color variation, from reddest to bluest area, was about 60%. A frequency distribution of the red to blue intensity ratio between 0.4μ and 0.8μ , as compared to the standard spot in Mare Serenitatis, was plotted (Figure 4) to illustrate this conclusion.

3. The shape of the relative spectral reflectivity curves is discussed in two parts: (a) general curve shape over wavelength intervals of 500 Å to 1000 Å or more; (b) narrow spectral features of several hundred Angstroms.

> (a The general curve shapes were best studied by using the 3rd order polynomial curves fitted to the data. This eliminated any "high frequency" structure in the data. Some curves showed only a monotonous increase or decrease of reflectivity with wavelength; slopes were generally steeper in the blue than in the red. However, some curves were very nearly straight lines, especially for areas of larger (> 10%) color differences.
>
> On many of the spectral curves, features were noticed that suggested absorption bands. Two general features appeared: one, located in

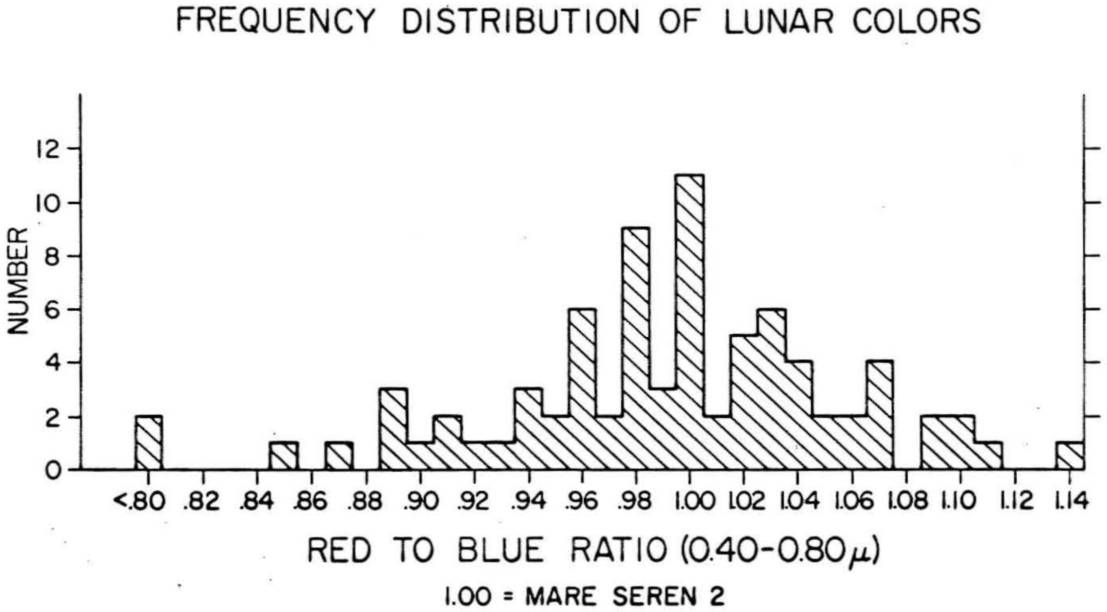
FREQUENCY DISTRIBUTION OF LUNAR COLORS
NUMBER
0
2
4
6
8
10
12
<.80
.82
.84
.86
.88
.90
.92
.94
.96
.98
1.00
1.02
1.04
1.06
1.08
1.10
1.12
1.14
RED TO BLUE RATIO (0.40-0.80μ)
1.00 = MARE SEREN 2

Figure 4

the red with center near .74μ, was the strongest and most common. It almost always appeared as a minimum and sometimes seemed to dominate the entire curve. A second feature, in the blue near 0.46μ, appeared less often and never as strongly ($<$ 4%) as the red feature. The blue feature was almost always a maximum. Both features appeared on some spectral curves creating the appearance of an inverted, reclining "S". At only one specific group of lunar objects (some bright craters) did the blue feature appear alone.

It must be kept in mind that these data represent relative reflectivity and not absolute reflectivity. Thus a spectral feature may appear strongly at both lunar areas but only weakly in the relative curve. However, the converse is not true. Also, the assignment of a spectral feature to one of the area-pairs is difficult if only relative data are available.

b) No obvious narrow-band (100-500 Å) spectral features were evident in any of the spectral curves. A search for small amplitude features was conducted by plotting the deviations of the measured data points from the curves fit through the data. In some cases spectral structure was noted that repeated in several measurements (Figure 5, note the scale). The actual data and curves for two cases are shown in Figure 6. These features show only the inability of a third order polynomial to fit the data points and may not necessarily correspond to actual absorption or emission bands. They do, however, indicate sudden changes in the differential reflectivity. These features appeared to be time stationary, although the case for Upland South is questionable. No relation between the broad and narrow spectral features was noticed, although there are not enough data to completely rule out such a relation.

4. Systematic dependence of differential color on lunar phase was found for some area-pairs. The effect was in the sense of decreasing color contrast for decreasing phase angle, and its amplitude over 90° change in phase angle was about 2% to 3% from 0.4μ to 0.8μ. Depths of the red spectral feature also seemed to decrease with the contrast. A sequence of relative reflectivity curves for different phase angles is shown in Figure 7

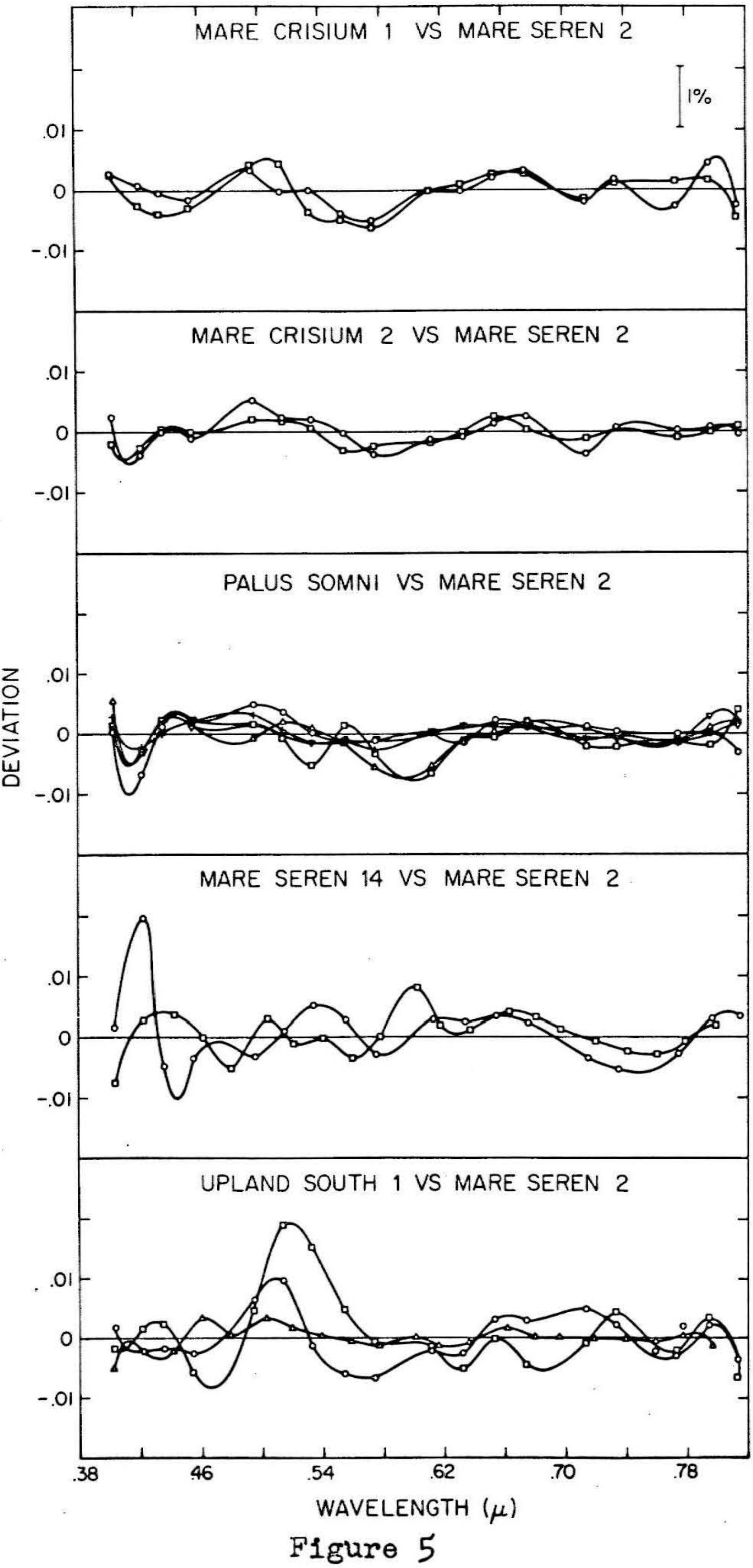
MARE CRISIUM 1 VS MARE SEREN 2
1%
MARE CRISIUM 2 VS MARE SEREN 2
PALUS SOMNI VS MARE SEREN 2
MARE SEREN 14 VS MARE SEREN 2
UPLAND SOUTH 1 VS MARE SEREN 2
.01
0
-.01
DEVIATION
.38
.46
.54
.62
.70
.78
WAVELENGTH (μ)

Figure 5

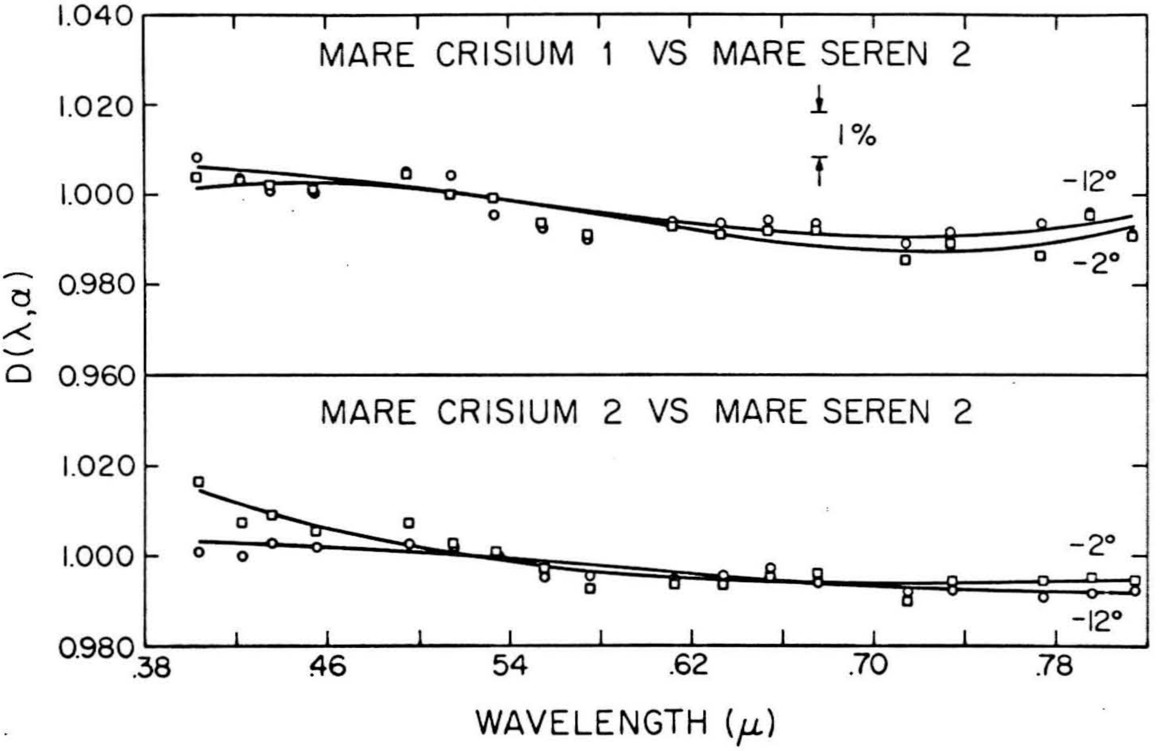
MARE CRISIUM 1 VS MARE SEREN 2
1%
-12°
-2°
MARE CRISIUM 2 VS MARE SEREN 2
-2°
-12°
D(λ,α)
1.040
1.020
1.000
0.980
0.960
1.020
1.000
0.980
.38
.46
.54
.62
.70
.78
WAVELENGTH (μ)

Figure 6

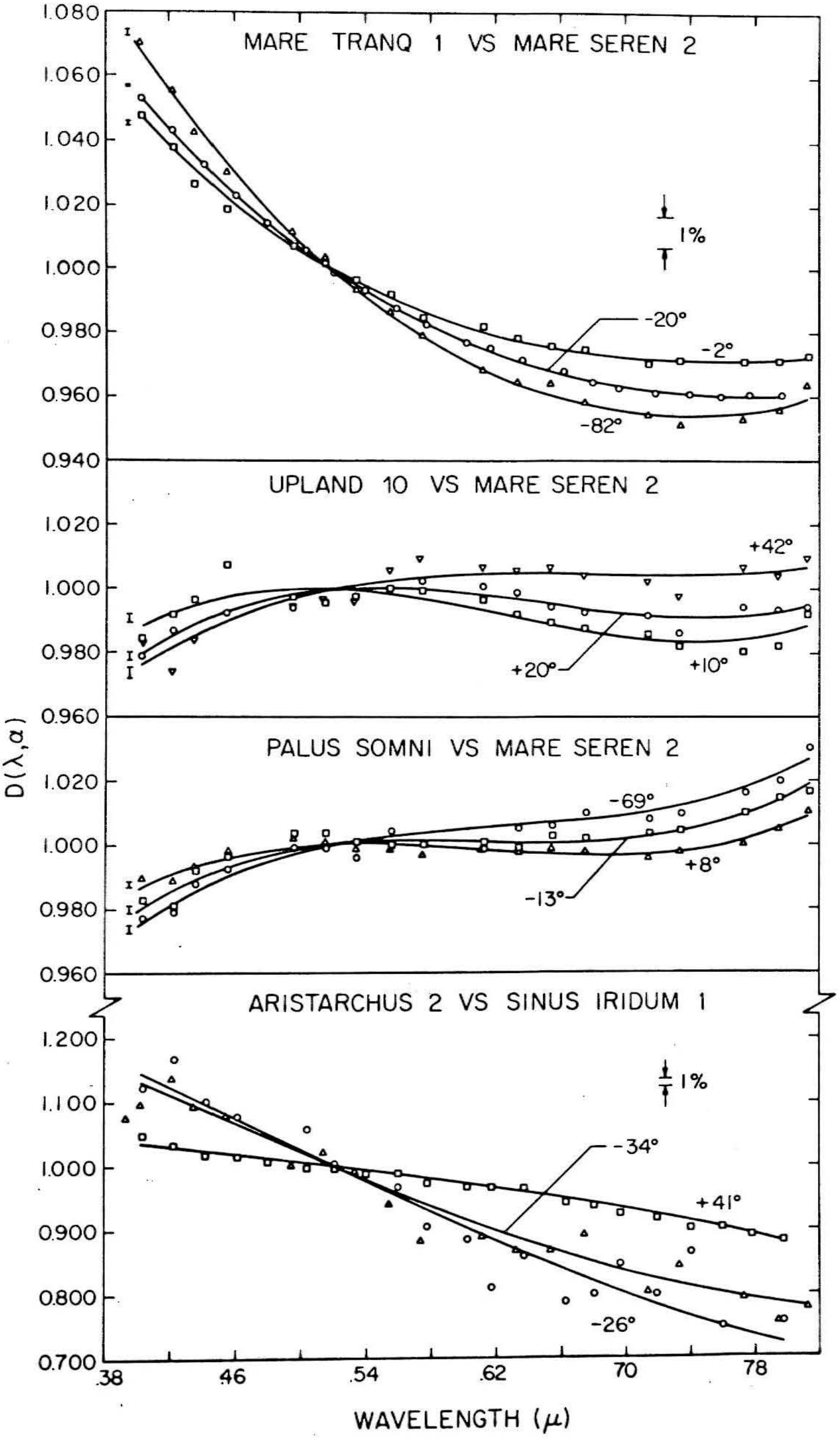
MARE TRANQ 1 VS MARE SEREN 2
1%
-20°
-2°
-82°
UPLAND 10 VS MARE SEREN 2
+42°
+20°
+10°
PALUS SOMNI VS MARE SEREN 2
-69°
-13°
+8°
ARISTARCHUS 2 VS SINUS IRIDUM 1
1%
-34°
+41°
-26°
1.080
1.060
1.040
1.020
1.000
0.980
0.960
0.940
1.020
1.000
0.980
0.960
1.020
1.000
0.980
0.960
1.200
1.100
1.000
0.900
0.800
0.700
.38
.46
.54
.62
.70
.78
D(λ,α)
WAVELENGTH (μ)

Figure 7

for several lunar areas. Both the data points and the fitted polynomial curves are shown as an example. (To avoid cluttered figures most of the subsequent figures show only the curves with an error bar indicating the standard deviation of the deviations of the data points from the curve.)

Change of the color contrasts with phase is illustrated in Figures 8-10 by plotting the red to blue ration, R/B, between 0.40 μ and 0.76 μ, of a curve against the value of the phase angle at which the curve was obtained. The most data exist for the area-pair Mare Serenitatis 2 - Mare Tranquillitatis 1, which straddled the albedo (and color) boundary between the two maria. The rate of change of the color contrast increases near 35° phase and it seems to decrease as zero phase is approached. It is also evident that the effect is symmetric about zero phase. The other plots further illustrate the effect. The vertical error bars were defined in the previous paragraph.

The Aristarchus 2 region (near Cobra Head) shown at the bottom for Figure 7 (note the scale change), is an extremely blue region where the phase effect seemed to operate in the opposite sense. The greatest color contrast occurred at large phase angles and, in

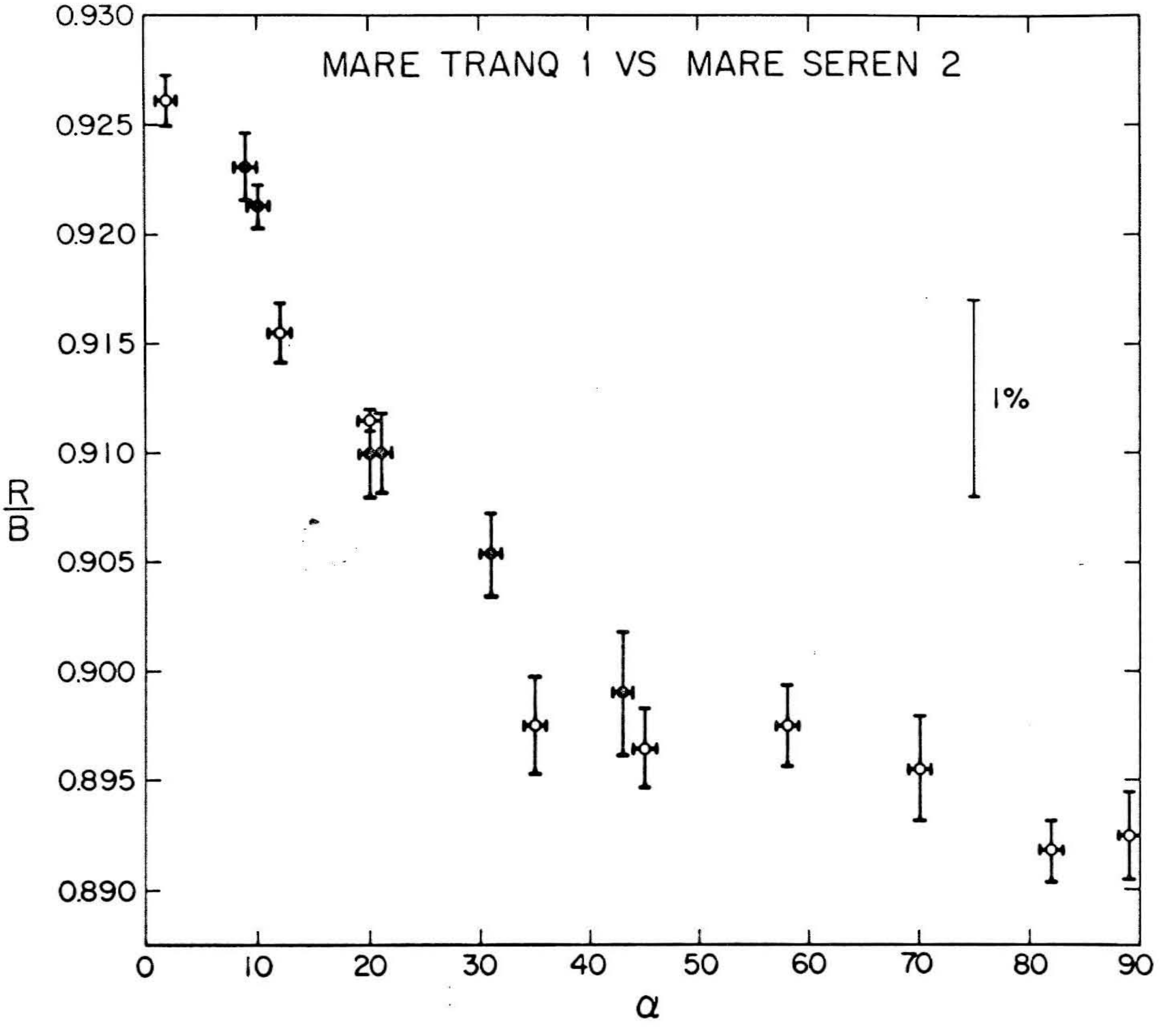
MARE TRANQ 1 VS MARE SEREN 2
0.930
0.925
0.920
0.915
0.910
0.905
0.900
0.895
0.890
R/B
0
10
20
30
40
50
60
70
80
90
α
1%

Figure 8

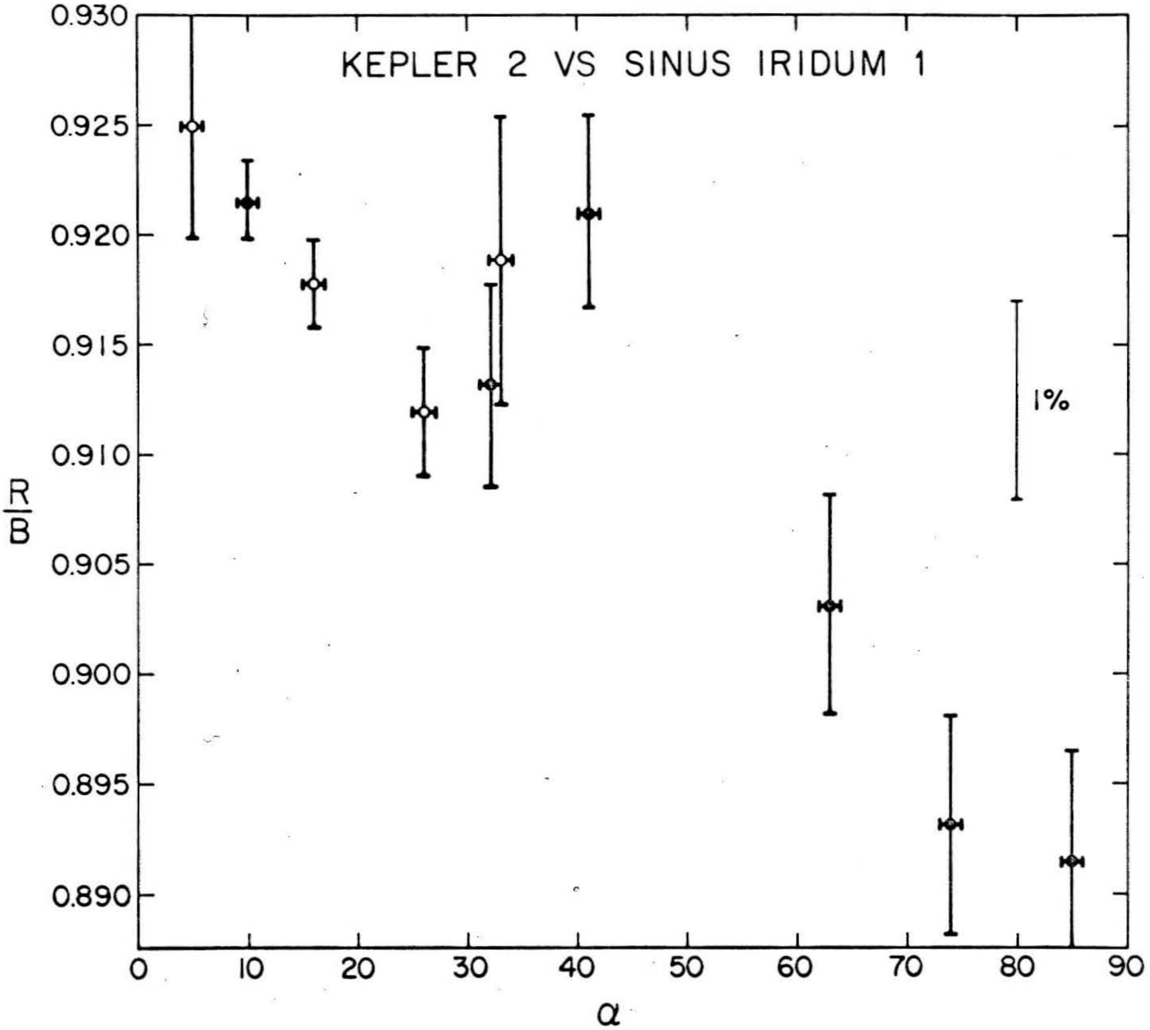
KEPLER 2 VS SINUS IRIDUM 1
0.930
0.925
0.920
0.915
0.910
0.905
0.900
0.895
0.890
R/B
1%
0
10
20
30
40
50
60
70
80
90
α

Figure 9

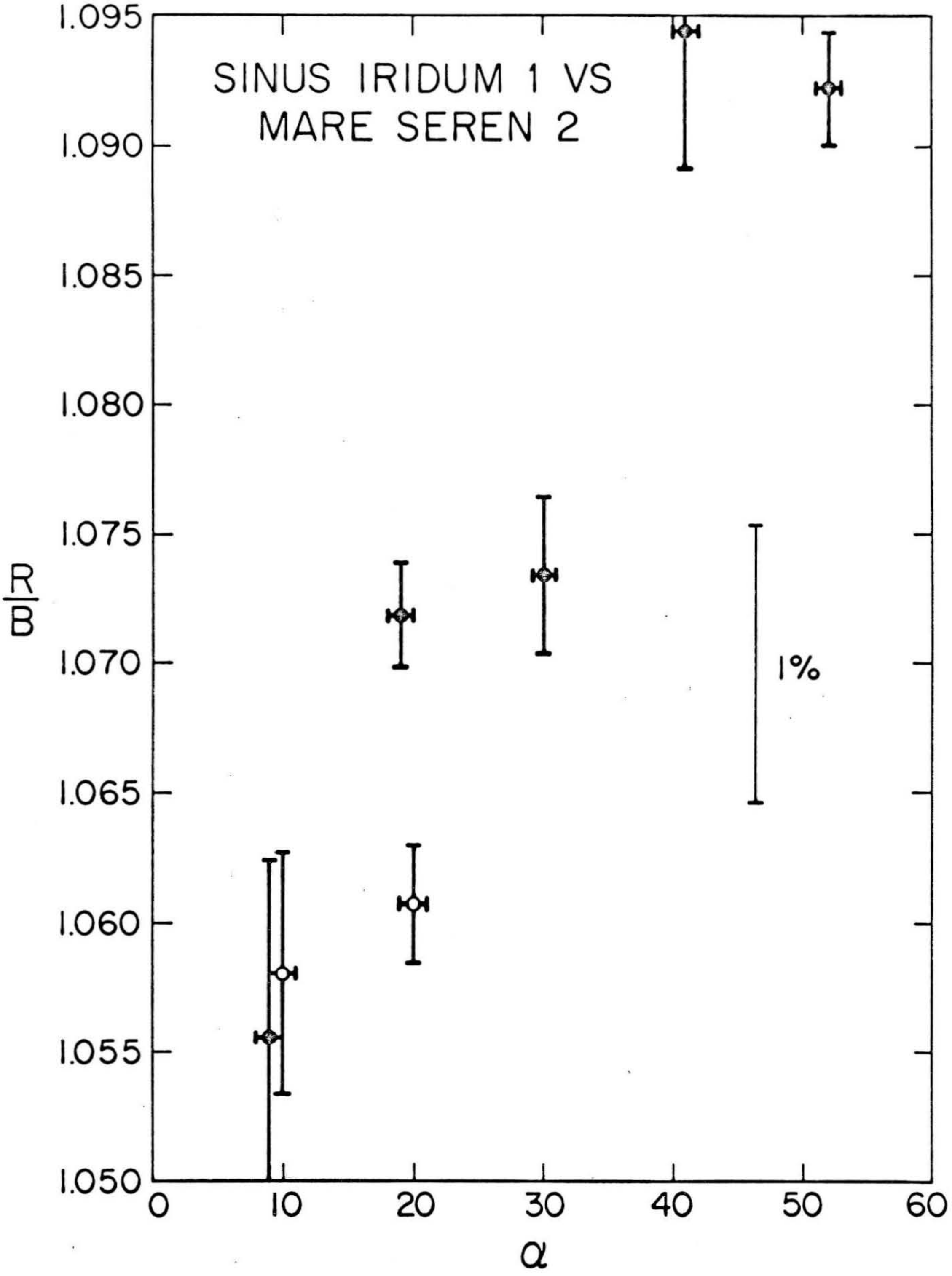
SINUS IRIDUM 1 VS
MARE SEREN 2
R/B
1.095
1.090
1.085
1.080
1.075
1.070
1.065
1.060
1.055
1.050
0
10
20
30
40
50
60
α
1%

Figure 10

particular, when this region is just entering the morning terminator. Then, only light reflected from the sides of vertical relief in this region is observed. At a later time, when the region is fully lighted and light reflected from the valleys is also observed, the spectral contrast is decreased. The greater color contrast at lunar dawn was noted during two different lunar days. This is one of the regions where lunar transient events (red spots) have been reported (Greenacre, 1963).

The color-phase effect varies in intensity with lunar position and/or with the magnitude of the color contrast itself. A large number of observations will be needed to completely define the effect, however.

5. The presence of a time-dependent emission phenomenon has been reported by several authors. Such an effect was not noticed in any of the observations made in the course of the present study, as was the case in an earlier search by the present author (McCord, 1967). The spectral features found appeared to be stable in time except for a systematic phase dependence. Certainly, had a 10% emission occurred during more than one observation, even if it only affected one filter measurement, it would have been detected. A 1% effect would have beeen noticed had it occurred frequently.

The suggested presence of relatively

narrow-band, small-amplitude spectral features, discussed in part 3b, may be due to an emission rather than an absorption phenomenon. However these features do not appear to be time dependent, or at least they were present in most of the measurements made at the particular lunar regions showing this feature.

6. Dependence of lunar differential color on morphology is discussed by considering three types of features; (a) maria, (b) uplands, and (c) bright craters. Some special features will be discussed later.

(a The color contrasts found in the maria are shown in Figures 11, 12, 13. All regions are normalized to the main standard area in Mare Serenitatis (Mare Serenitatis 2; $\lambda = -21\overset{\circ}{.}4$, $\varphi = +18\overset{\circ}{.}7$). Those lunar areas not measured directly against the main standard area were measured against more convenient intermediate standard areas and later reduced to the main standard area and are indicated by a symbol along with the name of the secondary standard area given at the bottom of the figure.

Variations in the Mare Serenitatis region, shown in Figure 11, were small (2% to 3%), and the spectral curves were generally smooth with little suggestion of relative spectral features

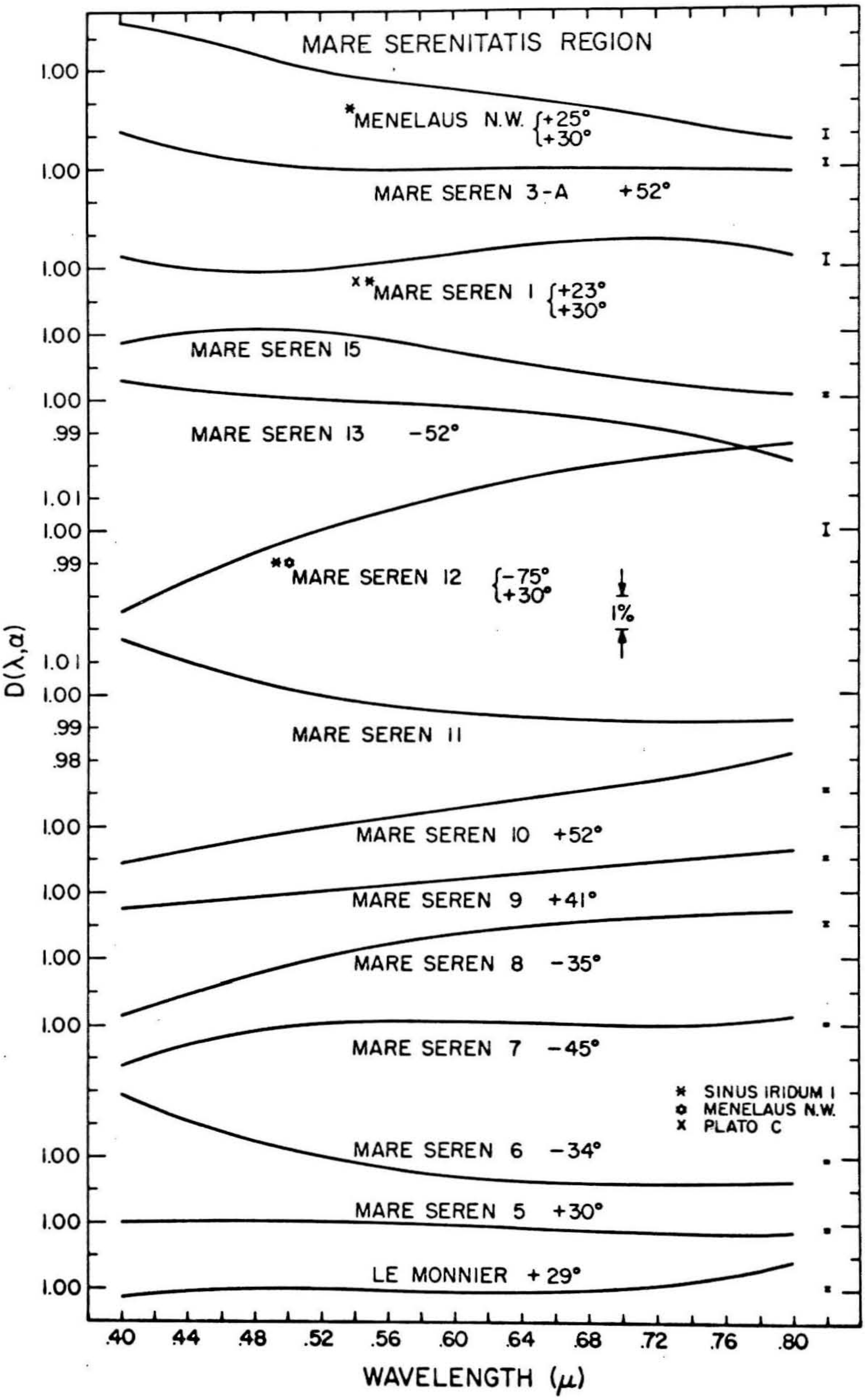
MARE SERENITATIS REGION
*MENELAUS N.W. {+25° +30°
MARE SEREN 3-A +52°
x*MARE SEREN 1 {+23° +30°
MARE SEREN 15
MARE SEREN 13 -52°
*○MARE SEREN 12 {-75° +30°
1%
MARE SEREN 11
MARE SEREN 10 +52°
MARE SEREN 9 +41°
MARE SEREN 8 -35°
MARE SEREN 7 -45°
* SINUS IRIDUM I
○ MENELAUS N.W.
x PLATO C
MARE SEREN 6 -34°
MARE SEREN 5 +30°
LE MONNIER +29°
1.00
1.00
1.00
1.00
1.00
.99
1.01
1.00
.99
1.01
1.00
.99
.98
1.00
1.00
1.00
1.00
1.00
1.00
1.00
D(λ,α)
.40
.44
.48
.52
.56
.60
.64
.68
.72
.76
.80
WAVELENGTH (μ)

Figure 11

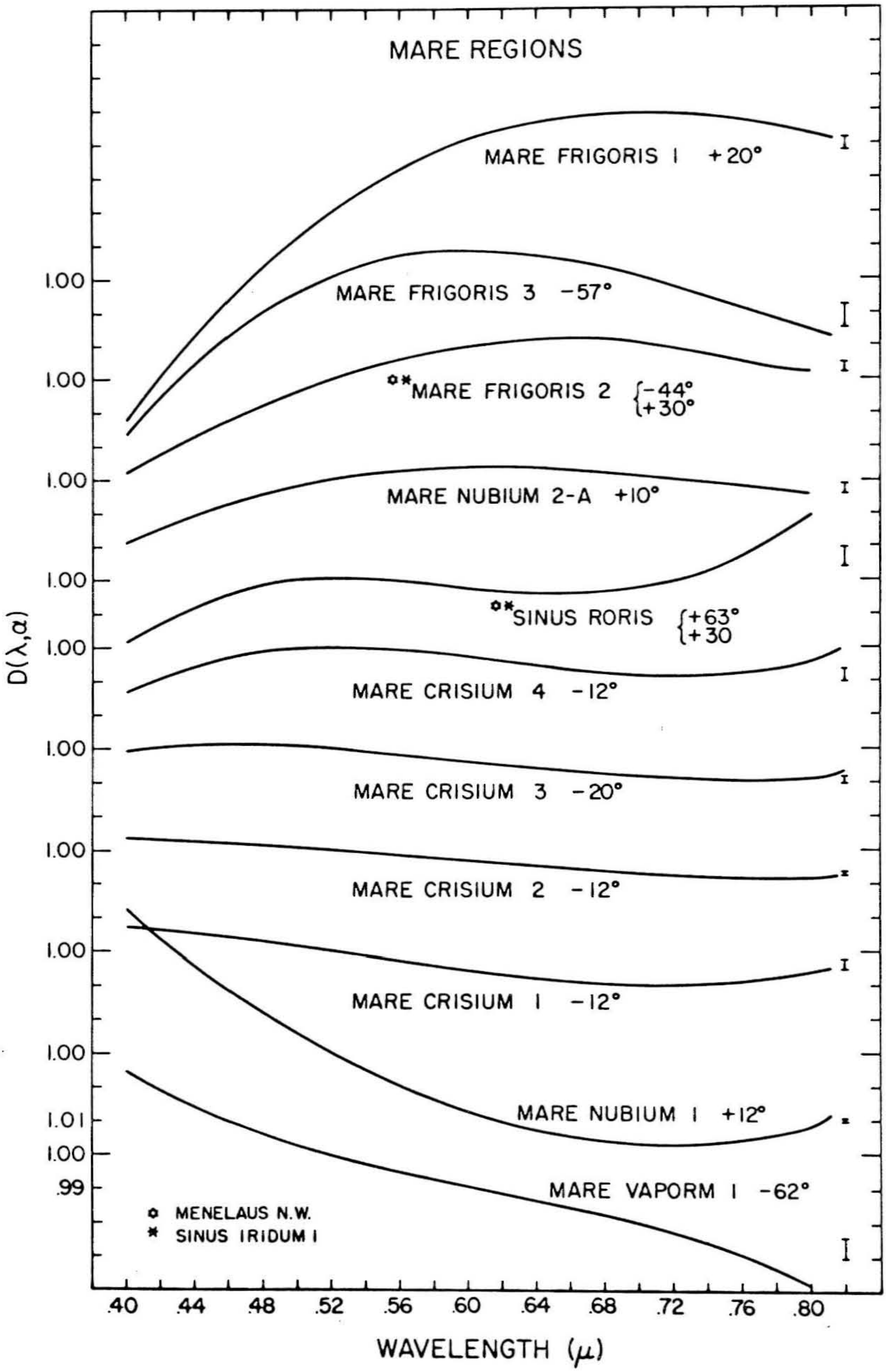
MARE REGIONS
MARE FRIGORIS 1 +20°
MARE FRIGORIS 3 -57°
MARE FRIGORIS 2 {-44° +30°
MARE NUBIUM 2-A +10°
SINUS RORIS {+63° +30
MARE CRISIUM 4 -12°
MARE CRISIUM 3 -20°
MARE CRISIUM 2 -12°
MARE CRISIUM 1 -12°
MARE NUBIUM 1 +12°
MARE VAPORM 1 -62°
MENELAUS N.W.
SINUS IRIDUM I
1.00
1.00
1.00
1.00
1.00
1.00
1.00
1.00
1.00
1.01
1.00
.99
D(λ,α)
.40
.44
.48
.52
.56
.60
.64
.68
.72
.76
.80
WAVELENGTH (μ)

Figure 12

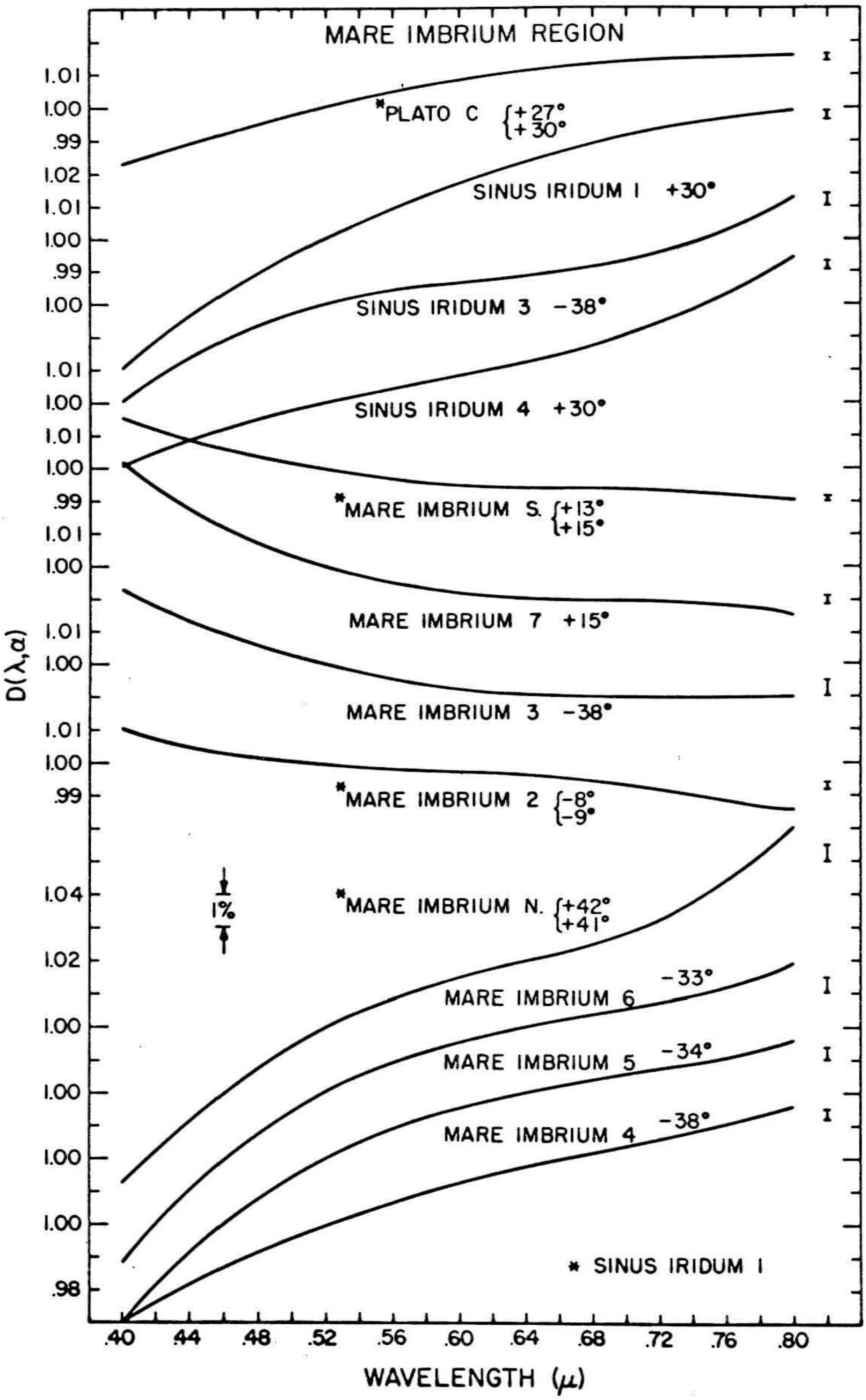
MARE IMBRIUM REGION
*PLATO C {+27° +30°
SINUS IRIDUM 1 +30°
SINUS IRIDUM 3 −38°
SINUS IRIDUM 4 +30°
*MARE IMBRIUM S. {+13° +15°
MARE IMBRIUM 7 +15°
MARE IMBRIUM 3 −38°
*MARE IMBRIUM 2 {−8° −9°
*MARE IMBRIUM N. {+42° +41°
MARE IMBRIUM 6 −33°
MARE IMBRIUM 5 −34°
MARE IMBRIUM 4 −38°
1%
* SINUS IRIDUM 1
D(λ,α)
1.01
1.00
.99
1.02
1.01
1.00
.99
1.00
1.01
1.00
1.01
1.00
.99
1.01
1.00
1.01
1.00
1.01
1.00
.99
1.04
1.02
1.00
1.00
1.00
1.00
.98
.40
.44
.48
.52
.56
.60
.64
.68
.72
.76
.80
WAVELENGTH (μ)

Figure 13

although the curve for Mare Serenitatis 1, Le Monnier and Mare Serenitatis 15 did suggest some spectral features. It appeared that there are small but real color contrasts within the mare that vary over relatively short distances. There also seemed to be regional differences with the southwest region bluer and the northwest region redder than the eastern area. The so-called colored ring (an albedo ring to the eye) around Mare Serenitatis appeared to be not very different in color from the center of the mare: Menelaus N.W., Mare Serenitatis 6 and Mare Serenitatis 15 all in the dark ring were bluer by about 2% to 3% than the center area but; Le Monnier was virtually identical in color to the mare center. Two exceptions to this were found. A dark region south of Le Monnier near the mare edge (Mare Serenitatis 14) was very blue (11%) relative to the mare (see Figure 14). Also the albedo boundary at the southeastern edge of the mare near Mare Tranquillitatis was found to be a strong color boundary (~ 10%), the lighter Mare Serenitatis region being redder (Figure 11). This boundary

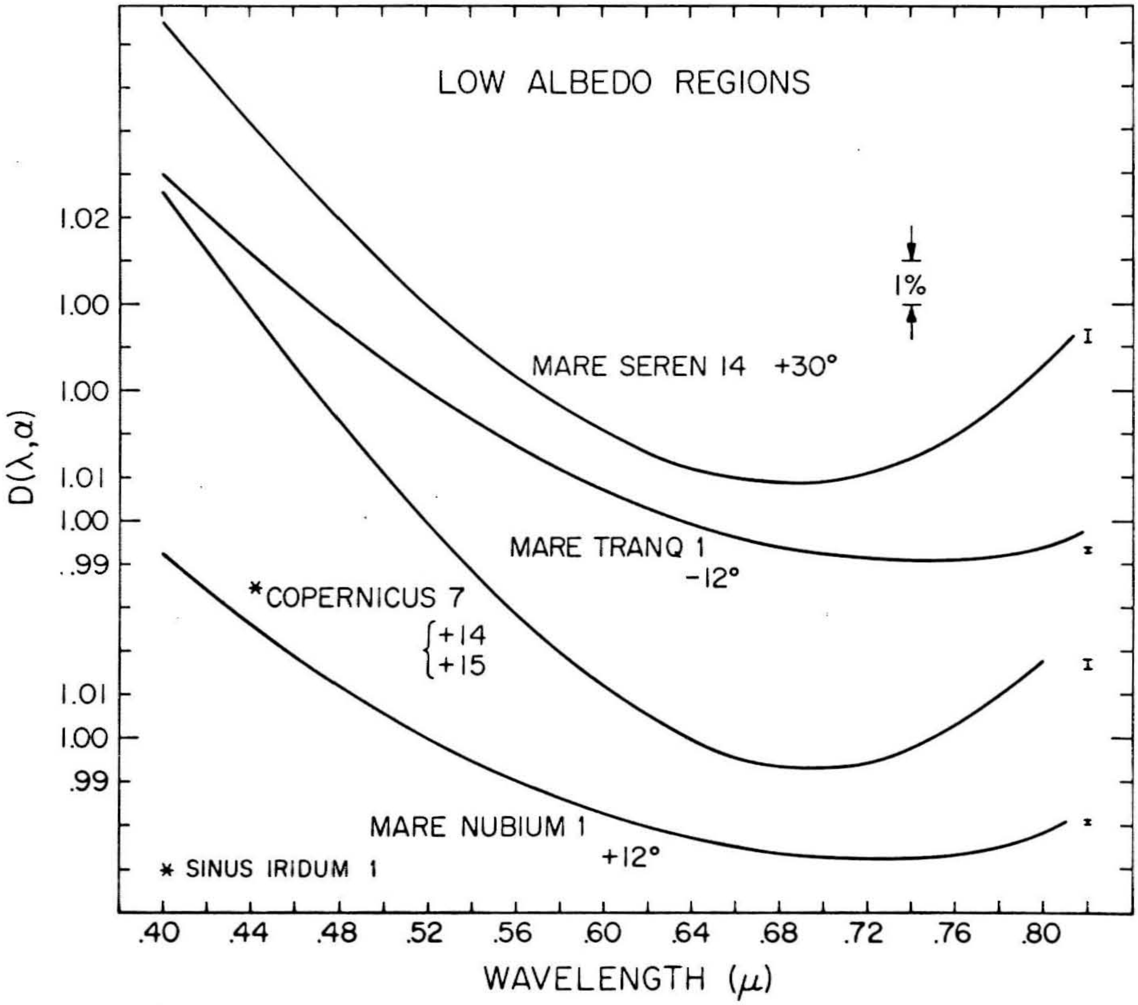
LOW ALBEDO REGIONS
D(λ,α)
1.02
1.00
1.00
1.01
1.00
.99
1.01
1.00
.99
1%
MARE SEREN 14 +30°
MARE TRANQ 1
-12°
*COPERNICUS 7
+14
+15
MARE NUBIUM 1
+12°
* SINUS IRIDUM 1
.40
.44
.48
.52
.56
.60
.64
.68
.72
.76
.80
WAVELENGTH (μ)

Figure 14

was very sharp ($<$ 15 km).

Fewer measurements were made in Mare Crisium than in Mare Serenitatis, but those made (Figure 12) showed very little color variation either within the mare or with respect to Mare Serenitatis. There appeared narrow-band departures of the reflectivity from a smooth curve, as was mentioned above. Broad-band spectral features also appeared, as shown by the curves for Mare Crisium 1 and especially for Mare Crisium 4.

The Mare Imbrium region was found to be colorful with two classes of areas evident, one much redder (up to 13%) and one somewhat bluer (to about 4%) than the standard area in Mare Serenitatis (see Figure 13). Curves for several places in Sinus Iridum and Plato exhibited similar trends. The curves were generally smooth but spectral features appeared on several curves, especially Mare Imbrium N, and Sinus Iridum 3. Mare Imbrium appeared different in its color characteristics from Mare Serenitatis or Mare Crisium.

Two measurements in Mare Nubium (Figure 12) in the same locality gave different color curves the brighter being redder, indicating a variety of colors in this region also.

Three measurements (Figure 12), all closely spaced, in Mare Frigoris north of Plato gave different curves, indicating again that color varies over small distances. All curves show Mare Frigoris, in this region, to be 5% to 10% redder than Mare Serenitatis. These spectral curves were different from those discussed thus far, except for Mare Nubium 1, in that a definite U-shape is evident. It is also unusual that the red spectral feature is a maximum rather than a minimum. This feature differs from place to place in Mare Frigoris.

One measurement in Sinus Roris clearly showed the red broad-band spectral features (Figure 12), although it was shifted toward the shorter wavelengths somewhat from the "usual" position.

Several areas were observed in the extreme northwestern edge of Mare Tranquillitatis near Mare Serenitatis. The entire region appeared much bluer ($\sim$ 10%) then nearby Mare Serenitatis (Figures 14, 15) and is the bluest mare area mentioned thus far. The red spectral

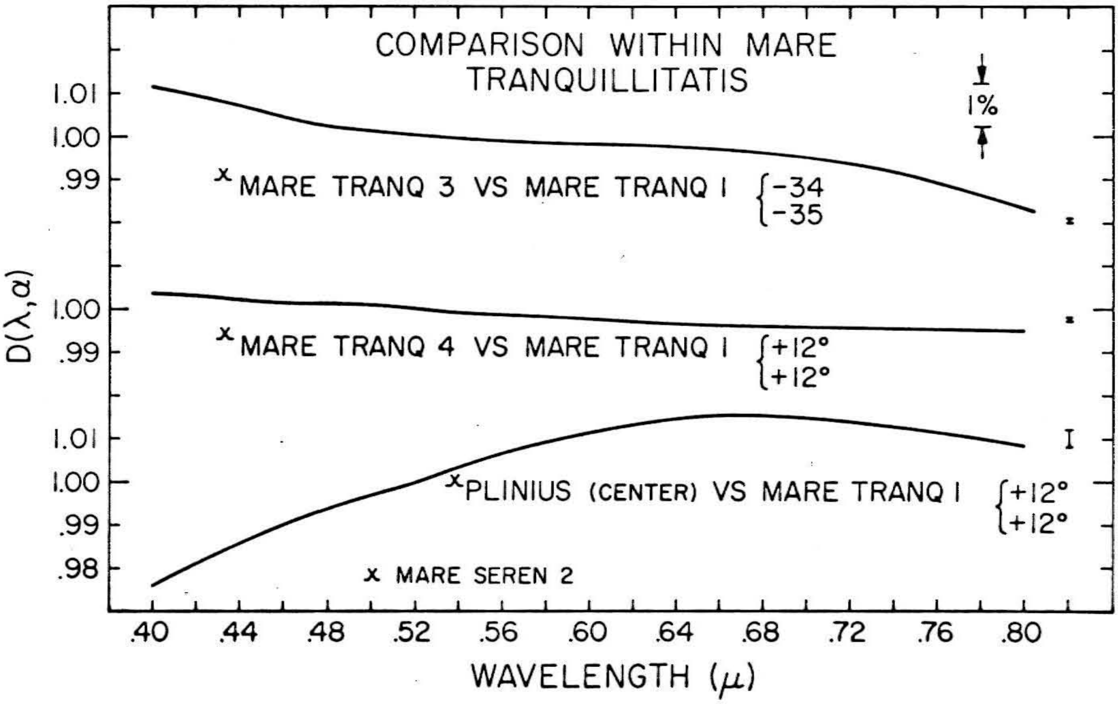
COMPARISON WITHIN MARE TRANQUILLITATIS
1%
MARE TRANQ 3 VS MARE TRANQ I
-34
-35
MARE TRANQ 4 VS MARE TRANQ I
+12°
+12°
PLINIUS (CENTER) VS MARE TRANQ I
+12°
+12°
MARE SEREN 2
D(λ, α)
1.01
1.00
.99
1.00
.99
1.01
1.00
.99
.98
.40
.44
.48
.52
.56
.60
.64
.68
.72
.76
.80
WAVELENGTH (μ)

Figure 15

feature shows strongly in the curves for the area, and as usual it is a minimum.

The Mare Tranquillitatis region is typical of most very low albedo areas (Figure 14). Copernicus 7, a dark mare area east of Copernicus, Mare Nubium 1, Mare Serenitatis 14 and Mare Tranquillitatis all appeared quite blue and showed a relatively deep, broad spectral feature in the red. An exception to this rule is the Wood's Spot area (Figure 13) west of Aristarchus. This low albedo area appeared quite red relative to Mare Serenitatis.

b) The upland regions (Figure 16) possessed a particular type of relative spectral curve at almost every area measured. This curve had an inverted, reclining "S" shape indicating either a red band or blue band or both, depending on how the curve is interpreted. Overall color differences from the standard region or among different upland regions, however, was small, less then 1% in many cases. Two regions in the Apennine Mountains (Apennine 1 and Upland 9) were noticably redder and one region on the south rim of Plato (Upland 9) was very red— the reddest area

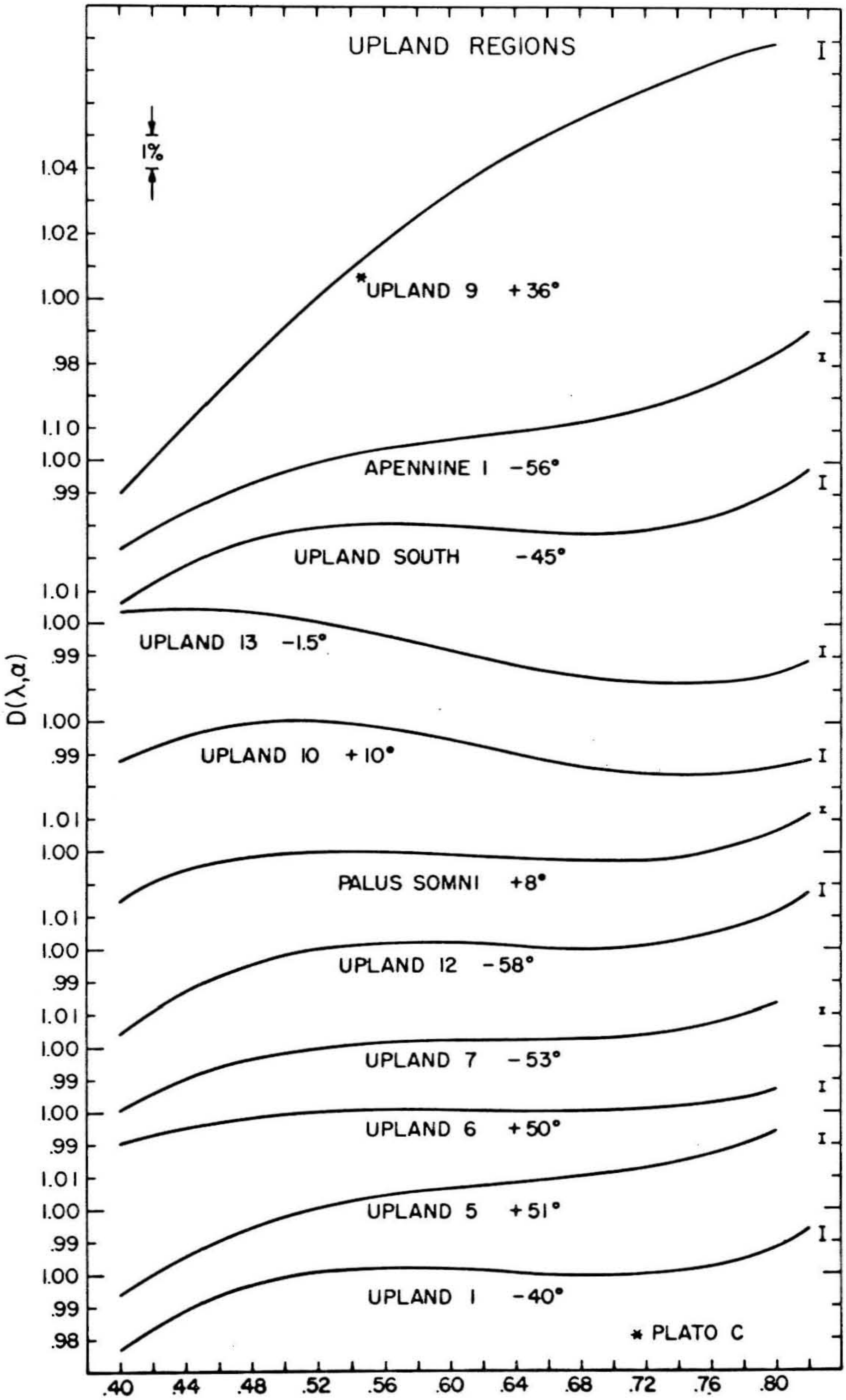
UPLAND REGIONS
1%
1.04
1.02
1.00
.98
1.10
1.00
.99
1.01
1.00
.99
1.00
.99
1.01
1.00
1.01
1.00
.99
1.01
1.00
.99
1.00
.99
1.01
1.00
.99
1.00
.99
.98
D(λ,α)
*UPLAND 9 +36°
APENNINE I -56°
UPLAND SOUTH -45°
UPLAND 13 -1.5°
UPLAND 10 +10°
PALUS SOMNI +8°
UPLAND 12 -58°
UPLAND 7 -53°
UPLAND 6 +50°
UPLAND 5 +51°
UPLAND 1 -40°
* PLATO C
.40
.44
.48
.52
.56
.60
.64
.68
.72
.76
.80
WAVELENGTH (μ)

Figure 16

found in the study. These last two regions might more accurately be classed as disturbed upland regions.

Upland regions appeared uniform in color and in the shape of the spectral curve, in contrast to the mare regions which exhibited large color differences and a variety of spectral curve shapes.

(c The bright craters studied appeared to be some of the most highly colored features on the lunar surface. Two distinct color groups of craters were defined with Tycho, Plato B and Aristarchus (Figure 17) appearing extremely blue and Kepler, Proclus, Copernicus and the bright feature west of Reiner (Figure 18) appearing less blue. The spectral curve shape for the very blue craters was almost a straight line but the curves for the other bright craters had a distinctive hump in the blue. Again, the interpretation of this hump as the center of an absorption feature or as the extreme wing of a feature with its center far in the red was not clear from these data. It is clear, however, that distinctive features do appear at these particular craters and not at others.

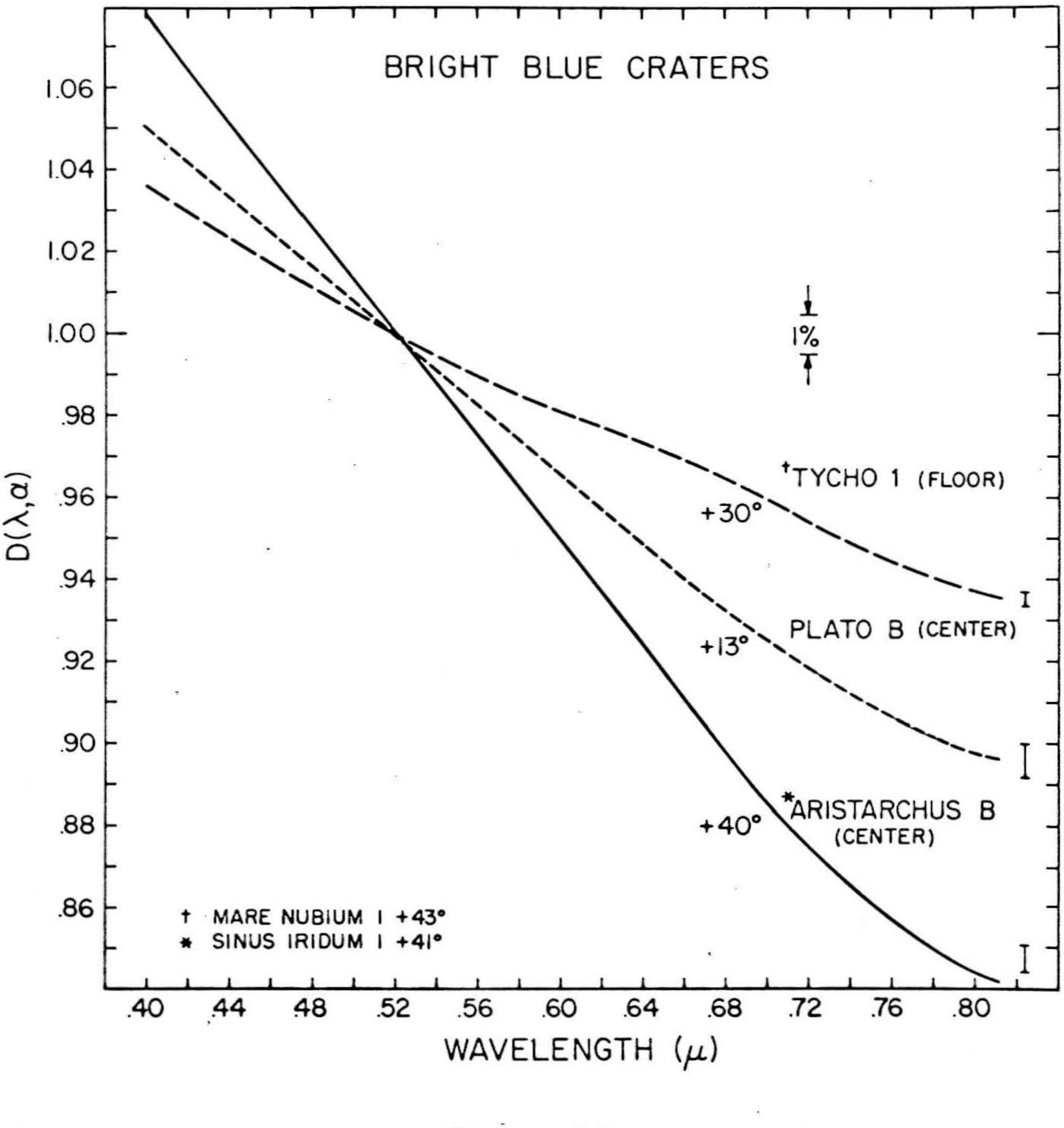
BRIGHT BLUE CRATERS
1.06
1.04
1.02
1.00
.98
.96
.94
.92
.90
.88
.86
D(λ,α)
1%
†TYCHO 1 (FLOOR)
+30°
PLATO B (CENTER)
+13°
*ARISTARCHUS B
(CENTER)
+40°
† MARE NUBIUM I +43°
* SINUS IRIDUM I +41°
.40
.44
.48
.52
.56
.60
.64
.68
.72
.76
.80
WAVELENGTH (μ)

Figure 17

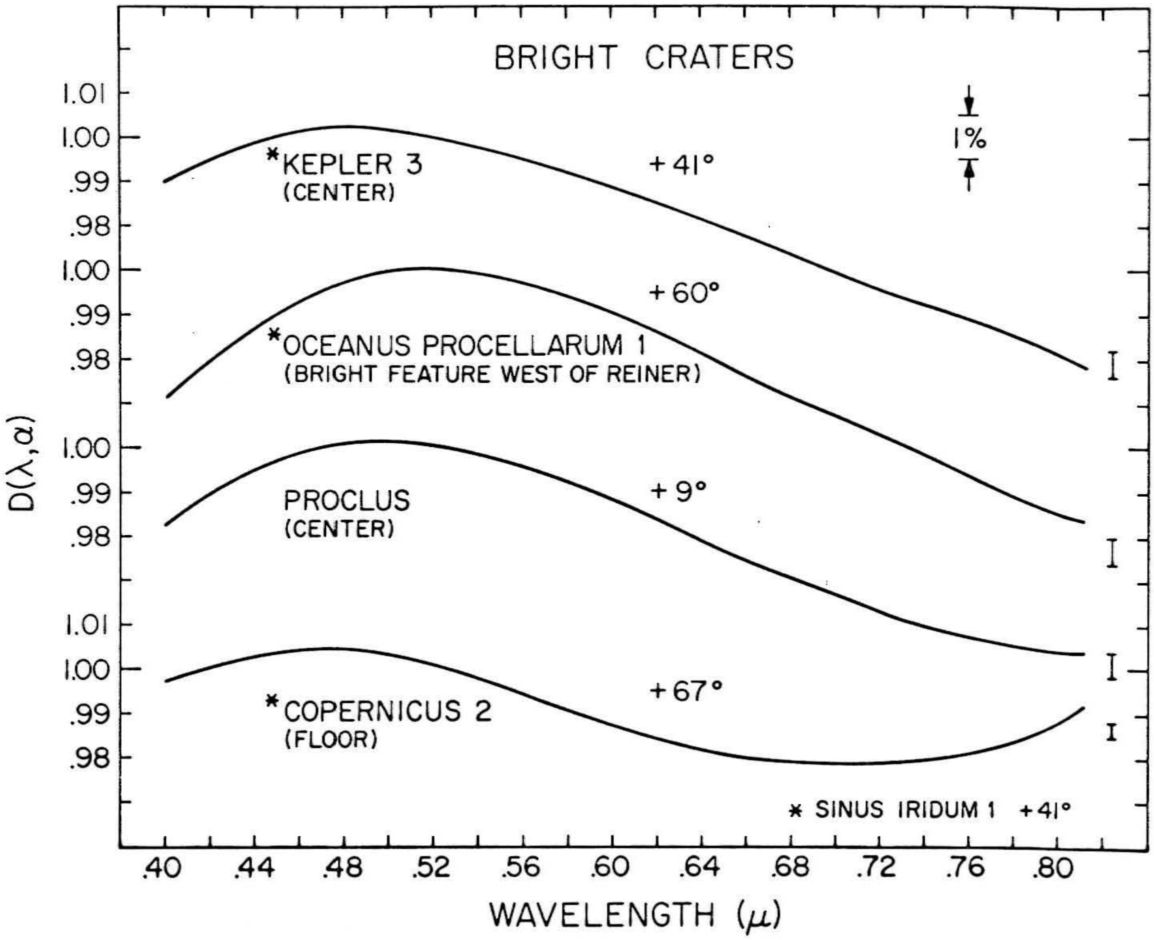
BRIGHT CRATERS
1%
*KEPLER 3
(CENTER)
+41°
+60°
*OCEANUS PROCELLARUM 1
(BRIGHT FEATURE WEST OF REINER)
PROCLUS
(CENTER)
+9°
*COPERNICUS 2
(FLOOR)
+67°
* SINUS IRIDUM 1 +41°
D(λ,α)
1.01
1.00
.99
.98
1.00
.99
.98
1.00
.99
.98
1.01
1.00
.99
.98
.40
.44
.48
.52
.56
.60
.64
.68
.72
.76
.80
WAVELENGTH (μ)

Figure 18

In summary, each of the three morphologic groups shows distinctive differential reflection curves. The mare areas vary in color from place to place within a particular mare and from mare to mare. The boundaries of the color regions seem to be very sharp. The very dark regions appear to be blue in general. The upland regions are generally of uniform color with a distinctive relative spectral curve shape found in only a few mare locations. The disturbed upland regions appear redder. The bright craters contain two distinct color groups, each with a distinctive color curve.

7. At several places the color of a mare area and a nearby upland area were measured. The Le Monnier-Upland 7 pair (Figures 11, 16) were very similar in color with the Upland 7 curve showing slightly more of the typical shape for upland regions.

The Mare Crisium-Proclus-Palus Somni area (Figures 12, 18, 16) varied in color with the depth of the red spectral feature (or the height of the bluer feature) changing from deepest at Proclus to almost non-existent in Mare Crisium.

Sinus Iridum 3-Upland 10 also showed a difference, not in the shape of the curve, but it its tilt; Sinus Iridum 3 is redder.

A complicated region is exposed by the

Upland 1-Plato B-Plato-Upland 9- Mare Imbrium N set of measurements (Figures 16,17,13). Upland 1, north of Plato, is characterized by a typical upland curve. Plato shows a variety of colors within its crater walls (Figure 19) but the curve shapes are different from those of Upland 1. Upland 9 to the south is very red and not at all typical of upland regions; it resembles Plato itself. In fact it may be erroronous to classify this region as an upland region. Mare Imbrium N completes the reddening trend from north to south. It again shows the curve shape found at Upland 1 and not so common in the mare. Plato B is completely different with an extremely blue color and a straight line spectral curve. Mare Frigoris to the north is quite different from Upland 1 and somewhat resembles Plato. This is a complex region. It may be significant that it was in the Plato region that Goetz (1967) reported an anamolous 8μ emissivity.

The color changes near craters are shown in Figures 20, 21, 22, for the Tycho, Kepler and Copernicus regions. Near Tycho, all curves are similar in shape. The areas outside the crater are redder than the crater, with the throwout ring reddest. The Kepler area also possesses similar curves with a small blueing trend as the crater is approached. However this set of curves differs from the Tycho set just as the curves for the two

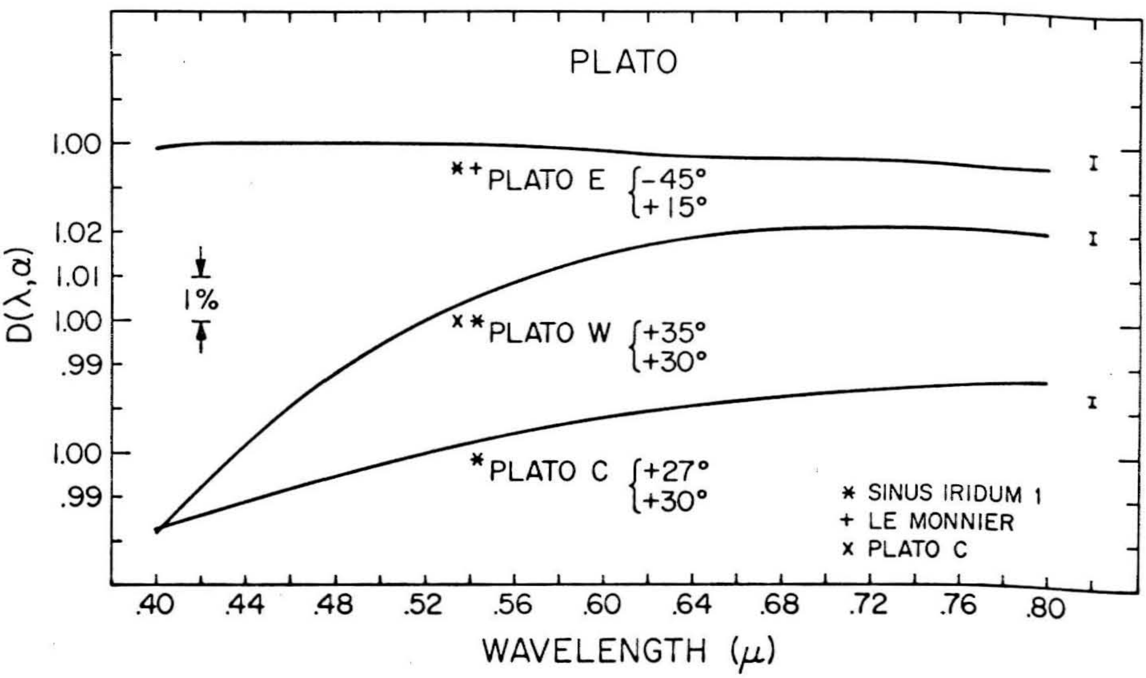
PLATO
1.00
1.02
1.01
1.00
.99
1.00
.99
D(λ,α)
1%
*+PLATO E {-45° +15°
x*PLATO W {+35° +30°
*PLATO C {+27° +30°
* SINUS IRIDUM 1
+ LE MONNIER
x PLATO C
.40
.44
.48
.52
.56
.60
.64
.68
.72
.76
.80
WAVELENGTH (μ)

Figure 19

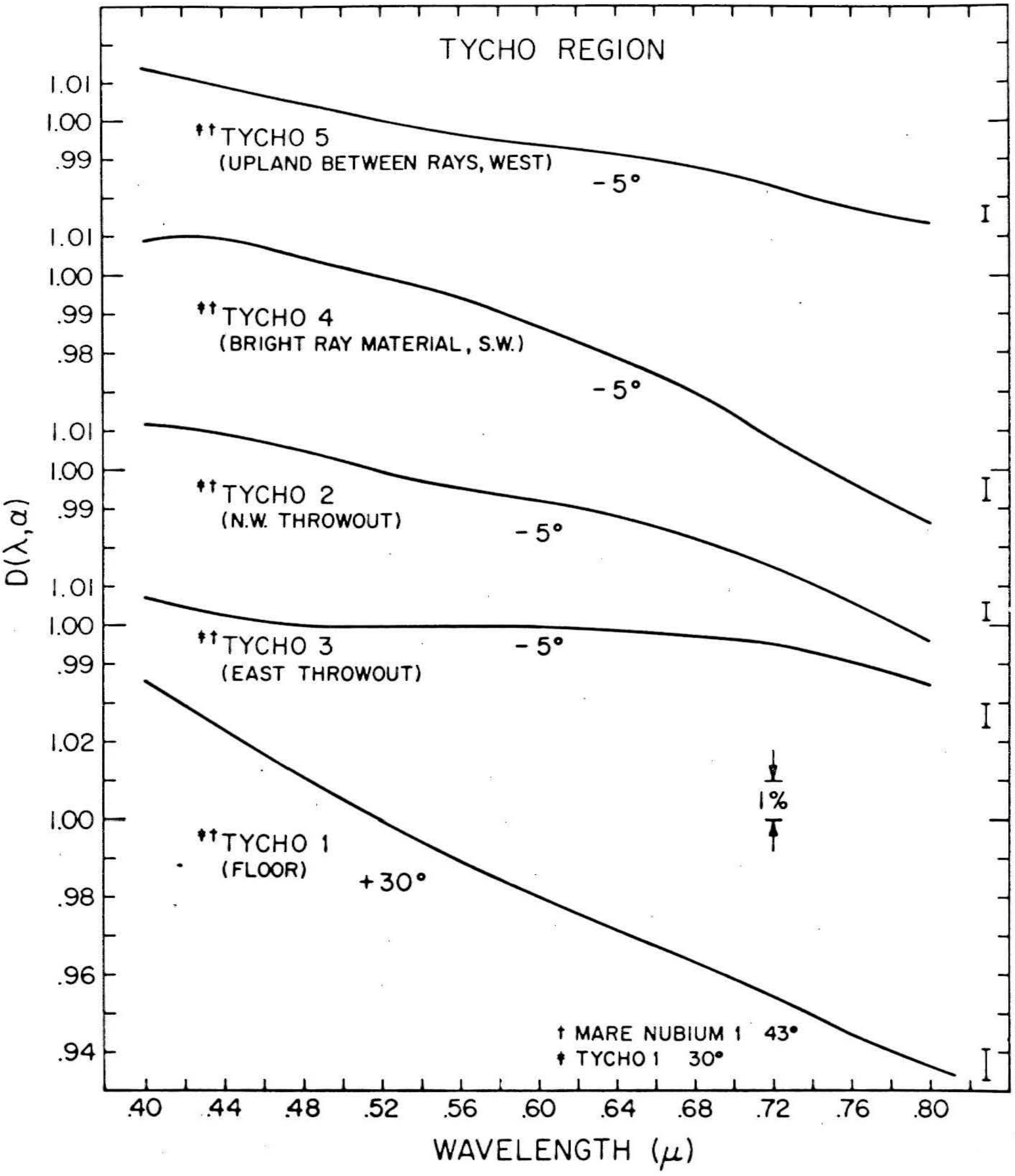
TYCHO REGION
D(λ,α)
WAVELENGTH (μ)
.40
.44
.48
.52
.56
.60
.64
.68
.72
.76
.80
1.01
1.00
.99
‡† TYCHO 5
(UPLAND BETWEEN RAYS, WEST)
-5°
1.01
1.00
.99
.98
‡† TYCHO 4
(BRIGHT RAY MATERIAL, S.W.)
-5°
1.01
1.00
.99
‡† TYCHO 2
(N.W. THROWOUT)
-5°
1.01
1.00
.99
‡† TYCHO 3
(EAST THROWOUT)
-5°
1.02
1.00
.98
.96
.94
‡† TYCHO 1
(FLOOR)
+30°
1%
† MARE NUBIUM 1 43°
‡ TYCHO 1 30°

Figure 20

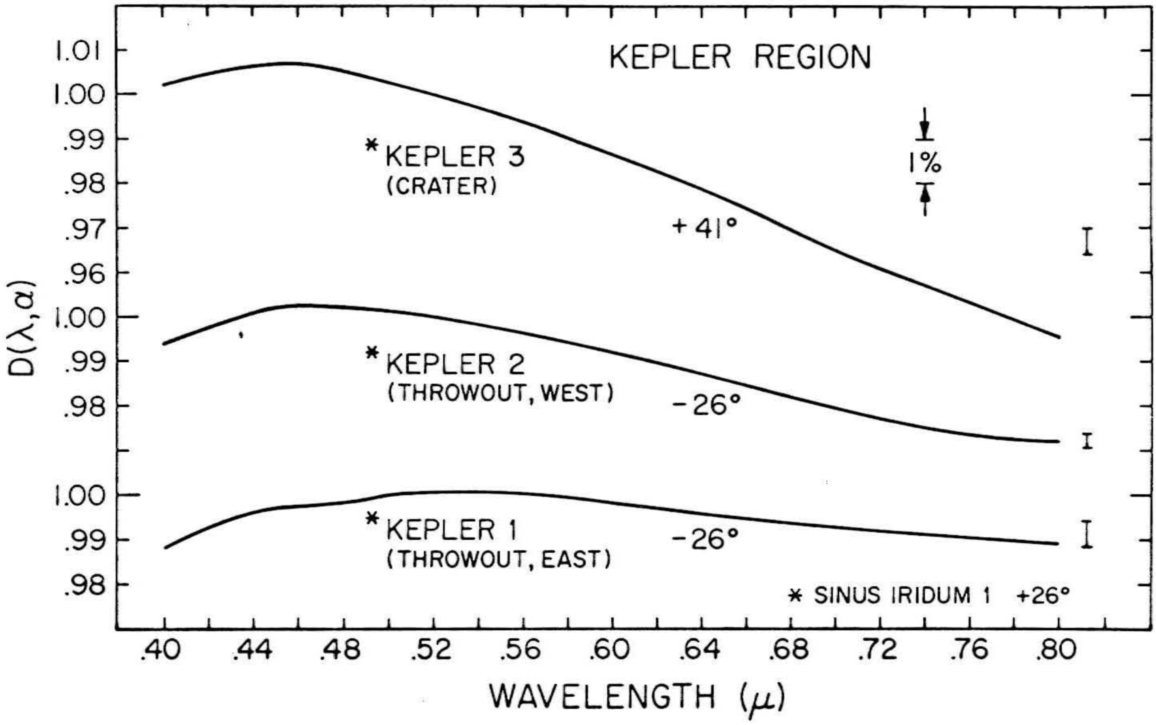
KEPLER REGION
D(λ,α)
1.01
1.00
.99
.98
.97
.96
1.00
.99
.98
1.00
.99
.98
*KEPLER 3
(CRATER)
+41°
1%
*KEPLER 2
(THROWOUT, WEST)
-26°
*KEPLER 1
(THROWOUT, EAST)
-26°
* SINUS IRIDUM 1 +26°
.40
.44
.48
.52
.56
.60
.64
.68
.72
.76
.80
WAVELENGTH (μ)

Figure 21

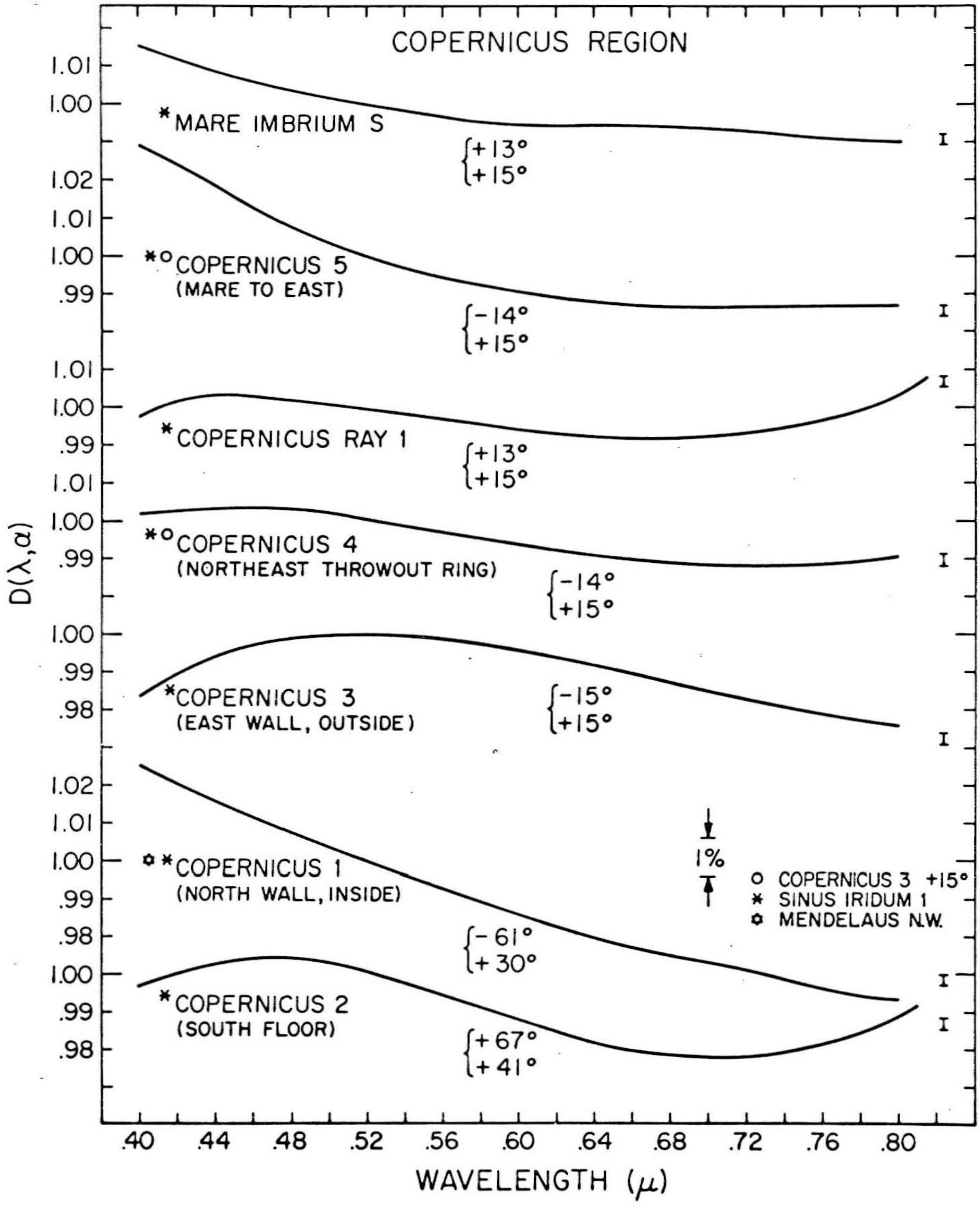
COPERNICUS REGION
1.01
1.00
*MARE IMBRIUM S
{+13° +15°
1.02
1.01
1.00
.99
*○ COPERNICUS 5 (MARE TO EAST)
{-14° +15°
1.01
1.00
.99
*COPERNICUS RAY 1
{+13° +15°
1.01
1.00
.99
*○ COPERNICUS 4 (NORTHEAST THROWOUT RING)
{-14° +15°
1.00
.99
.98
*COPERNICUS 3 (EAST WALL, OUTSIDE)
{-15° +15°
1.02
1.01
1.00
.99
.98
✡*COPERNICUS 1 (NORTH WALL, INSIDE)
{-61° +30°
1.00
.99
.98
*COPERNICUS 2 (SOUTH FLOOR)
{+67° +41°
1%
○ COPERNICUS 3 +15°
* SINUS IRIDUM 1
✡ MENDELAUS N.W.
D(λ,α)
.40
.44
.48
.52
.56
.60
.64
.68
.72
.76
.80
WAVELENGTH (μ)

Figure 22

craters differ.

The Copernicus area is more complicated. The crater floor has an upland-like curve, less evident in the throwout ring and ray. The crater wall is quite different and resembles the mare region just beyond the throwout ring.

It is evident that the color structure of the lunar surface is complex and that the albedo and/or topographic boundaries are not necessarily color boundaries. Similarily, color boundaries are not necessarily accompanied by striking albedo or topographic boundaries.

In two cases a comparison of ray material with nearby mare material was made (Figure 23). The ray north of Bessel in Mare Serenitatis was redder then the darker mare material, however the color curves had the same shape. In the case of a ray north of Copernicus and the nearby Mare Imbrium S. region, a difference in the shape of the two curves appeared with the ray curves appearing similar to the curve for the crater itself.

8. After completing the discussion of the color properties of uplands, mare and bright craters, it is evident that a general law yielding a redder color for a higher albedo does not hold. In fact very bright craters were some of the bluest features observed. The uplands are rather bright but darker mare regions are

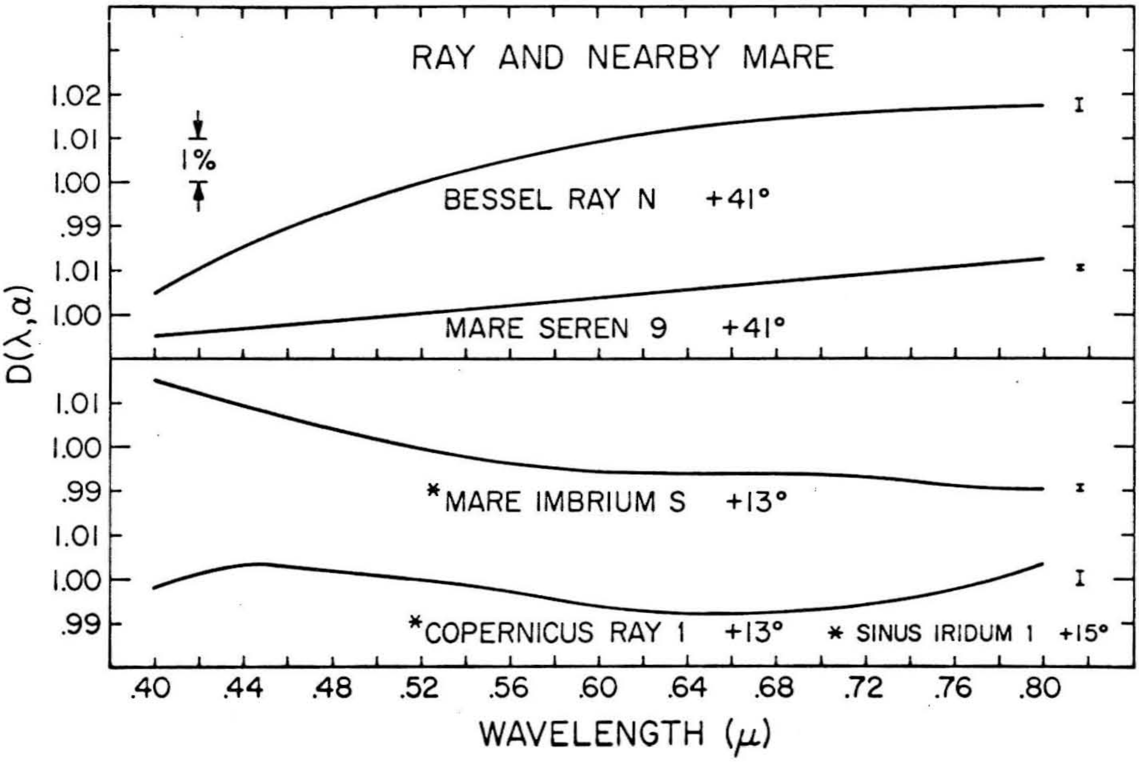
RAY AND NEARBY MARE
1.02
1.01
1.00
.99
1.01
1.00
1.01
1.00
.99
1.01
1.00
.99
1%
BESSEL RAY N +41°
MARE SEREN 9 +41°
*MARE IMBRIUM S +13°
*COPERNICUS RAY 1 +13°
* SINUS IRIDUM 1 +15°
D(λ, α)
.40
.44
.48
.52
.56
.60
.64
.68
.72
.76
.80
WAVELENGTH (μ)

Figure 23

consistantly both bluer and redder than the uplands. Within the mare itself, where the strongest evidence for a reddening law has been gathered, a more careful analysis is required.

The very dark regions generally are quite blue, except for Wood's Spot which is quite red. At other areas such as the dark ring around Mare Serenitatis and at some places in Mare Imbrium a correlation between brightness and redness does seem to hold. In the Plato crater area (Figure 19) there is a general reddening with increasing albedo but in the northwestern Mare Tranquillitatis region (Figure 15) the opposite is true. The crater Plinius formed in this dark mare is lighter than the mare and also redder. However, the brighter ring around the crater Dawes is bluer than the darker surrounding mare material. The entire area, including the bright center of Plinius, is much bluer than nearby Mare Serenitatis. There are also exceptions to the reddening law in the Mare Imbrium region where Sinus Iridum 1 is darker than Mare Imbrium 7 or Mare Imbrium 5 but Mare Imbrium 5 is about the same in color and Mare Imbrium 7 is much bluer than Sinus Iridum 1. Other contradictions occur. Although there seemed to be a trend for darker areas to be bluer in the maria, no definite rule was evident.

Conclusions

From these data it can be concluded that: (1) color differences to 10% occur commonly and differences to 60% have been observed. (2) Differential color changes with lunar phase, with a decrease in color contrast as phase decreases. The change is about 2% to 3%, i.e., a 10% color contrast at 90° phase may reduce to a 7% color contrast at 0° phase. (3) Broad spectral features appear on the spectral curve for some lunar regions. The existence of spectral features centered near 0.74 μ , and 0.44 μ, seems clear, and narrowband spectral features are suggested by some measurements. (4) A lunar luminescence phenomenon larger than about 1% differentially and with band width wider than about 200 Å did not occur commonly during the time the observations were made. (5) There are systematic differences in the reflectivity of regions of differing morphology. Upland regions show the most uniform reflectivity. Bright craters form two groups, with one crater group appearing extremely blue. Mare regions vary in color and are both redder and bluer than uplands. The appearance of band structure on the relative spectral curve is somewhat predictable. It appeared weakly at almost all upland regions, more strongly at very dark mare regions and in moderate strength at the less blue crater areas. Because these data are relative measurements, it is not possible to determine to which lunar area the spectral features belong without having an absolute spectral curve for at least one area. (6) When the entire Moon was considered, a relationship was not found between brightness and the color of areas of the lunar surface. Within the maria there was a tendency for darker areas to be bluer, but many exceptions were found.

Comparison of New Measurements with Other Works

A comparison of the results of this new observational study with those of earlier studies is useful at this point.

It had been firmly established previously that spectral differences in reflectivity exist on the lunar surface. The more accurate studies, such as those of Van den Bergh (1962), Wildey and Pohn (1964), Gehrels, et. al. (1964), Coyne (1965) as well as the present work agreed that the magnitude of the difference in the visible spectral region commonly ranges to 10% with some variations to 20% or higher. In this work several areas differed by more than 50%. A frequency distribution for the red to blue ratio of all lunar areas measured is given in Figure 4.

The observational study reported here is the most accurate study to date and presents the most complete spectral coverage of the extended visible region of a significant sample of lunar surface area. Therefore the shapes of the spectral curves are defined principally by this work. Some relative absorption features such as those existing between the general mare regions and the low albedo mare region could have been detected by previous workers with sufficient spectral coverage. Unfortunately no previous study of differential lunar reflectivity provided such coverage. Thus most earlier work has not been suitable for geologic interpretation. The requirements for future studies are indicated.

In Chapter II it was pointed out that a luminescent phenomenon had been reported to occur on the Moon. An earlier attempt by the present author (McCord, 1967) to observe this phenomenon was unsuccessful except for the possible detection of some activity below 1%. Again in the present study no time dependent spectral features exceeding 1% were noted. In particular the Kepler area, where luminescence had been reported, was measured repeatedly for several months. Existence of a 1% or stronger emission phenomenon occurring during a significant period of time and on a significant portion of the lunar surface is not supported by the studies made by the present author.

A change of color contrasts with phase was found in the present study. The magnitude of the effect is about 2% to 3% for areas of 5% to 10% color difference between 0.4 μ and 0.8 μ, and is in the sense of smaller color contrast for smaller phase angles. All evidence presented by Coyne (1965) indicated no systematic dependence of color contrast on phases greater than about 0.5%. However his measurement spanned only a part (.44 μ to .56 μ) of the spectral range covered by the present study and thus the effect would have appeared in Coyne's data as about a 1% effect. Also, Coyne plotted the measurements at all lunar areas together rather then studying specific areas separately. Thus he diluted the effect for all areas for all areas do not show a phase effect. It seems there is no real contradiction between the results of this study and the earlier studies as far as a phase effect is concerned.

A comparison of measurements made by all previous workers at common lunar areas included in this study might be desirable to check the validity of each group of data, and it would be the first step in a program to collate all existing lunar color data into what might be a useful catalogue. Because of the wide variety of observational techniques and the multitude of forms in which the data are presented, this is a major undertaking and will not be included in this study. However, a comparison of some of the most recent, and presumably most accurate, results can be made rather easily with the measurements presented in Chapter III. Figure 24 is a scatter diagram of the color excesses obtained by Coyne (1965), Wildey and Pohn (1964), Gehrels, et. al. (1964) and Van den Bergh (1962) against those obtained in this study (as calculated from the spectral curves) for those lunar positions measured by more than one observer. The exact location of the areas observed are not always accurately known and, since lunar color has been shown to vary over small distances, some lack of correlation can probably be explained in this way. The correlation is generally within the error (~ 1%) quoted by the authors, indicating general agreement among recent studies. Note that the measurements by each author have not been normalized one to another in Figure 24.

As was pointed out in Chapter II, the two-dimensional nature of a lunar color mapping program surely requires a two-dimensional data gathering technique. One possible technique is the photographic imagery

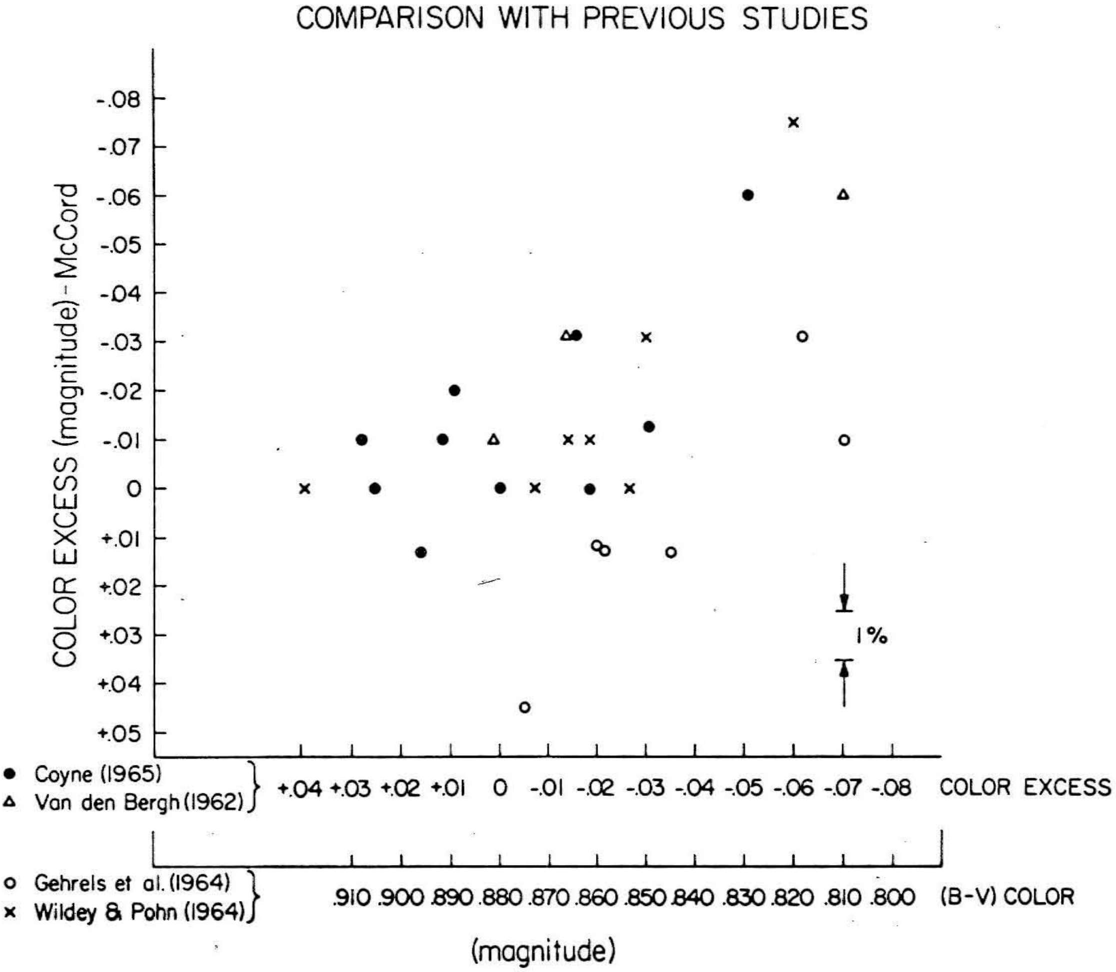
COMPARISON WITH PREVIOUS STUDIES
COLOR EXCESS (magnitude) - McCord
-.08
-.07
-.06
-.05
-.04
-.03
-.02
-.01
0
+.01
+.02
+.03
+.04
+.05
1%
● Coyne (1965)
△ Van den Bergh (1962)
+.04 +.03 +.02 +.01 0 -.01 -.02 -.03 -.04 -.05 -.06 -.07 -.08
COLOR EXCESS
○ Gehrels et al. (1964)
× Wildey & Pohn (1964)
.910 .900 .890 .880 .870 .860 .850 .840 .830 .820 .810 .800
(B-V) COLOR
(magnitude)

Figure 24

method also discussed in Chapter II. To determine the reliability of the existing data obtained by this method, and then to get an idea of how useful this technique might be, a comparison was made of several color-indicating photographic images with the photoelectric data present in this dissertation.

Photographs by Whitaker, Wright, and Scott (Appendix I) were considered. A number of lunar regions of differing colors were chosen and the results of the three photographs and of the photoelectric program were compared. Table 3 gives the results for the Mare Imbrium area. There is general agreement for larger (5%-10%) color differences but some contradictions arise for smaller differences. Part of the difference in the data may be due to different color normalization levels for each photograph and to the lack of quantitative information in the images.

A further comparison of these works for the Mare Serenitatis area indicates general agreement with photoelectric measurements, except for Whitaker's photograph which erroneously shows Le Monnier to be bluer than the center of Mare Serenitatis. Whitaker's photograph also shows Mare Crisium to be bluer than Mare Serenitatis, a result not found in the present author's study.

Comparison of Photographic Imagery with Photoelectric
Measurements for the Color of the Mare Imbrium
Area Compared to Extreme Southern Sinus
Iridum

	McCord's Spot Number	Whitaker	Wright	Scott	McCord (p.e.)
Mare Imbrium	2	B	B	B	B (10%)
	6	B	B	B	same or slightly redder
	5	B	B	B	same
	7	B	B	B	B (14%)
	3	B	B	B	B (11%)
	4	R	R	R	B (1%)
	N	same	same	R	R (2%)
	S	B	B	B	B (10%)
Sinus Iridum	3	same	R	R	R (2%)
	4	R	unclear	B	R (2%)
Mare Frigoris		B	same	same to red	B (3%)
Sinus Roris		B	B	B (?)	B (3%)
Upland	9	R	same	same to red	R (6%)
Upland	1	same	bright	bright	B (5%)

Table 3

The lack of dynamic range in the photographic process is made evident by considering the color variation between uplands and most mare regions. The photoelectric data showed very little difference between these regions but the photographs showed either very great differences or only bright regions, with perhaps the exception of Whitaker's work.

Some recent work by Adams (unpublished data) indicated that the photographic imagery method might be improved to give 1% accuracy, but the published photographs are not consistent to that accuracy. Efforts to improve this potentially very useful technique should certainly be continued.

IV. INTERPRETATIONS

Compositional Implications

Color differences on the lunar surface have been interpreted as indicating compositional differences, age differences, particle size differences, or a combination of these effects. The complete absence of an aging (weathering) phenomenon, such as radiation effects and/or solar wind contamination (Hapke, 1966; Nash, 1967), probably can not be proven until onsite samples are analysed. Particle size variations quite possibly do modify the spectral curves if the particle size is very small (Adams and Filice, 1967; Adams, 1967).

It is argued here that lunar color contrasts are due primarily to compositional differences, although particle size variations and aging processes may modify the spectral curves somewhat. This argument is based on the size and location of color contrasts and the variation in the shape of spectral curves for various lunar areas.

The seven bright craters for which spectral curves were obtained in this study, form two distinct color groups; Tycho, Plato B, and Aristarchus (Figure 17) are very blue features with a relative red to blue ratio of from 0.902 to 0.776, no spectral features appear in the spectral curves for these craters, although a decrease in slope occurs in the red. Copernicus, Kepler, Proclus and the bright feature west of Reiner in Oceanus Procellous (Figure 18) have red to blue ratios within 4% of unity and a clear hump appeared in their spectral curves in the blue, with the suggestion of another feature in the red. These craters are all youngish appearing features; some of each group occur in the uplands and some occur in the maria; they vary in size and are widely distributed. There is nothing apparent to distinguish the groups except their spectral curves. It would seem that had all crater sites been composed of the same material, both aging processes and the mechanism generating particle size distributions should have operated equally, or at least not in this selective way, at all sites. The conclusion is drawn, therefore, that two different compositions exist and that the spectral curves reflect this basic difference.

The spectral curves for upland regions showed little variation from place to place except a reddening in the Apennines region. The red to blue ratio, again relative to the standard area, is very nearly unity. This uniformity suggests either uniform composition with uniform (or large) particle size or that an aging process operated and has reached saturation in these apparently ancient regions. The presence of the shallow minimum in the red and a maximum in the blue in the spectral curves for all upland regions, if a property of the upland material and not of the standard area, indicates uniform composition of the surface layer, since particle size effects do not include the creation of absorption features. The other alternative is that the absolute spectral curve for the uplands is featureless and the shape of the relative curve is due to the properties of the standard area in Mare Serenitatis. In this case, very little can be said other than to remark on the uniformity of the reflecting properties of the upland regions. Material presented later in this dissertation will make this second alternative less likely.

Within the maria a wide variety of colors exist. This indicates again that, if an aging process operates to destroy color contrasts, it has not yet reached saturation in most maria areas. The lack of a firm relation between color and brightness argues against a change in particle size explaining all the color differences, since a change in the red to blue ratios is accompanied by a change in albedo where the particle size distribution is the controlling factor. For example, compare the red-colored dark region called Wood's Spot (Figure 13) with the blue-colored dark regions in Figure 14. Both areas appear "young" and have low albedo but they are quite different in color. Their spectral curves are also different in shape with a strong minimum appearing in the curves in Figure 14. It is difficult to explain these differences except by assuming compositional differences.

If it is granted that color differences are primarily indicative of compositional differences, then variations of color over short distances and in a complex way over entire maria indicate a complex geologic history for the Moon. In addition, the difference in the reflectivity curves of bright craters from those of the surrounding regions and the variation of the reflectivity curve from crater floor to crater wall to crater throw-out at Copernicus indicates a stratified or compositionally layered structure for regions of the Moon. Perhaps this structure is quite different from the visible topography.

Appearance of structure in the spectral curves which varies across the lunar surface is extremely important, for it strongly suggests that composition and mineralogy of rocks composing the lunar surface is directly affecting these curves. Effects proposed for aging or modifying the lunar surface layer will tend to degrade the spectral curve structures, none would seem to create structure in the curve. The conclusions to be drawn are: (1) that an aging or weathering mechanism has not acted to completion on the lunar surface, including the apparently ancient upland regions, or there is a competitive erosion process operating which exposes new material; (2) that since the spectral curve shape changes from lunar area to lunar area so must the composition change; (3) that these spectral features might be used to determine to some extent the composition of the lunar surface.

Absolute Spectral Curves and Interpretation of Broad Band Spectral Features

Determination of the composition of the lunar surface is not possible from data presented thus far. However, recent laboratory work (Adams, 1968; Adams and Filice, 1967; Hovis and Callahan, 1966) indicated that it may be possible to determine the general composition of the lunar surface by using the shape of the reflectivity curves between 0.4μ and 2.5μ. They reported that characteristic absorption bands due to electronic transitions in transition metal ions appeared in the reflection spectrum of powders and that these bands are diagnostic of general classes of rock-forming minerals. The lunar data just presented in the present report show that broad absorption features do appear in the lunar spectral curves and can be well defined if measurement accuracy is better than 1%.

To interpret these spectral features in terms of composition, it is necessary to use an absolute spectral reflectivity curve for at least one lunar area measured in the present study. Such a spectral curve was obtained by R. Younkin (unpublished data) for the center of Plato. Using standard stars to obtain the spectral response of the telescope-instrument-detection system and a measured spectral energy distribution of the Sun, he obtained reflectivity curves for the region 3125 Å to 11125 Å A red sensitive and blue sensitive photomultiplier were used, yielding two sets of data. The red cell data were obtained on the night of 02/18/65 U.T. and the blue cell data were obtained on 02/13/65. The lunar phase angles were $+33^{\circ}$ and -34° respectively. The data are shown in Figure 25 for the spectral region of interest in the present study. The data will be presented in full by Younkin in a future publication. The reflectivity values have been normalized arbitrarily to unity at 0.527μ . The mismatch in slope of the red cell (circles) and the blue cell (dots) measurements is probably artificial and the slope of the reflectivity curve is probably linear from at least 0.4μ to 0.82μ (Younkin, private communication). Certainly the red cell measurements follow a straight line with no systematic departure less than 1% over a band width greater than .04 μ . The blue cell data show some narrow band irregularities (to be discussed by Younkin) but no broad features greater than about 1% appeared in this wavelength interval.

The relative reflectivity of the center of Plato (Plato C) and the standard area (Mare Serenitatis 2) is given in Figure 13. This curve was obtained by using an intermediate standard (as explained elsewhere in this chapter), and therefore it could be assumed to be unreliable. However, the curve was also obtained by using a different secondary standard, with an identical curve resulting.

The relative curve is a straight line to about 0.52 μ and then smoothly deviates from a straight line between 0.54 μ and about 0.64 μ . The curve is almost horizontal beyond 0.64 μ, indicating no color differences in this spectral region. From this information the absolute reflectivity of the standard area was calculated and is shown as a dashed line in Figure 25. A very shallow minimum appears in the absolute curve, with center near .56 μ, (ignoring the artifical mismatch of the two sets of data) but no absorption bands appear. Therefore the spectral features which appeared in some of the relative spectral reflectivity curves apparently are

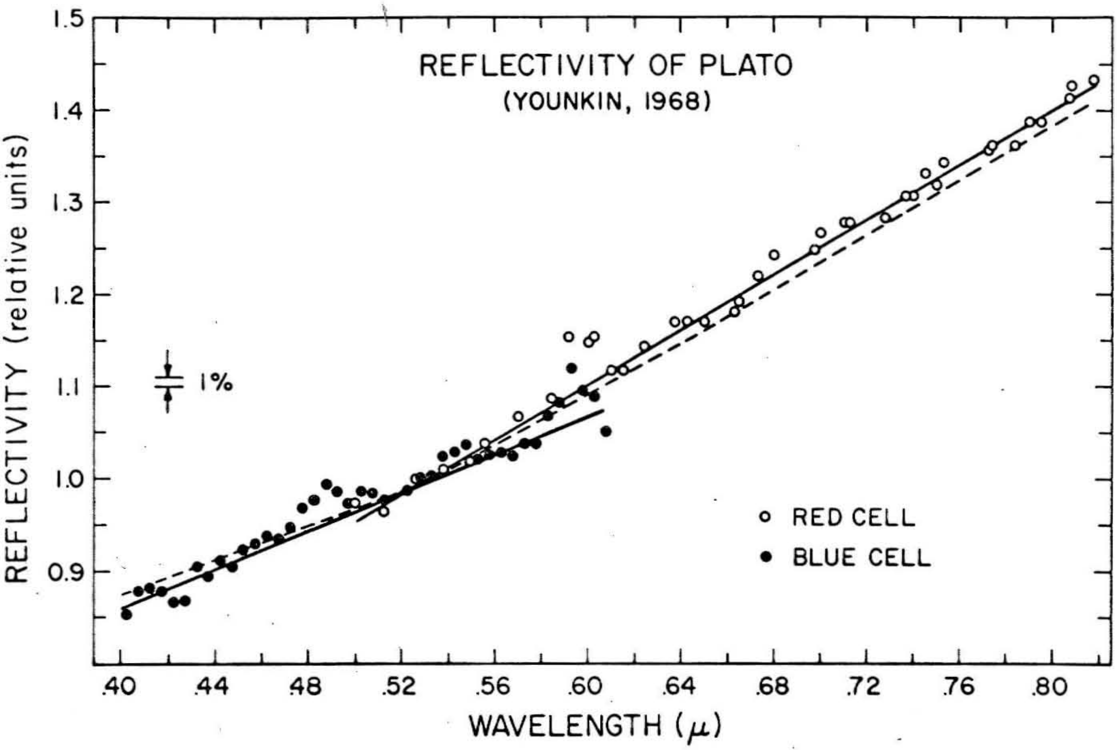
REFLECTIVITY OF PLATO
(YOUNKIN, 1968)
REFLECTIVITY (relative units)
1.5
1.4
1.3
1.2
1.1
1.0
0.9
1%
○ RED CELL
● BLUE CELL
.40
.44
.48
.52
.56
.60
.64
.68
.72
.76
.80
WAVELENGTH (μ)

Figure 25

a result of the reflecting properties of the individual areas and not of the standard area. For example, the minimum that appeared in the curves for the very low albedo mare areas (Figure 14) should be interpreted as an absorption band, in the reflected spectrum of these areas. The regional assignment of the spectral features found in all upland curves is somewhat less certain because of the amplitude of the features (a few percent), but all evidence suggests they are a property of the upland region. The following statements can now be made based on the data presented and the absolute reflectivity curve for Plato. (1) The basic color of all lunar features observed is red; some features are redder than others. (2) Reflectivity curves for all very low albedo mare areas measured, except for Wood's Spot, contained a broad absorption band centered between .68μ and .74μ with a depth of 5% to 10%, depending on the shape of the curve beyond .82μ. (3) A few other mare areas showed a similar but much shallower band. (4) A few mare areas, the reddest areas, showed a reflectivity maximum between about 0.6μ and 0.72μ. (5) All upland areas possessed a red absorption band centered in about the same region. (6) One group of bright craters showed local reflectivity maximum at about 0.44μ to 0.50μ with the possibility of an absorption feature in the near infrared. (7) The other bright crater group showed the least increase in reflectivity toward longer wavelength of any area observed (except for the anomalous Cobra Head region) but no absorption features were evident.

The presence of these absorption features apparently indicate that by using ground based observational techniques, it is possible to observe effects that are controlled by the crystal structure and composition of the minerals composing the lunar surface. Certainly it indicates that the surface is not covered with a substance such as a sputtered metallic coating that would mask these spectral features. Because this particular observational study did not include the near infrared portion of the spectrum, where spectral features may be more diagnostic, it is not possible to make a definite determination of the composition of the areas showing the absorption features. Also, because of the mineralogic complexity of some rocks, it may not be possible to definitely determine the exact rock type at a certain lunar location, even if a complete and accurate spectrum were available (Adams, private communication). However, a determination of general rock type and major mineral constituents should be possible, thereby limiting the possible range to geologically useful bounds.

Using spectral reflectivity curves for silicate

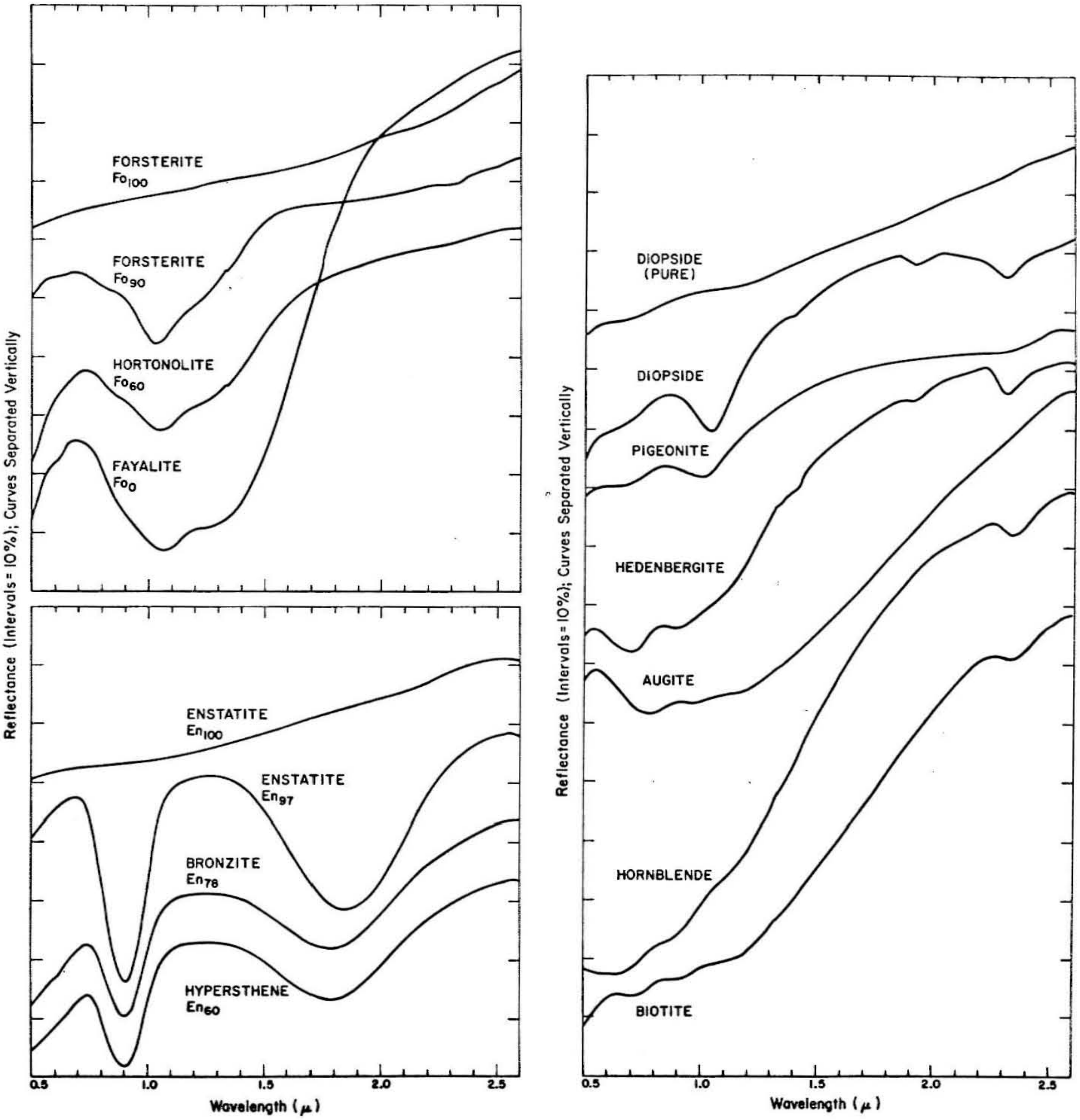
Reflectance (Intervals = 10%); Curves Separated Vertically
FORSTERITE
Fo$_{100}$
FORSTERITE
Fo$_{90}$
HORTONOLITE
Fo$_{60}$
FAYALITE
Fo$_{0}$
ENSTATITE
En$_{100}$
ENSTATITE
En$_{97}$
BRONZITE
En$_{78}$
HYPERSTHENE
En$_{60}$
0.5
1.0
1.5
2.0
2.5
Wavelength (μ)
Reflectance (Intervals = 10%); Curves Separated Vertically
DIOPSIDE
(PURE)
DIOPSIDE
PIGEONITE
HEDENBERGITE
AUGITE
HORNBLENDE
BIOTITE
0.5
1.0
1.5
2.0
2.5
Wavelength (μ)

Figure 26

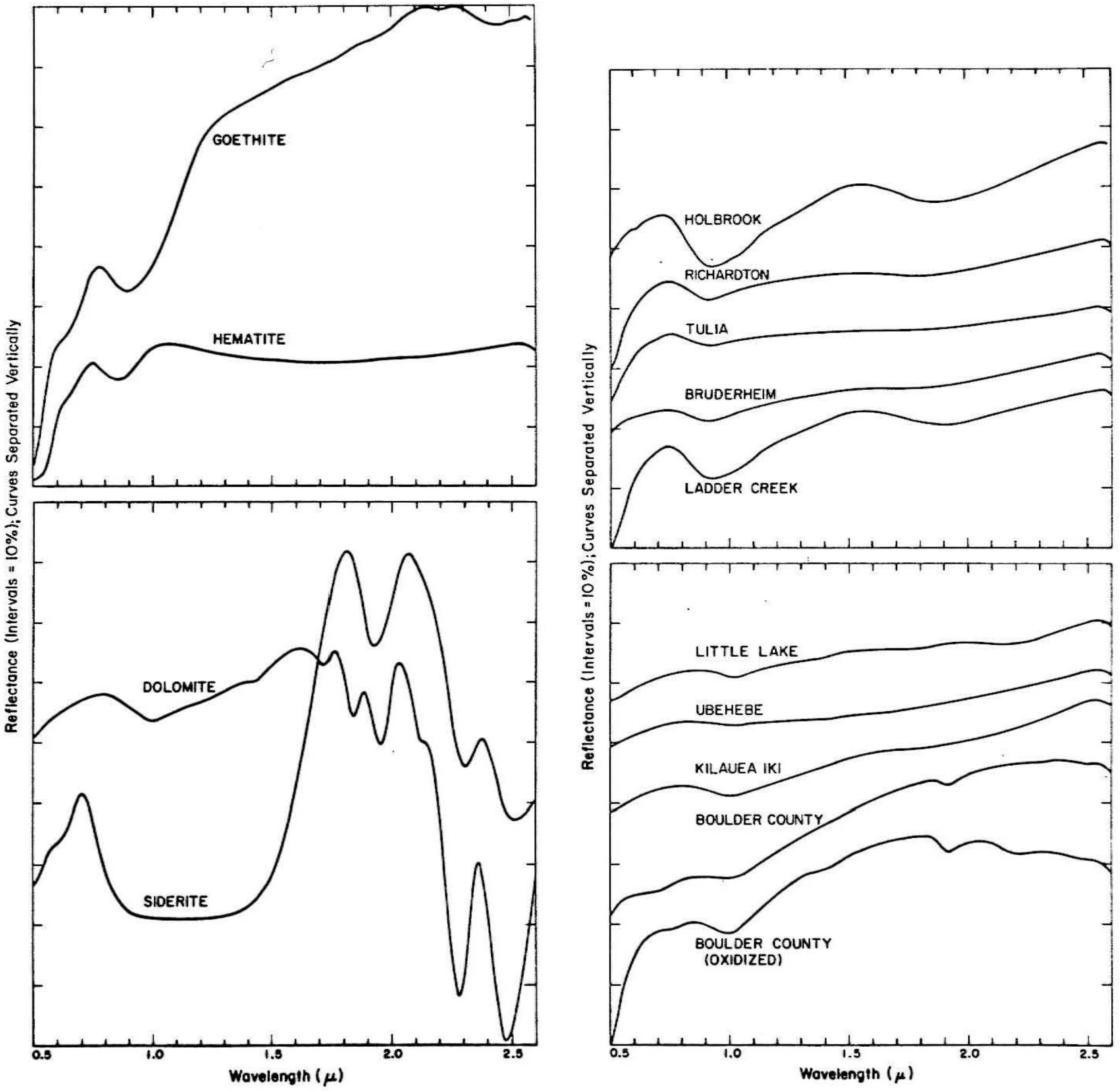
GOETHITE
HEMATITE
DOLOMITE
SIDERITE
Reflectance (Intervals = 10%); Curves Separated Vertically
0.5
1.0
1.5
2.0
2.5
Wavelength (μ)
HOLBROOK
RICHARDTON
TULIA
BRUDERHEIM
LADDER CREEK
LITTLE LAKE
UBEHEBE
KILAUEA IKI
BOULDER COUNTY
BOULDER COUNTY (OXIDIZED)
Reflectance (Intervals = 10%); Curves Separated Vertically
0.5
1.0
1.5
2.0
2.5
Wavelength (μ)

Figure 27

minerals and rock powders as measured by Adams and Filice (Adams and Filice, 1967; Adams, 1968) (Figures 26,27) it is possible to make some suggestions as to the minerals and elements most likely to cause the observed lunar spectral features.

The absolute spectral curve for the standard area in Mare Serenitatis (Figure 25) showed no departure from linearity except a slight bend near 0.56μ . On the basis of the laboratory measurements, the possible constituents of the standard area are forsterite, enstatite or diopside, in other words iron poor olivine, orthopyroxene and clinopyroxene, respectively, or also "basalt". It may be very important however that even a fairly small amount of opaque grains such as magnetite, if present, will smooth the spectral curve to a relatively straight line (Adams, private communication). Therefore, a smooth spectral curve is somewhat ambiguous. A basaltic composition for areas having curves similar to Mare Serenitatis is consistent with these data.

The absorption feature near 0.74μ, which appears especially strongly at the low albedo mare areas and weakly in the uplands, is a more unique feature in that it is consistent with only one class of minerals studied by Adams: the calcium-iron-bearing clinopyroxenes such as augite, hedenbergite and possibly pigeonite.

The maximum in the lunar spectral curve near 0.50μ may be caused by titanium which can produce structure in the spectral curve at shorter wavelengths (Adams, private communication).

Two other pieces of evidence of the mineralogy and composition of the lunar surface are (1) the results of the alpha-scattering experiments carried by Surveyor V and VI and (2) the composition of basaltic achondrite meteorites. The petrology of eucrites, howardites and mesosiderites (basaltic achondrites) has been discussed by Duke and Silver (1967). They suggested that these objects may have a lunar origin. Results from the α -scattering chemical analysis experiment carried by Surveyor V (Turkevich, Franzgrote and Patterson, 1967) indicated a composition for the Surveyor V landing site (a dark mare area) consistent with that of basaltic achrondrite meteorites. Major constituents of eucrites are pigeonite, sub-calcic augite and ferroaugite, with small amounts of titanium. Although it is not possible to draw frim conclusions at this stage, the evidence at hand is at least consistent with the existence of a calcium bearing mineral containing some titanium such as some from of augite, or perhaps a less calcium rich pigeonite. A material containing abundant opaques, such as some basalts, or an extremely iron-poor mineral, or the predominance of particles smaller than 10μ is suggested for the lunar regions showing a smooth spectral curve. Extending the spectral curves into the infrared may eliminate much ambiguity, and with the possibility of calibrating these curves to returned lunar rock samples an earth-based lunar compositional mapping program should be effective.

Phase Effect

The discovery of a differential color-phase effect should not have been unexpected, although it was not predicted. Gehrels, et. al (1964) published polarization curves as a function of lunar phase in three colors (0.36μ, 0.54μ, 0.94μ) for seven lunar areas. The polarization is greatest at large phase angles and decreases to zero at about $\alpha = 23^{\circ}$; it then becomes negative, reaching a minimum near 10° and returns to zero at $\alpha = 0^{\circ}$. The degree of polarization depends on wavelength and is greater at shorter wavelengths. Different lunar areas showed different polarizations. The polarization curves can be reproduced using Fresnel's reflection laws. The polarization implies a selective absorption of one component of the electric vector and results in a decrease in the light intensity in one polarization plane. Since this intensity decrease varies

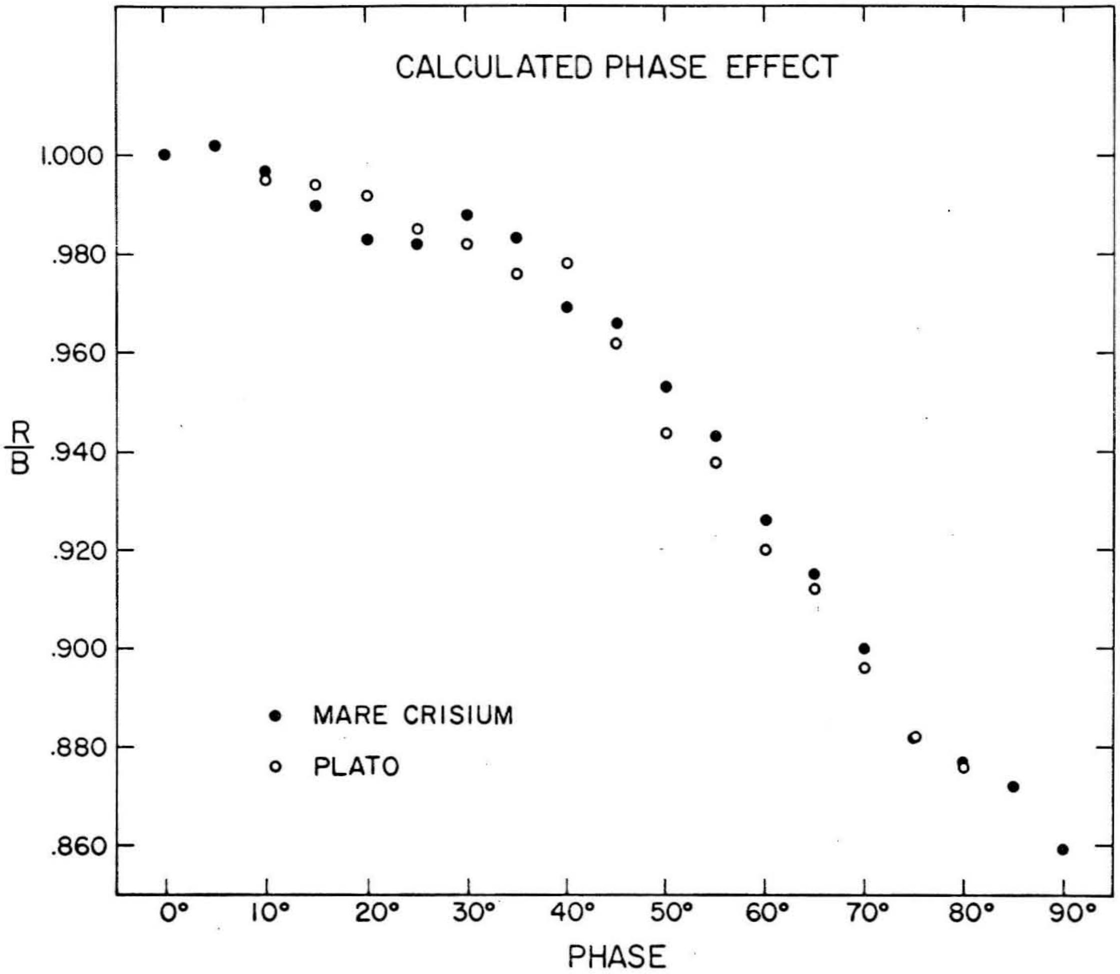
CALCULATED PHASE EFFECT
1.000
.980
.960
.940
.920
.900
.880
.860
R/B
● MARE CRISIUM
○ PLATO
0°
10°
20°
30°
40°
50°
60°
70°
80°
90°
PHASE

Figure 28

with wavelength and lunar area as well as with phase, differential color must vary with lunar phase as the polarization (absorption) varies. Values taken from Figure 7 of Gehrels, et. al. (1964) were used to compute the expected color-phase effect, and a plot of the maximum expected change of the red to blue ratio between 0.36 μ and 0.94 μ for two cases is shown in Figure 28. This plot is similar to the plot of the measured change in the red to blue ratio between 0.4 μ and 0.74 μ (Figures 8-10) The size of the calculated effect is larger because the case of maximum effect was considered. The decrease in color contrast with a decrease in phase angle is clear. The calculated color-phase effect curve does not have the shape of the measured curve, however. This could indicate the operation of a second mechanism which retards the color contrast decrease until smaller phase angles are reached.

A possible mechanism is one that would be expected to operate on a surface covered with fine grains of material such as has been shown to exist on the lunar surface. The grains must have an opacity and size such that a significant amount of light incident can traverse one or more grains.

Light returned by a lunar surface area can be considered to have two components: light reflected from the first surface of a mineral grain (I_1), and light reflected from a second grain after passing through the first grain (I_2). The light I_1 will have certain polarization properties; light I_2 will have polarization properties tending to cancel the properties of I_1. In addition, I_2 will have spectral properties imposed while traversing the first grain which I_1 will not have, and these imposed spectral properties will reflect the composition of the mineral grain. The relative amount of I_2 present will decrease with decreasing phase angle, for the probability of a second reflection returning light to space decreases as the angles of incidence and reflection become the same. The net effect would be to increase color contrasts at large phase angle. When only polarization is measured the total color effect, including that due to the transmitted light, is not observed.

This mechanism would explain the differences between the observed color-phase effect and that calculated from the polarization data. Furthermore, it suggests once more that compositional differences in lunar surface material are the primary cause of color differences.

V FUTURE STUDIES

There are several complementary studies that should be undertaken to further define the properties of lunar color variations and of the lunar surface. A study of the color-phase effect would be useful as would a more careful analysis of the color-brightness relation. The most useful observational program would be one designed to extend the measurements through the near infrared spectral region. Such measurements should reveal the presence of more absorption features which will probably be more diagnostic of lunar composition. The accuracy requirements are probably as strict as in the visible region, and the spectral resolution should be at least 0.05μ . Because of large atmospheric transmission variations in the near infrared region, differential measuring techniques are required.

The possibility of using the photographic imagery method for recording and presenting the lunar color data for geologic mapping should be explored further. Two-dimensional electronic intensity measuring devices may be the ultimate answer to this requirement because of their speed, dynamic range, data handling flexibility and possible accuracy.

APPENDIX I

LITERATURE ABSTRACTS

Investigations of spectral reflectivity differences across the lunar surface are listed here in abstract form according to the observational method used. Each observational method is described before the associated data are discussed.

Qualitative Visual Observations

One method of studying the color of the lunar surface has been to simply look at the Moon through a telescope and describe the colors as perceived by the observer. This has been a popular method, especially among amateur astronomers, because of the simplicity of the equipment required. However, results are far from quantitative and the descriptions vary with the individual color characteristics of the observer's eye and his telescope.

There are two general results that can be stated concerning these qualitative visual observations. (a) Color differences were seen by almost all observers. The differences often agreed with the major results found by using more exact methods, but many more and contradictory color features were also reported. (b) Colors were said to change both throughout the lunation and on longer time scales. Terminator and limb effects were often reported.

For a review of this literature and a list of major references, the interested reader should see Fielder (1957) and Firsoff (1958).

Quantitative Visual Observations

The more quantitative method of making visual observations utilizes a standard light source with which the object of interest is compared. The instrument that has been used almost exclusively is the Rosenberg blue wedge colorimeter (Rosenberg, 1921; Radlova, 1941). When using this instrument the region of the Moon to be measured is visually matched in intensity, by adjusting a standard lamp, and matched in color, by manipulating filters, to an illuminated comparison field. The filter setting required to accomplish a match yields a standard color index by using a calibration scale. This calibration scale is determined by measuring many standard stars. The internal consistency of the measurements made by this method seems to be very good, about 0.01 magnitude (1%) for one observation. However, the accuracy over several nights with different observers is nearer 5% to 10% (Sharonov, 1962), this being partly due to changes in atmospheric transparency.

By this method, point measurements are made and one color parameter, the standard color index, is produced. A comparison of the color indexes for various lunar areas observed gives a measure of relative redness or blueness of an object in the visible region of the spectrum. However, it tells very little about the actual structure of the spectral reflectivity curve.

One advantage of this method is the rapidity (10 measurements per minute) with which a lunar region can be surveyed for relative color.

The first quantitive visual study of any importance was that by Wilsing and Scheiner (1921) which utilized a standard lamp and a prism. In two series of observations beginning in 1908 they compared the brightness of 6 lunar areas at 10 spectral intervals between 4510 Å and 6420 Å and 2 lunar areas at 5 spectral intervals between 4480 Å and 6380 Å. They also observed 47 terrestrial rock samples in an attempt to determine the composition of the lunar surface. Their data, presented as color temperatures, have been reworked by Sharonov, (1956) and were presented by him as reflectivities at each effective wavelength. The mean quadratic error of the measurements is given as about 5%. A plot of the spectral curves according to Sharonov's values showed a general reddening of some areas with respect to other areas. The curves also exhibited humps of as much as 20% which are not consistant with later work. The main conclusion stated was that the lunar reflectivity differences were not conspicuous enough to allow a determination of its composition, but a lava character was nevertheless suggested for the maria. Perhaps for the first time, a correlation between redness and brightness was mentioned.

The visual studies of lunar chromatic reflectivity variations were made using the Rosenberg photometer. Rosenberg (1921) measured the visual brightness of the same lunar spots which Goetz (1919) measured photographically. Rosenberg combined the measurements of 55 lunar areas and subtracted the magnitudes to form a color index. Although the errors were too great to determine the precise color index of any particular spot, a group of red reflecting and blue reflecting areas were determined and were found to be in agreement with the two-color photographic images produced by Miethe and Seegert (1914). It was also pointed out that the red reflectors were brighter than the blue reflectors.

Fessenkoff (1929) obtained the color temperatures of 8 maria. All maria were first compared to Mare Tranquillitatis and then this locality was compared to different stars and to Jupiter. A maximum of 310 degrees color temperature difference (about 10%) was found and a general agreement in the color of the maria with earlier data was apparent. Unfortunately, the exact spots observed were not given and the error for each measurement was not estimated.

More careful use of the Rosenberg blue wedge visual photometer was made by Radlova (1941) when she observed 35 lunar regions as well as some terrestrial rock samples. Her measurements were given as color indexes. Measurement error was given as ± 0.06 magnitude for one reading or ± 0.01 to ± 0.02 magnitude for an average of several measurements. The range of color indexes for the Moon was found to be 0.21 magnitudes, corresponding to a temperature range of 770 degrees. This was a much smaller range than that found for terrestrial minerals. The same was found for the brightness range. She compared her results with the Miethe and Seegert pictures and found good agreement. Radlova also investigated the color-brightness relation found by earlier observers and found that, although the brighter regions were redder, the darker regions exhibited the full range of colors.

Sharonov (1955) reported on a series of visual measurements he made between 1953 and 1955 at full moon. He found only a few noticeable color differences and concluded that the maximum differences in color on the Moon's surface were approximately equal to the threshold of the color distinction of the eye and certainly did not exceed a standard color index range of ± 0.05 magnitude. No data were given in this report by Sharonov.

A combined visual-photographic study was made by Radlova (1961) using plates made in 1939 and visual observations made in 1956. She investigated the color variations along some bright rays of the craters Tycho, Copernicus and Kepler. Her data were given as standard color indexes at various distances from the crater centers. The visual observations showed that the differences in the color of the rays was not much more than the range of random error, which was given a ±0.01 magnitude. Nevertheless, within this range the color index showed a systematic variation with the distance from the crater center. She reported that this variation was different for different craters.

Sharonov (1962) used an improved version of the blue wedge photometer to visually measure 115 lunar details. The color excess, defined as the difference in the color index of the sun and the lunar area, was tabulated. The error was given as ± 0.038 magnitude and was defined as rms error for measurements made in different months; this, he stated, is a more realistic error for the blue wedge technique. The most extreme color difference found was 0.11 magnitude. The lunar areas measured corresponded to those of Sytinskaya (1953), who measured the albedos of those spots. Thus a check of the color-brightness relation could be made. A plot of color versus albedo showed a triangular distribution with the base of the triangle along the color axis of the plot. This confirmed Radlova's statement that the dark regions contain all colors while the bright regions were mostly red. A comparison (performed by the present author) of the color excesses measured by Sharonov with those measured by Radlova (1941) at the same lunar positions showed a strong correlation within the measurement accuracy quoted by the two observers.

Imagery

The method of photographic imagery involves the production of an image or images which give a visual display of color differences. There are several ways to accomplish this. One is simply to photograph the Moon through two different filters and then examine the two images for contrast differences. Two regions of the Moon that have equal reflectivity in one filter range and different reflectivity in another filter range will show no contrast in one image but will show a contrast in the other image. If the two photographic plates have been adequately calibrated, quantitative data can also be obtained from the plates; the method which uses the plates to obtain quantitative data is called photographic spectrophotometry.

Additional processing of the photographs taken in two spectral regions can result in the presentataion of the color contrast in one image. This is extremely useful for displaying results that can be visually interpreted easily and rapidly. However, the display is purely qualitative and subject to systematic errors. A major difficulty is the small linear dynamic range inherent in the photographic process. For the small color contrasts which must be detected, a range of a factor of two in source intensity is probably the limit for accurate comparitive work. Also, photographic emulsions have different intensity-to-density constants (so-called plate gamma) even in the linear region; this can produce additional error when combining images made in different spectral regions.

Wood (1912, 1914) was the first to announce a photographic imagery study. He photographed the Moon through a thin silver film which only transmitted light shorter than about 3100 Å. This work revealed a dark region near Aristarchus which is now known as Wood's Spot. A later series of photographs made in three spectral regions (3100 Å, what he called violet, and yellow) showed more differences in the spectral contrasts of lunar features. This simple but effective study demonstrated the existence of several colored regions on the Moon. In addition, Wood studied mineral samples and concluded that a mineral containing only a very small amount of sulphur would produce such UV-absorbing features as Wood's Spot. No photometric calibration of the plates was reported.

Shortly after Wood began his work, Miethe and Seegert (1911;1914) reported a photographic study using the two spectral intervals 3300-3600 Å and 6000-7000 Å. They produced photographic images of the Moon in each region and then superimposed the two images on a screen after passing the projecting light beams through complementary colored filters. Any color on the screen showed differences in the density of the photographs. In their work they reported confirming Wood's Spot as well as finding other color features. In producing this print, an attempt was made to standardize the individual negatives to prevent spurious density differences from effecting the results. An attempt was made (1914) to photograph at the still shorter wavelengths used by Wood. Problems with the telescope mirror reflecting surface prevented complete success, although much of their earlier work was confirmed.

Miethe and Seegert were the first to report a dependence of lunar color contrasts on lunar phase. They stated that Mare Tranquillitatis did not assume its full "green" color until full moon but that Mare Serenitatis appeared "red" even at early phase. The lack of color at lunar sunrise, they suggested, might be due to a shadowing effect.

The first reported attempt at using direct color photography was made by Hargreaves (1924). He used "Agfa Farbenplatten" with several filters to photograph the Moon through a refracting telescope. His work was troubled by carelessness and a lack of standardization but he did report confirming the color differences between Mare Serenitatis and Mare Tranquillitatis as well as several other features. No plate was published.

Wright (1929) produced photographic images of the Moon through 6 filters. He published a series of very sharp images made through the two extreme filters (3600 Å, 7600 Å). The plates were also calibrated by using a density wedge, a procedure he found imperative for quantitative or even serious qualitative work. A set of positive copies that were suitable for accurate comparative study were produced. A large number of color contrasts with much detail were noted on these prints and most of the color features reported in earlier works were confirmed.

Recently N. Scott (personal communication,1967) prepared a three color "marked" print from Wright's original negatives, according to a process described in his publication (Scott, 1964), which shows quite plainly the density differences in the negatives. An abundance of color detail is evident.

In 1952 Barabashov (1953) obtained color photographs of the Moon showing color contrasts in the range 5% to 15%, according to his report. He also stated that the uplands are easily seen to be different in color from the maria. The color features gave qualitative agreement with earlier work.

N. Scott (1964), a professional photographer and amateur astronomer, used several photographic methods to obtain an image of the Moon showing color contrasts. He tried commercial color photographic material but decided the contrasts were not great enough to be shown easily this way. Then color correcting masks (transparent film positives having about 70% of the contrast shown in the negative) applied to high-contrast negatives made from suitable transparencies yielded, on color paper, clear local variations in color for different parts of the lunar surface. These differences did not appear to change with phase, lunation or different image scales on the telescope. Also, high contrast black and white film was used to make 3-color filter photographs. These photographs were enlarged and masked and then color prints were made which had substantially greater color saturation than those made from regular color transparencies. The same results were obtained. The results of this work are quite similar to those of Wright and of Miethe and Seegert. As stated earlier, Scott processed Wright's negatives for comparison with his own. Color variations in the integrated light of the Moon with lunar phase were reported.

Whitaker (Kuiper, 1966) produced two-color composite images of several regions of the lunar surface which showed sharp color contrast boundaries in the maria. The colored regions were the same as those found by other workers. Whitaker's images showed the least difference in color between upland and maria which may indicate his control of the dynamic range problem in the photographic process. This problem is evident in the images of other workers.

Adams (private communication, 1966) undertook a detailed program to make more quantitative the basically qualitative method of photographic imagery. He experimented with a wide variety of techniques and obtained many colored images of the Moon. The best were 3-color composites made from negatives taken through narrow-band filters. These images again showed the color features found by other workers and demonstrated the great wealth of color detail present on the lunar surface. Adam's work is not yet completed.

Photographic Spectrophotometry

The method of photographic spectrophotometry involves making photographic images through filters of regions of the lunar surface on intensity standardized plates. The plates are then measured photometrically using a microdensitometer or similar device to obtain intensity versus wavelength curves for each picture element of the photograph. This is potentially a very useful method for it provides both two dimensional spatial coverage and the possibility of quantitative accuracy over a wide spectral range. However, because of the very large data reduction problem, the two dimensional spatial coverage has not been fully used; usually only a few point-measurements are made on the image. Another problem is the inaccuracies inherent in the photographic process; some of these have been mentioned previously. Work is under way to solve some of these problems, as will be mentioned later, but at present the full value of this method has not been realized.

The earliest work of this type was performed by Barabashov (1924), who made full moon measurements of 46 lunar areas at three wavelengths (6200, 5000, and 4000 Å). He presented his data as albedoes and absolute magnitude intensities in three colors; the coordinates of the lunar positions observed were also given. His absolute error was listed as ±0.03 magnitude, although the relative error may be less. The study revealed color differences amounting to a maximum of about 0.25 magnitude. Comparing his results with those obtained by Wilsing and Scheiner for terrestrial rocks, Barabashov concluded that the lunar surface resembled a volcanic material with a predominance of basaltic lava.

Later Keenan (1931) reported on a 6 color (7400, 7000, 5300, 4400, 4100, 3300 Å) study of 36 lunar areas. Coordinates are given of the areas measured as well as a pictorial display of their positions. The data are presented for all 6 filters as brightness in terms of the average lunar brightness for each filter. Probable error for each spot ranges from 0.005 to 0.124 magnitude with 0.020 to 0.030 magnitude common. General qualitative agreement with previous workers was found. It was shown that Wood's Spot is 20% brighter in infrared then in UV, a 10% color difference exists between Mare

Serenitatis and Mare Tranquillitatis, and a green maximum is present in some maria.

Radlova (1943) reported the relative albedos of 98 lunar areas at three wavelengths (4300, 5600, 8100 Å). She also computed absolute color indices and color excesses relative to an average of all points. Coordinates of the spots measured were given and are the same as those studied in her previous visual work (1941). She found the variations in the color indices to be not much more than the estimated mean error of 0.05 magnitude. However, she did suggest that some real color differences were detected. She also found a color-brightness relation indicating that the darker regions possessed all colors while the brighter regions were mostly red. She described a plot of color index versus brightness at 5600 Å which gave a triangular distribution with the base along the color axis of the plot. She found Aristarchus and some of the other bright craters to be an exception to this rule. The colors of the mare and upland regions intersected indicating that these morphologic units did not represent clear color units. The spectral curves for all objects as defined by only 3 wavelengths were linear for the most part.

Comparison was also made of lunar color and brightness ranges to those for meteorites, asteroids and terrestrial. These results were inconclusive.

Although Radlova did not compare the numerical results of the study with those of her visual study (1941), the present author attempted unsuccessfully to find a correlation.

Barabashov and Chekirda (1954) reported on a careful program in which they observed 72 lunar positions at 5 wavelengths (8400, 6800, 5020, 4150, 3650 Å). They presented their data as color excesses relative to 5020 Å and a spot in Oceanus Procellarum. An accuracy of ±0.006 magnitude is quoted. Color differences were found to be similar to those shown in the color photographs by Barabashov (1953) and others. The maximum color excess deviations were found in the ultraviolet where the minimum deviation was in the red. A study of the data by morphology revealed that rayed craters, maria, crater bottoms and the throwout ring around Tycho were reddish when compared to the standard spot. Mountainous regions and irregularly outlined maria were greenish.

A comparison was made by Barabashov and Chekirda of this data with those obtained by earlier workers. Barabashov's earlier work (1924) was found in qualitative agreement but the color excess values were found to be too high. The magnitude of the color contrasts reported by Tihov (1924), and Markov (1950), were found to be too high and those of Radlova (1943) too low. The work of Keenan was in close agreement with Barabashov's results.

Barabashov and Chekirda (1955) followed their earlier work with a study of the color of the bright rays of the crater Tycho, Copernicus, and Kepler as a function of distance from crater center. Plates were made at full moon through the same 5 filters used in the previous work. Brightnesses along the rays were measured relative to those of the center of the craters. Four rays of Tycho, 6 rays of Copernicus and 2 rays of Kepler were measured and the data displayed. Strong color differences with distance along the rays were reported with the rays for different craters varying differently. The color differences were not monotonic with wavelength.

Wegner (1960) published an abstract describing a filter photographic and spectrometric observational program to measure color features on the Moon. A comparison of 110 terrestrial minerals was also mentioned. The photographs through 8 spectral regions extending to 1.3 microns were said to give the best results, however no data were given. Maria were said to resemble igneous materials while bright areas reflected light highly in the infrared and did not match terrestrial substances very well. Maria were found to vary in color over short distances; a flow structure was suggested.

Radlova (1961) also studied the color variations along the rays of the craters Tycho, Copernicus and Kepler She used both visual and filter photographic techniques. Filters centered at 3800, 4300, and 5600 Å were used and errors were given as 0.15 magnitude for the photographic study. The plates were taken in 1939. Color indexes relative to 5600 Å were computed as a function of distance along the ray from the crater center. She claims to have found real but small color variations along the rays with the rays colored in a variety of ways. The color trends she found are qualitatively similar to those found by Barabashov and Chekirda (1954).

Rackham (1964) published a preliminary report on a narrow-band filter photographic program showing images of the Aristarchus-Copernicus region in UV (3900 Å) and IR (10200 Å) wavelength regions. A microdensitometric tracing across both images was shown and color differences were obvious. Also shown was an IR image of the northern part of Mare Imbrium showing a blue patch evident in photographs taken by other workers. No futher report on this work is known to this author.

Photographs on the Moon were made by Evsiukov (1966) at wavelengths 3700 Å and 10000 Å at lunar phases $-3\overset{\circ}{.}9$, $95\overset{\circ}{.}5$ and 110°. About 170 lunar spots were measured at the smallest phase angle and 100 spots at the others. The author claimed a systematic dependence of color on the selenographic longitude of the observed position; this dependence was said to change with phase. With a few exceptions, Evsiukov found a range for the color indicator of about 0.25 magnitude. The general colors he reports were in agreement with those found by earlier workers using both photometric and imagery methods.

Photographic Spectroscopy

Photographic spectroscopy studies as applied to the lunar color problem are a more recent type of observation; nevertheless, a great deal of data has been gathered. The studies involve passing light from some region on the lunar surface through a dispersing device such as a prism or grating and then recording the spectrum on photographic plates. The plates are intensity calibrated and are measured photometrically to yield intensity versus wavelength curves.

Again the problems and inaccuracies associated with the photographic method are limiting factors. However, since all wavelengths are recorded simultaneously as are several regions on the lunar surface, if a slit is used, errors due to atmospheric effects can be greatly reduced. Because of the large amount of data existing on one plate, a data reduction and handling problem arises, and consequently this method has not been fully utilized.

Although one very early study was reported (Petruskevski, 1878), the first program of interest was carried out by Yezerskii and Fedorets (1956). They used a prism spectrograph to determine the comparative spectral energy distribution curves for 8 pairs of spots on the Moon. The wavelengths at which measurements were given in 100 Å intervals was from 4500 to 6300 Å. Mean error was given as ±0.01 magnitude. The data were presented in a table as intensity ratios in units of magnitude for different wavelengths. Color differences were found to be neither monotonic nor uniform for different lunar regions and color differences to about 0.30 magnitude were listed for the spectral region. They concluded that the color contrasts obtained when comparing areas in the upland to areas in the maria were greater than when comparing areas within the same generic type of lunar feature, although the maria showed large color contrasts.

A plot of the color excesses against wavelength (not given in the article) show interesting narrow-band spectral features of about 5% to 10% that are similar in all spots relative to the reference area in the southern uplands, although some variation is evident among the lunar areas. Also, it can be seen that all features seem to have a general maximum reflectivity in the green and yellow of about 15% relative to the standard spot. This seems to support most earlier work which described the maria regions as appearing greener than the upland regions.

Vigroux (1956) determined the logarithm of the ratio of the intensities of 7 lunar features in the wavelength interval 3500 Å to 6300 Å. He found this function to decrease with wavelength for some features and increase for others. All variations were monotonic. Relative spectral curves were given with a general description of the observed lunar regions. The general color features found were similar to those reported previously (e.g. color differences between Mare Serenitatis and Mare Tranquillitatis).

Teifel, in a series of publications, reported on an extensive observational program using a slit spectrograph. At first, ninety areas within 15 lunar regions were observed between 3900 Å and 6200 Å, six to eight spectrograms being measured for each area. Spectral curves were constructed relative to a spot in

Mare Vaporum and presented for these 90 areas (1960a). The spectral distribution curves of most lunar objects showed a smooth intensity variation along the spectrum, with some changes in slope evident. For several features the differences in spectral intensities exceeded the mean square error of the result (0.02 to 0.03 magnitude) and contrasts to 0.01 and 0.20 magnitude appeared at some positions. No unusual spectral anomalies were noted in the intensity distributions in this spectral region, with the exception of a conspicuous decrease in the reflectivity for wavelengths less than 4200 Å for several objects in Mare Imbrium and some other regions.

Because of the almost monotonic distribution of reflected solar radiation with wavelength, Teifel felt that to characterize the color properties of regions of the Moon it was necessary only to compute color indexes for two wavelengths. Thus, a catalogue was compiled which gave the normal color indices of 262 areas of the Moon based on the measurements of 10 to 14 spectrograms of each of the 11 lunar regions studied (1960b). The two wavelengths used were 4430 and 5500 Å. The color excesses were measured with respect to the same reference point in Mare Vaporum, whose color index was measured with respect to a star. In a similar study spectrograms were obtained near full moon and were used to measure color indexes and the relative intensity of 1442 areas of the Moon in 62 regions (1961). Errors for both studies were about ±0.02 magnitude.

The results of these investigations were several. The range of color differences were found to be 0.21 to 0.25 magnitude with the range almost the same for both maria and continents. An extensive investigation of the color-brightness relation was made. The brighter objects were found to be redder, as reported earlier. However this relation was found to vary for different lunar regions. A gradient was defined as the rate of change of color index with brightness for each region. This gradient was found to be different in different lunar regions.

An examination of the crater Aristarchus and the region nearby was made (1960c). The color-brightness relations determined previously were found not to hold here, the bright regions not being red enough.

Barabashov, et. al. (1959) obtained spectra of 43 lunar areas between 4400 Å and 6000 Å relative to sun light reflected from a plate. The spectral curves for 14 lunar areas were given and the color excess between the effective wavelengths of visible and photographic magnitudes were determined with errors of 0.02 to 0.04

magnitude. For the remaining spots only the color excess was calculated. The color differences were usually under 0.10 magnitude with a few to 0.02 or 0.30 magnitude. The color-brightness relation mentioned before was evident in a majority of the studied regions. There was good agreement of these results with those of earlier workers.

Spectrometric measurements between 3900 and 6400 Å were carried out for the details in the bottoms of the craters Alphonsus, Copernicus, Eratosthenes, Theophilius and Posidonius by Barabashov and Yezerskii (1961). Spectral curves were shown with some color differences evident (central peak redder in some cases).

Sergeeve (1959) measured 80 spectral distribution curves for lunar details from "UV" to 7200 Å. The spots measured were only generally described and few intensity tracings were shown. However, the results given were that color contrasts were found to be sometimes 10% to 15% but seldom 20%. Various specific color areas were described and they generally agreed with past results. Craters and mountainous regions displayed a reddish tint when compared with maria. Spectral intensity curves were measured across some craters with color differences found; the red rim around Tycho was one feature mentioned which had been described in earlier work.

Polozhentzeva (1958) obtained spectra between 4000 Å and 6300 Å of 12 lunar areas. The measurements were made at several phase angles. Intensity curves relative to Sinus Iridum were given and color differences of 10% to 15% were evident above the estimated error of ±0.02 magnitude. The uplands were found to be somewhat redder than the maria. No dependence of color on phase was noticed.

Polozhentzeva (1961) analyzed the spectragrams taken by Kozyrev (1959) just before the detection of the well known gas emission in Alphonsus. The color excesses are plotted as a function of position across the crater. Some color differences were evident to about 0.10 magnitude and were attributed to spectral reflectivity differences at the lunar surface. The central peak appeared to be redder than the crater walls but about the same color as the crater floor.

Coyne (1962, 1963) made a detailed study of color differences on the lunar surface. Relative spectral intensity curves between 4380 Å and 6835 Å were produced for 44 paired areas. The mean error was given as 0.01 to 0.03 magnitude. The areas measured were shown on a lunar photo with all the spectral intensity curves displayed in the first reference. He found that the color contrasts were greater between mare and upland than in the maria although there were significant contrasts in the maria. The maria appeared more homogeneous in blue light than in red light. The color-brightness relations seemed to hold, with brighter areas being redder on the average. Coyne also noted bumpy features in the spectral curves that he attributed to luminescence of the lunar surface.

Photoelectric Photometry

The newest and most accurate technique for observing lunar color contrasts involves using the photomultiplier tube as a detector. Two methods have been used. Point measurements have been made by passing light from a selected lunar region through an aperture and a series of filters onto a photosensitive surface. Secondly a dispersing device is used instead of a filter. In this case the dispersing element, usually a grating, is moved, effectively scanning the spectrum past the photo detector. Both methods utilize the high accuracy and great dynamic range of the photomultiplier tube.

Markov, (1950) was the first to describe a lunar color study using a photoelectric detector. He measured the color indices of 10 lunar features between the wavelength of 3800 Å and 5270 Å. The results were given as stellar classes but a calibration table is given for converting these to stellar magnitude. The reddness of the rim of the crater of Tycho as compared to its floor was one feature noted. In general Markov states that his measurements gave color differences that were greater than those obtained by Radlova (1941), about the same as those obtained by Barabashov (1924) and smaller than those noted by Tihov (1924).

Murray and Liu (1961) used a photoelectric scanning spectrometer to obtain spectra from 3900 Å to 8100 Å of four small regions in Mare Serenitatis. They attempted to confirm the existance of a color contrast across the albedo boundary near the north and south edge of Mare Serenitatis. They found no color differences to within 0.3%. This contradicted much earlier work although the accuracy quoted was the highest achieved to that time.

Kozlova (1961) made photoelectric observations near full moon at 4200 Å and 5350 Å of 14 lunar craters. The bottom of the crater Manili was used as a standard area. Color excess was given relative to the standard area and to 5350 Å. Errors averaged 0.01 to 0.02 magnitude, and the color differences ranged to 0.13 magnitude at Flemstidius and Lambert.

Van den Bergh (1962) determined the color excesses of 14 lunar regions on the standard B-V color system. A spot in Mare Serenitatis was used as a standard. Errors were given as about 0.005 magnitude. He found color differences to exist with Mare Tranquillitatis being bluer than Mare Serenitatis. He also found the highlands slightly reddish. His results agreed well with those of most earlier workers.

Wildey and Pohn (1964), as a part of a more extensive lunar photometric observational program, measured the B-V colors of about 30 lunar areas, mostly craters, at various phase angles. Color differences to about 0.10 magnitude were recorded and only a very slight reddening with brightness was noticed.

At about the same time Gehrels,et. al., (1964) reported on an extensive lunar photometric study which was carried out over a period of several years. Measurements were made using both the UBV system (3600, 4500, 5600 Å) and the UGI (3600, 5400, 9400 Å). Data were obtained at different phase angles. Color data given are: G-I for 7 regions, U-G for 7 regions, and B-V and U-B for 13 regions with errors given as 0.006 to 0.008 magnitude. The color differences range over 0.09 magnitude for B-V. No change in differential color with phase was noted, although the color of the entire Moon was found to redden with phase.

Coyne (1965) determined the B-V colors for 36 lunar areas with respect to a standard area in Mare Serenitatis. The maximum color range was 0.08 magnitude with errors of 0.005 to 0.010 magnitude. An attempt was made to discover a change of color with phase but none was found. A comparison of these measurements with those of Van den Bergh's (1962) showed some correlation but differences of 0.02 magnitude were common.

Petrova (1966) used a photoelectric scanning spectrometer to observe 11 lunar areas from 3400 to 7200 Å. The relative reflectivity curves for 6 pairs of spots were given showing a generally linear trend for most areas. Humps were present in the spectral curves which the author ascribed to luminescence, but the scatter in the data was great.

APPENDIX II

INSTRUMENTATION

A DOUBLE-BEAM ASTRONOMICAL PHOTOMETER

Thomas B. McCord

Division of Geological Sciences
California Institute of Technology
Pasadena, California

Submitted to Applied Optics

October, 1967

Publication March, 1968

Contribution No. 1492 of the Division of Geological Sciences, California Institute of Technology, Pasadena

ABSTRACT

A double-beam photoelectric filter photometer has been designed and constructed to make simultaneous measurements of two astronomical objects. Both objects are imaged in the same focal plane so that the same aperture-filter-detector system is used for both beams. The device greatly reduces errors due to variable atmospheric extinction. Photometric measurements can be made under conditions normally suitable only for spectroscopic work. Measurement precision is also increased, and accuracies of a few tenths of one percent are routine under thin cloud conditions. A description of the instrument and its operation is given in this paper.

A DOUBLE-BEAM ASTRONOMICAL PHOTOMETER

INTRODUCTION

A significant portion of astronomical measurements involve the comparison of one energy source with another. The purpose of the measurement may be to determine color characteristics of a group of stars with respect to some standard star, to monitor the intensity of a variable source using a standard star or, particularly in the field of planetary astronomy, to determine the relative properties of different areas of an extended source. The standard technique used to make comparative measurements is to move the telescope from one source to another. A major source of error is change in sky conditions (e.g. extinction) during the time required to move the telescope. This error can be greatly reduced by using a double-beam photometer which monitors both sources simultaneously. In this case the energy from both objects travels very nearly the same path through the atmosphere at the same time and the effect of changes in atmospheric extinction on the relative measurement is greatly reduced. The accuracy improvement is less for sky emission at far infrared wavelengths for there the spatial coherence distance is only on the order of a few arc seconds.

A double-beam photometer was built and operated by Walraven[1] to study variable stars. His system used two separate focal plane diaphragms and photoelectric detection systems --one for the standard star and one for the object of interest. An optical switch was used to alternate the roles of the two photomultipliers to help remove the effects of changes in the detector responses. A calibrated density wedge was inserted in one beam and its position controlled by a servo system. The system was operated as a null detector with the wedge-servo system maintaining an intensity balance between the two channels. The position of the density wedge gave the ratio of the intensity of two stars.

Walraven's system, although apparently quite successful for certain types of measurements, is not versatile enough for many applications and, by recording only the intensity ratio, discards useful data. Disadvantages of this system include the fixed beam spacing and the use of two separate aperture and detection systems.

A double-beam, multi-channel filter photometer was designed and constructed to overcome the limitations of Walraven's instrument. The purpose of this paper is to describe the instrument and its operation.

PHOTOMETER

The general function of a double-beam photometer is to admit light from two sources located at two different positions in the sky and measure the intensity of each source simultaneously, or alternately, at a rapid rate. To be truly versatile the instrument must satisfy at least three requirements: (1) The two beams of the photometer must have easily varied spacing within wide extremes, so that a variety of objects can be observed during one night; (2) It is also desirable that the aperture-filter-detector system be the same for both beams. This eliminates the need for continuous careful calibration of one beam with respect to the other, because the bandpass and detector sensitivity for each beam is identical; (3) The intensity of light passed by each beam should be recorded separately so that all available information is retained; ratios can be formed later if that is the desired result.

To meet the first two requirements a system of mirrors was designed which allows the beam spacing and thus the separation of the objects in the sky, to vary continuously over a wide range while both beams remain in focus on the same aperture regardless of the beam spacing.

The mirror system, shown in Figure (1), consists of four mirrors, one of which, is a three bladed chopper. With a blade of the chopper in place, beam X, which is on the optical axis of the telescope, travels from mirror A to the chopper blade and then onto the aperture, which is at the real focal plane of the telescope. When the chopper blade is not in place, beam Y reflects from mirror C onto mirror D and then between chopper blades onto the same aperture. Mirrors A and B are fixed in the photometer. Mirrors C and D are mechanically linked so that C moves on a path inclined at 45 degrees to the path along which D moves. Both mirrors C and D move in the same plane. By adjusting mirrors C and D in beam Y, areas on the sky of different angular separation can by chosen for comparison.

The photometer is joined to the telescope in such a way that it can be rotated 360° about the optical axis, which is colinear with beam X. Thus by moving mirrors C and D and by rotating the entire photometer on the telescope a plane polar coordinate system is set up onto which the sky is mapped. The origin is on the optical axis of the telescope; the radial degree of freedom is along the path beam Y follows as mirrors C and D are adjusted; the azimuthal degree of freedom is controlled by rotating the photometer about beam X.

The two beams are always in focus on the same aperture because the beam path-lengths from the primary mirror of the telescope to the aperture remain the same regardless of the beam spacing. When the movable mirror C is moved away from the fixed mirror A, it moves an equal distance, <u>a</u>, down and to the right (as Figure 1 is drawn) of mirror A, but mirror D moves only a distance, <u>a</u>, down from the chopper mirror B. The path length to the aperture along beam Y with respect to that of beam X has become shorter in the horizontal direction by a distance <u>a</u>, but longer in the vertical direction by an equal amount and the overall pathlength remains constant.

The range of beam separations possible is controlled by the thickness of the chopper blade mirror and the size of the telescope beam and the photometer. For very small beam separations the beam pathlength compensator is no longer needed and mirror C is lowered out of position to prevent interference with beam X.

The advantages of this system are: (1) objects are always in focus on the same aperture regardless of the beam spacing and both objects are available for constant viewing; (2) the aperture, filter and detection systems can be identical for both beams because both beams are approximately colinear after chopper mirror B.

This eliminates detector drift as a source of error for comparative measurement; (3) the same number of reflections at the same angles occur in each beam minimizing differential polarization effects; (4) because the beam separation is continuously adjustable, any areas of the sky, with angular separations which the size of the telescope beam and the photometer allow are available for comparison.

The particular instrument presently in existence has a beam spacing range of from 1 mm to 75 mm in the focal plane. This corresponds to a 10 minute of arc range for an f/16, 60 inch telescope. The mirror chopper is a three-bladed aluminized glass flat 0.031 inch thick which is driven at 30 cycles per second. The beam spacing is controlled externally by a single adjustment and the entire photometer is mounted on the telescope using a radial thrust bearing which allows the instrument to rotate 360° about the optical axis with less than 0.001 inch flexing over an 8 inch bearing.

After traveling through the mirror system, both beams are imaged on an aluminized, polished stainless steel plate set at 45° to the beams (Figure 1). In this plate is drilled the aperture aligned with the incoming beam. The light not passing through the aperture is reflected by the aluminized plate and is directed onto a beam splitter (Figure 2). The transmitted light passes through a lens and beam-length compressor to a camera mounted on the side of the photometer. The light reflected by the beam splitter is directed through a lens system into a periscope and finally to an eyepiece.

Immediately before the beam splitter in the path of the viewing beam is another three-bladed chopper, which is blackened and driven by a synchronous motor of the same speed as the mirror chopper motor. The motor and blade unit is mounted so that it can be manually phased by rotating the unit about the motor spin axis. This allows the observer to adjust the phase of the blackened chopper or strobe with respect to the mirror chopper so that only beam X, only beam Y,or both beams superimposed can be seen through the eyepiece and at the camera focus. Either or both beams can be monitored continuously and pictures can be taken as a permanent record of the exact area of the sky from which light was sampled. This is especially useful when observing star clusters or extended sources.

An off-axis guiding eyepiece is also used to view a larger field than reflected from the aperture plate. It is placed directly behind mirror A and can be moved to view the field around mirror A.

The light passed by the entrance aperture, either from beam X or from beam Y, passes through one of many filters mounted in a wheel directly behind the aperture and then is focused onto the photocathode surface by a field lens.

DETECTION AND ELECTRONICS

The detector presently used is either an ITT FW-118 or FW-130 photomultiplier tube mounted in a cold box. The cold box is mounted on the photometer directly behind the filter wheel. The photomultiplier tube output signal is a square wave, 30 cycles/second in this particular device. Beam X is read for half the cycle while the mirror chopper blade is in place; the current due to beam Y composes the other half of the cycle.

Two detection and data processing systems have been developed for use with the photometer. One system treats the photomultiplier as a current source and measures the voltage over a 1 megohm load using a.c. amplification and synchronous detection techniques. The other system is a two channel pulse counter and digital-data system.

In the first system, the signal is fed to a driven switch or chopper which is phased-locked to the mirror chopper. The chopper alternately switches the photomultiplier output between two amplifications, synchronous detection and rectification channels. Each channel sees the same ground or zero level at the load resistor when not looking at the phototube. The rectified voltage in each channel is then read by a two channel chart recorder and by a digital voltmeter-paper tape punch system yielding digital output suitable for computer processing. The functional block diagram is shown in Figure 3, with the signal history given in Figure 4.

The handling of the signal from the phototube is straightforward except for the first stage. In a two channel system such as this, care must be taken to insure that the signal at the chopper input is a true square wave. If not, energy is effectively transferred from one channel to another and a false ratio will be recorded which is dependent on the relative signal size from beam X and beam Y. This limits the size of the input impedance of the preamplifier to that which, with the cable and component capacitance, will give an appropriate time constant for this part of the circuit. An analysis of the circuit for a square wave imput at the photocathode and a time constant in the input circuit RC shows that the ratio of the output of the two channels is in error from the true ratio as follows:

$$\frac{V_1}{V_2} \longrightarrow \frac{V_1 - E}{V_2 - E}$$

$$E \sim 2 \quad \Delta V \frac{RC}{T} \qquad\qquad T \gg RC$$

Where R is the load resistor and C is the capacitance in the circuit, about 10 pf for this system. ΔV is the difference in the signals of beam X (V_1) and beam Y (V_2), $\Delta V > 1$; T is one-half the chopping period (1/60 sec.). For $\Delta V = 2$, $R = 10^6 \Omega$ the error is about 0.1%. This is a basic limitation for a two channel detection system of this type, unless a switching device is used to block out that part of the signal near the square wave edges.

The second detection and data handling system utilizes pulse counting techniques. Each beam of the photometer has its counter channel which is switched on and off synchronously with the mirror chopper blade. Counts are made in each channel for a specific length of time before switching to the other channel. This insures that each channel counts for the same length of time before data punch-out occurs. The counter gate is regulated so that no counts are made when the chopper blade edge passes from one beam to the next. Again data are punched out on paper tape at a maximum rate of 120 characters/second for later computer processing. Part of this system is similar to one developed by Dennison and Oke of Mt. Wilson and Palomar Observatories and reported in the 1965 yearbook of the Carnegie Institution of Washington.

In both of these systems the intensity measured in each channel is recorded so that the maximum information is retained. It is also possible to operate the analogue system in a direct differencing mode by bypassing the electronic switch and using only one data channel.

OPERATION

Two objects to be compared are located and positioned on the aperture by adjusting the mirror separation and rotating the photometer on its mount. This is not an easy task for the inexperienced, but with a little practice the photometer can be set in less than 1 minute. As the system is presently used the filter wheel drive and the data sampling system is programmed to run automatically; the operator need only guide the telescope. The beams are periodically inverted by rotating the photometer 180° and a measurement is repeated.

This allows for the elimination of any color characteristics peculiar to the instrument, although none have been experienced when clear mirrors were used. It also provides a check for such problems as scattered light.

RESULTS

The instrument has been used successfully in a variety of both stellar and planetary programs using the 24, 60 and 100 inch telescopes at Mt. Wilson as well as the 200 inch telescope at Mt. Palomar. One program involved the use of the instrument with the 100 inch telescope at Mt. Wilson Observatory to detect and measure small amplitude variations in the intensity of visible radiation from the Cygnus x-ray source.[2] Variations limited only by photon statistics (~ 0.3%) in a 15th magnitude object have been measured easily even when extinction variations of 10% occurred during the observation.

A lunar colorimetry program is also underway using the 24 and 60 inch telescopes at Mt. Wilson. Figure 5 shows three typical runs made of two lunar areas with the 24 inch telescope on a night when thin high clouds caused 10% transmission variations. A 0.5 mm aperture was used at f/16. The points represent normalized ratios of the intensities of the two lunar positions as measured through each of 21 interference filters with about 0.001 magnitude (0.1 percent). The scatter of the points is slightly greater because of small guiding errors, however, the guiding problem is not nearly so great on stellar objects. The result of these and other programs presently under way will be reported in articles appearing elsewhere.

CAPTIONS

Figure 1: A diagram of the photometer optical system is shown. The centers of mirrors A,B,C, and D are in the same plane and mirrors C and D move in that plane. Two settings of the movable mirrors C and D are shown.

Figure 2: The viewing optical system is shown out of scale. This diagram is in a plane perpendicular to the beam passing through the aperture to the photocathode. Light entering this system is reflected from the mirror surface of the aperture plate.

Figure 3: Functional diagram of the ac synchronous detection system used with the photometer is shown.

Figure 4: History of the signal from the photomultiplier tube output through the switching operation to the input of the ac preamplifier in each channel.

Figure 5: Actual data obtained during three typical observation runs on two areas of the Moon. Transparency changes on the order of 10%

occurred with frequencies on the order of 10 seconds during these runs. Plotted is the normalized ratios of the intensities measured in each channel: the magnitude or logrithmic scale is used. The shape of the curve shows the variation in the reflecting properties with wavelength (i.e. color) between the two lunar areas observed.

ACKNOWLEDGMENTS

The author wishes to thank Bruce Murray for originally suggesting that such a device be designed, as well as James Westphal who was of considerable help with both the design and debugging of the instrument. Sol Giles contributed a great deal toward the detailed mechanical engineering and construction of the photometer. Robert Dickens is also to be thanked for assistance in debugging operations on the telescope.

This project was supported through NASA grant NSA 56-60. The author held a NASA Traineeship during this project.

REFERENCES

1. Walraven, T., "On the use of sevomechanisms in photometry of stars" in <u>Astronomical Photoelectric Photometry</u>, ed. Frank Bradshaw Wood, a publication of the American Association for the Advancement of Science, Washington, D.C., 1953.

2. Kristian, J., A. Sandage, and J.A.Westphas, <u>Ap. J.</u> <u>150</u>, 1967.

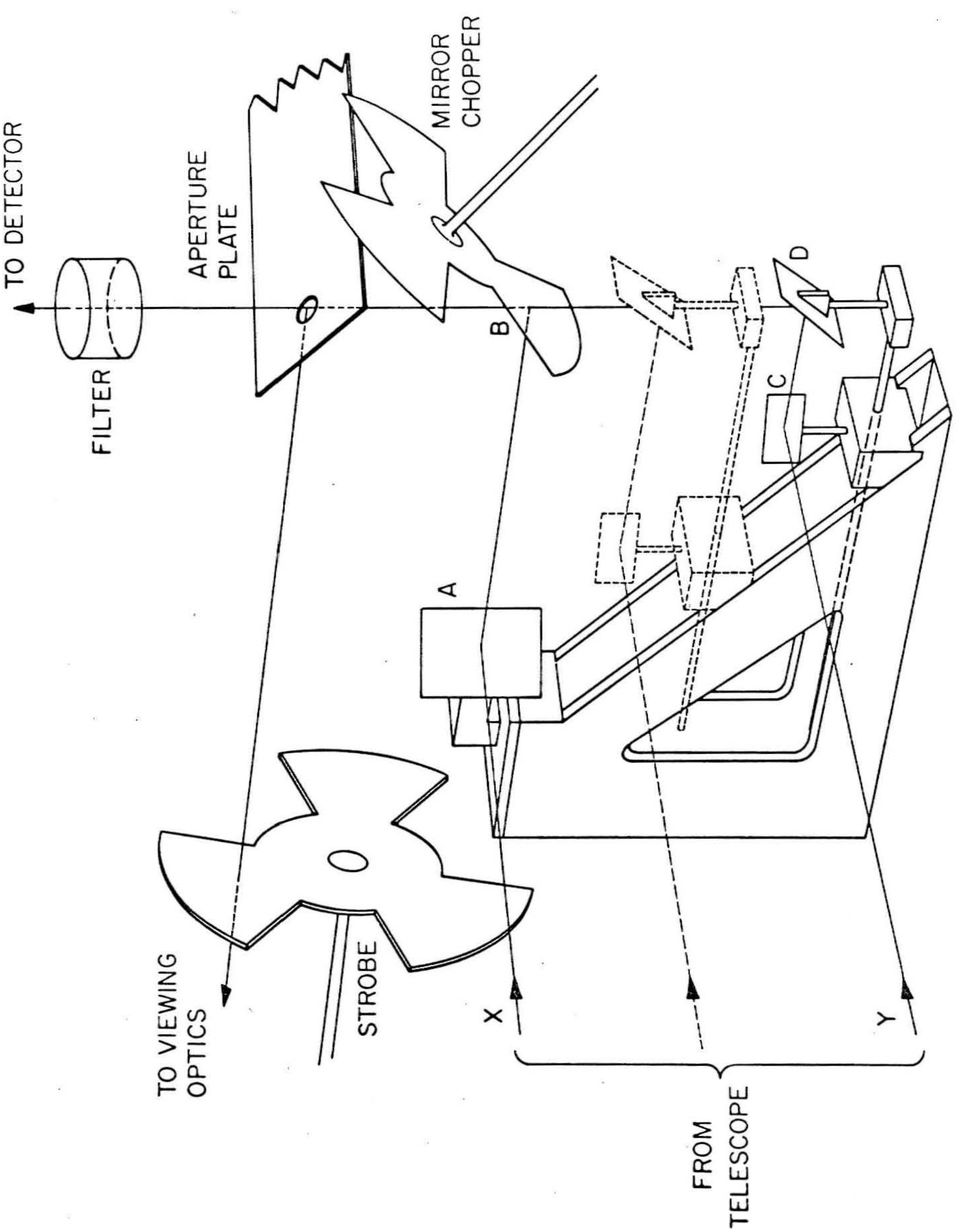
TO DETECTOR
FILTER
APERTURE PLATE
MIRROR CHOPPER
B
A
C
D
TO VIEWING OPTICS
STROBE
X
Y
FROM TELESCOPE

Figure 1

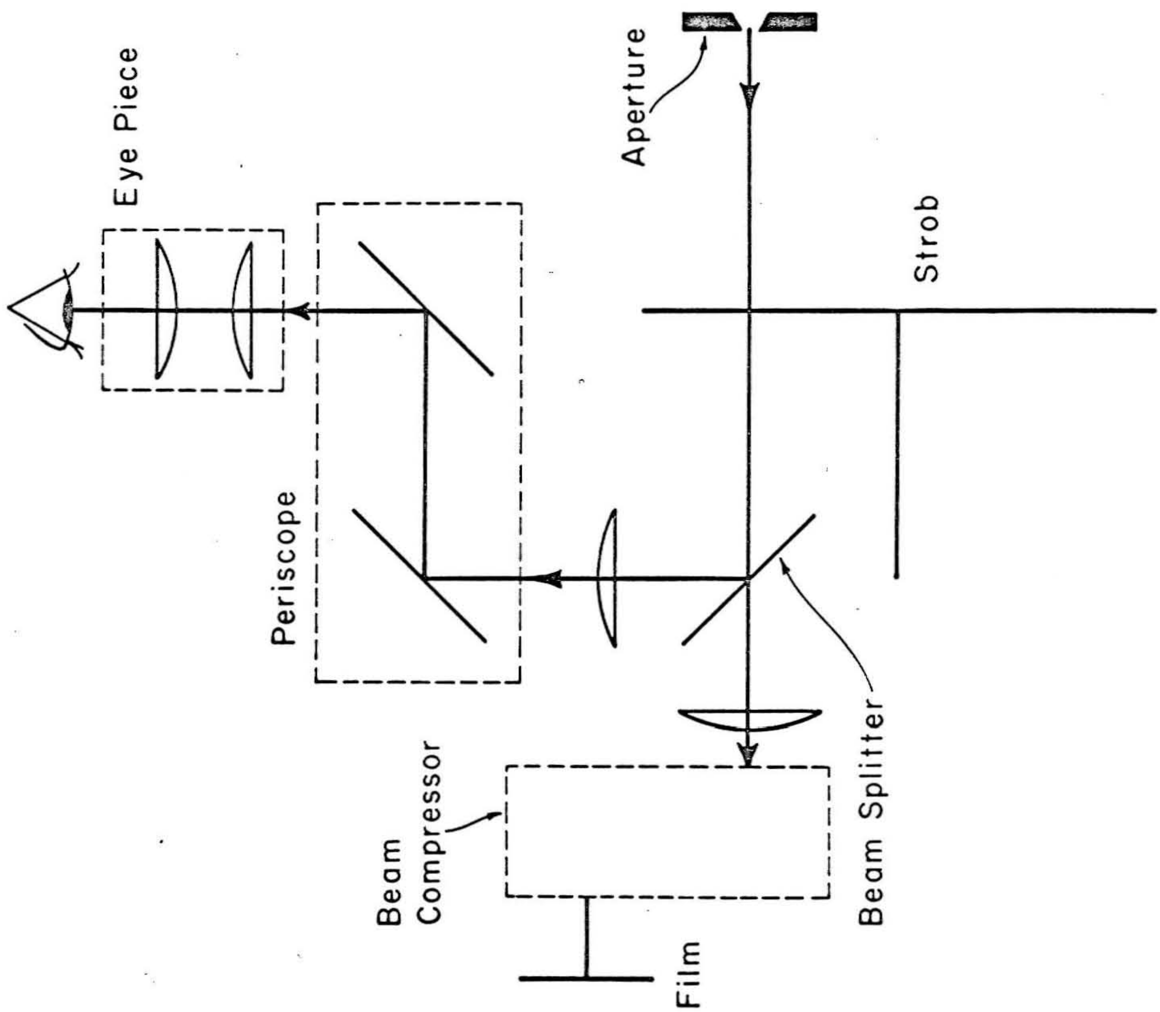
Eye Piece
Aperture
Strob
Periscope
Beam Splitter
Beam Compressor
Film

Figure 2

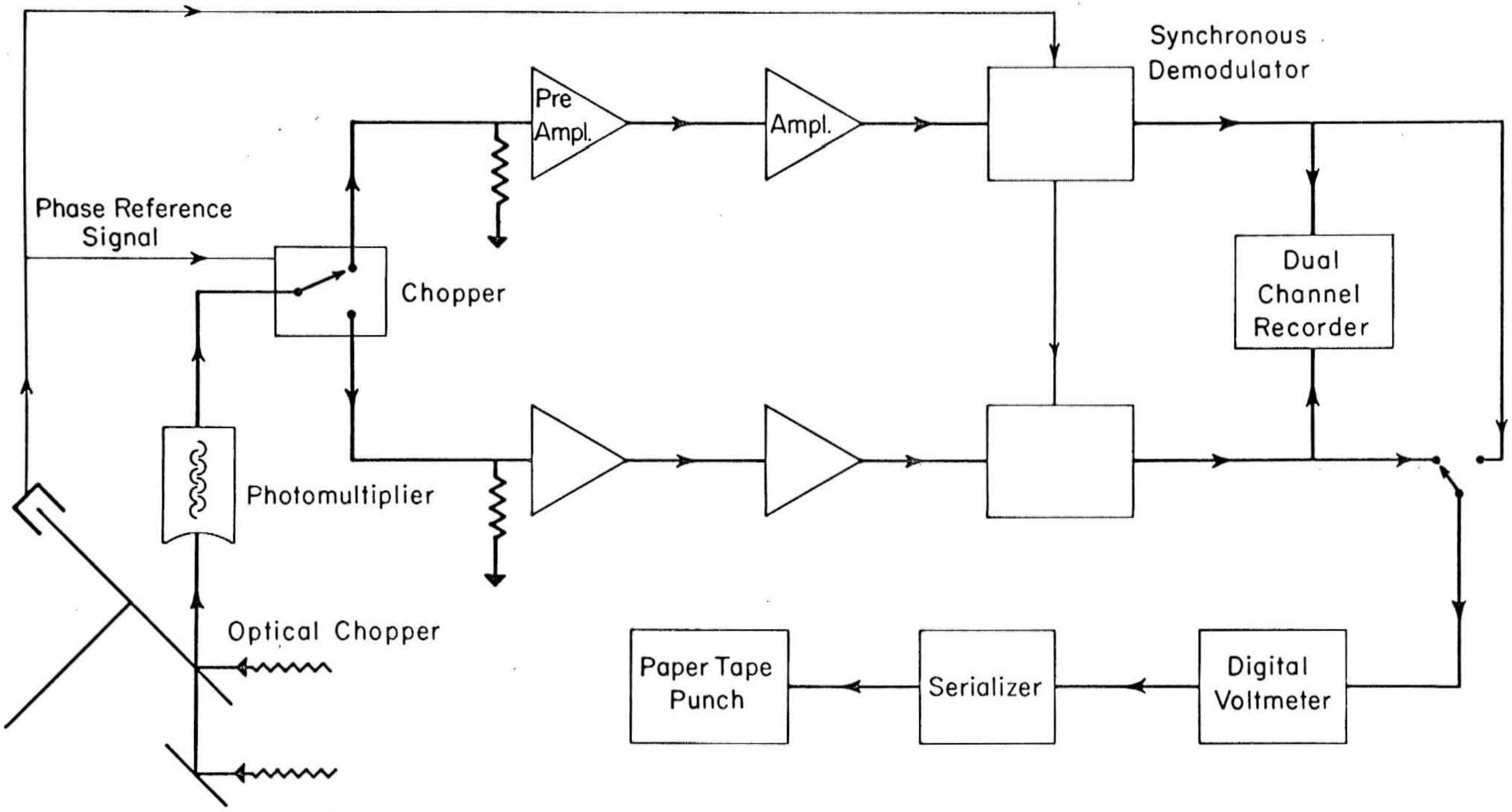
Synchronous
Demodulator
Pre
Ampl.
Ampl.
Phase Reference
Signal
Chopper
Dual
Channel
Recorder
Photomultiplier
Optical Chopper
Paper Tape
Punch
Serializer
Digital
Voltmeter

Figure 3

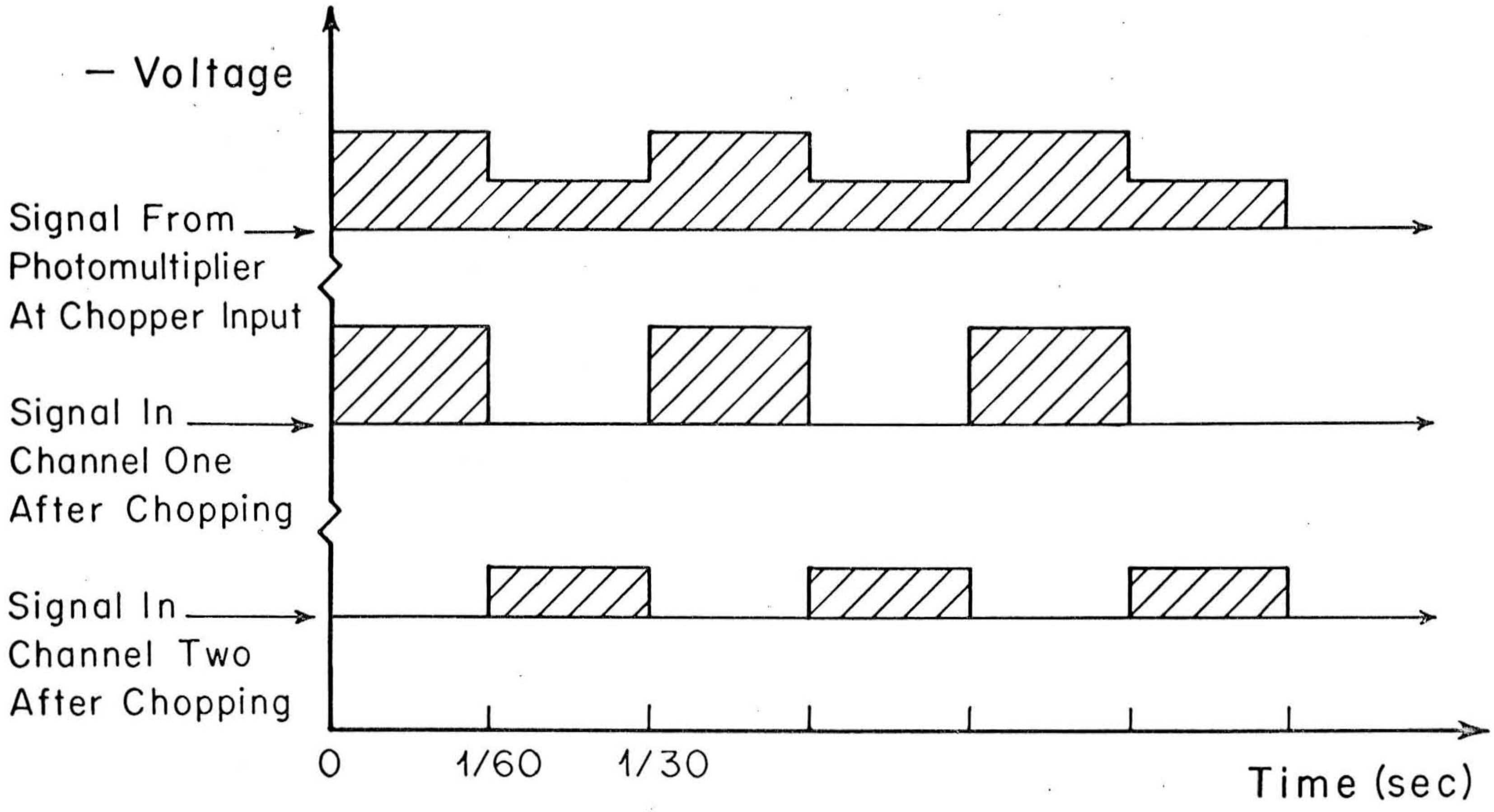
– Voltage
Signal From Photomultiplier At Chopper Input
Signal In Channel One After Chopping
Signal In Channel Two After Chopping
0
1/60
1/30
Time (sec)

Figure 4

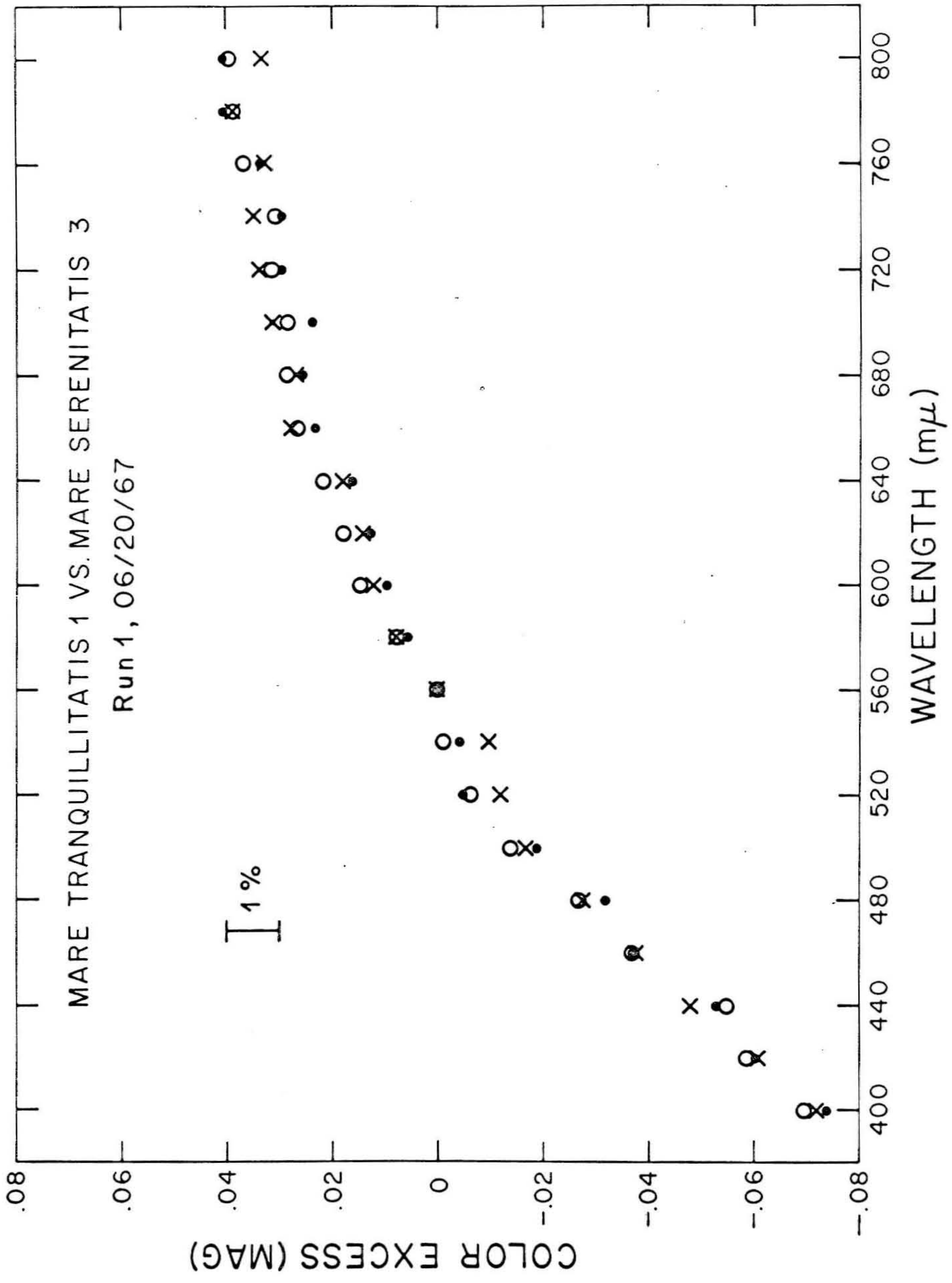
MARE TRANQUILLITATIS 1 VS. MARE SERENITATIS 3
Run 1, 06/20/67
1 %
WAVELENGTH (mμ)
400
440
480
520
560
600
640
680
720
760
800
COLOR EXCESS (MAG)
.08
.06
.04
.02
0
-.02
-.04
-.06
-.08

Figure 5

APPENDIX III

OBSERVATIONAL DATA

The graphs included in this Appendix represent the most useful and non-redundant data obtained in the observational portion of this study of relative lunar color differences. Plotted are the relative reflectivity ratios D (λ , α) against wavelength in microns. The scale is given at the top-left of each page.

This Appendix consists of three sections; the first, pages 162-168 , contains measurements as they were actually made. The data points are ratios as reduced directly from the raw intensity measurements. The curves are third order polynomials least-squares fitted to the points, which were weighted by their standard deviations. The phase angle at which the measurements were made is given at the right of each curve as is an error bar indicating the standard deviation of the deviations of the points from the curve.

The second section (page 169) is a continuation of the first except that the scale was reduced as indicated in the upper left corner of the graph.

The third section (pages 170-171) gives the spectral curves of some lunar areas given in part 1 of this Appendix but this time relative to the standard area (Mare Serenitatis 2) rather than to an intermediate standard area. The phase angle at which the original measurement was made is given along with the phase angle of the measurement used to transfer the curve. The intermediate standard area(s) used are indicated by the symbols placed to the left of each curve identification. The code is: ✱ Sinus Iridum 1, † Mare Nubium 1, ☆ Menelaus N.W., ‡ Tycho 1, ○ Copernicus 3, × Plato C, and + Le Monnier.

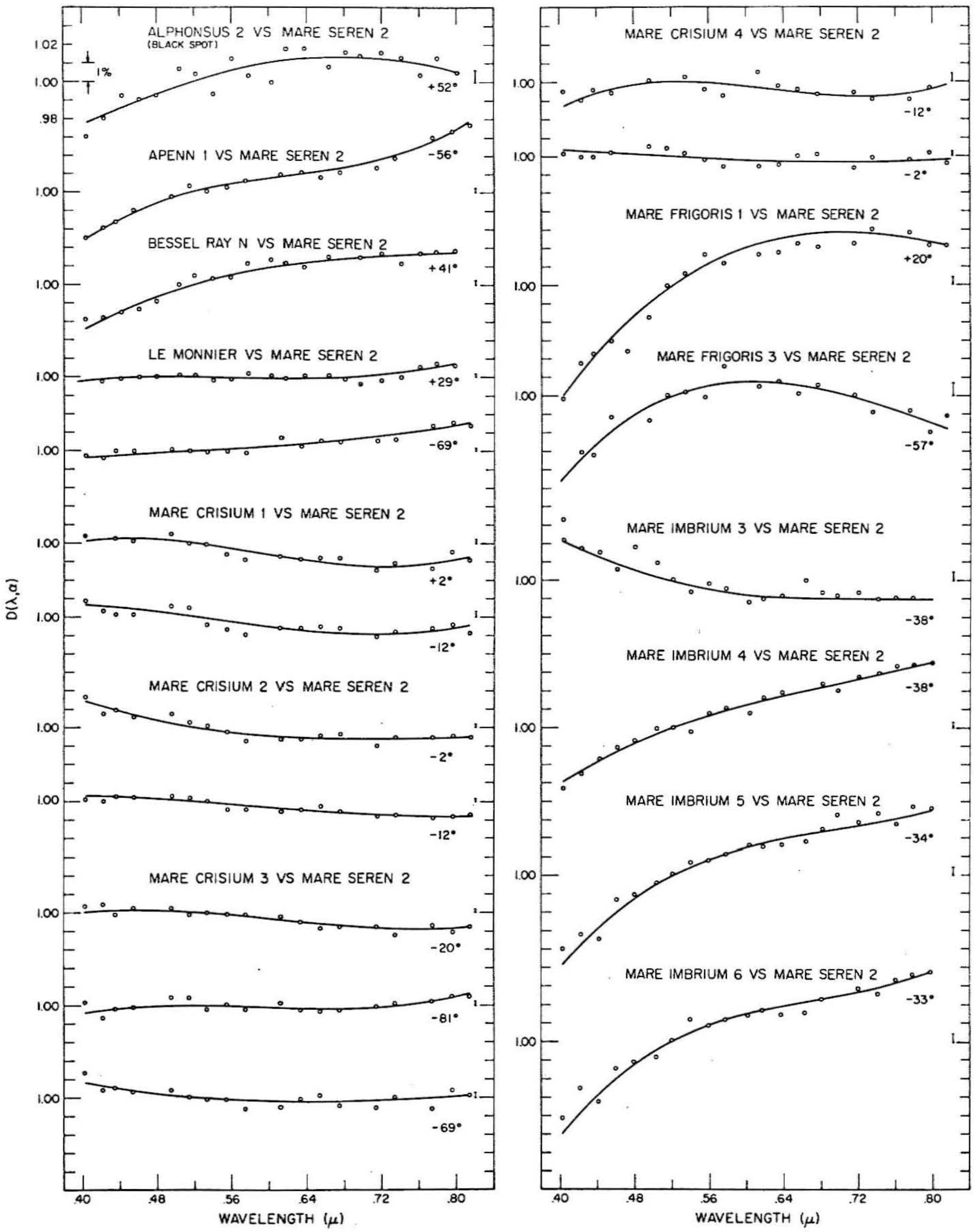
ALPHONSUS 2 VS MARE SEREN 2
(BLACK SPOT)
1.02
1.00
.98
1%
+52°
APENN 1 VS MARE SEREN 2
-56°
BESSEL RAY N VS MARE SEREN 2
+41°
LE MONNIER VS MARE SEREN 2
+29°
-69°
MARE CRISIUM 1 VS MARE SEREN 2
+2°
-12°
MARE CRISIUM 2 VS MARE SEREN 2
-2°
-12°
MARE CRISIUM 3 VS MARE SEREN 2
-20°
-81°
-69°
D(λ,α)
WAVELENGTH (μ)
.40
.48
.56
.64
.72
.80
MARE CRISIUM 4 VS MARE SEREN 2
-12°
-2°
MARE FRIGORIS 1 VS MARE SEREN 2
+20°
MARE FRIGORIS 3 VS MARE SEREN 2
-57°
MARE IMBRIUM 3 VS MARE SEREN 2
-38°
MARE IMBRIUM 4 VS MARE SEREN 2
-38°
MARE IMBRIUM 5 VS MARE SEREN 2
-34°
MARE IMBRIUM 6 VS MARE SEREN 2
-33°
1.00
WAVELENGTH (μ)

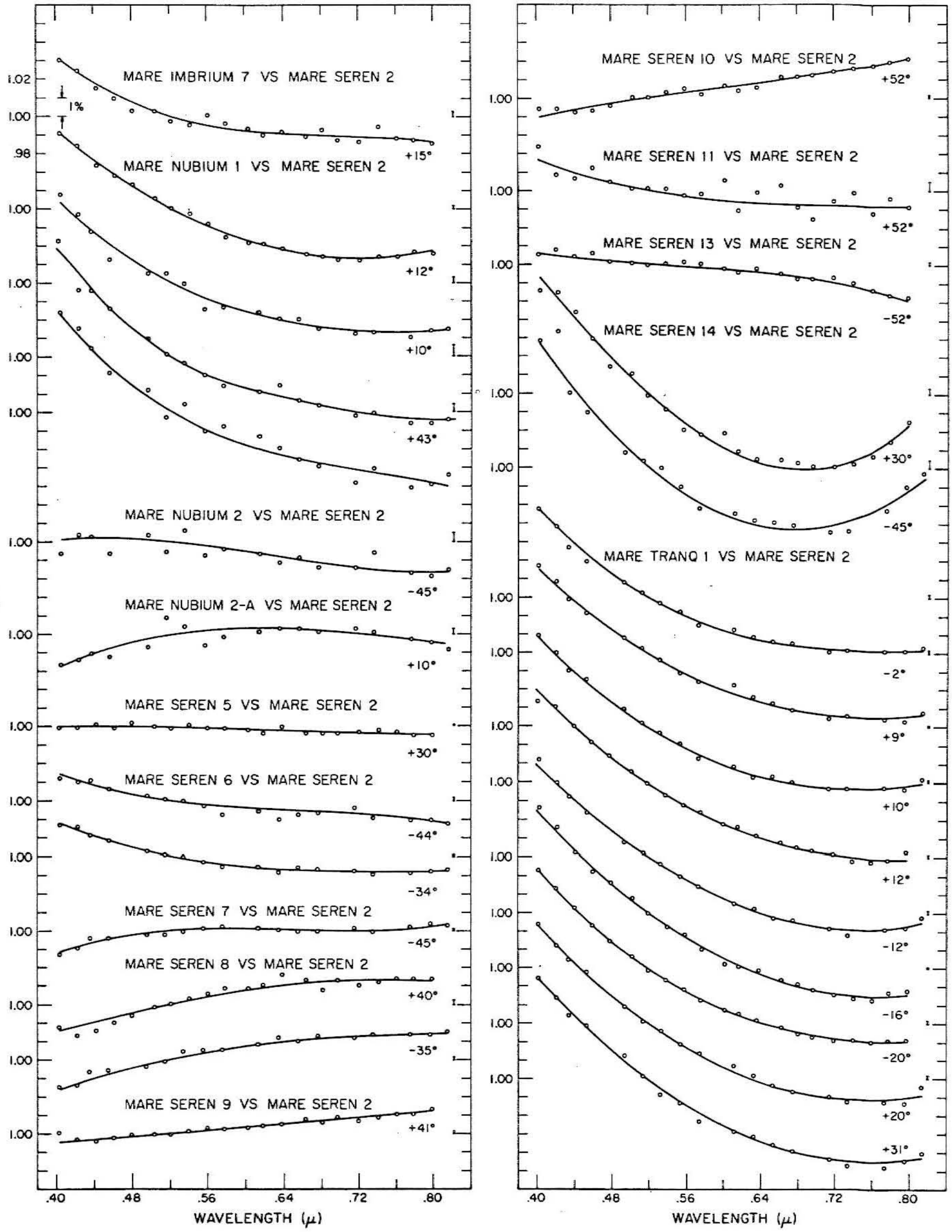
1.02
1%
1.00
.98
MARE IMBRIUM 7 VS MARE SEREN 2
+15°
MARE NUBIUM 1 VS MARE SEREN 2
1.00
+12°
1.00
+10°
1.00
1.00
+43°
MARE NUBIUM 2 VS MARE SEREN 2
1.00
-45°
MARE NUBIUM 2-A VS MARE SEREN 2
1.00
+10°
MARE SEREN 5 VS MARE SEREN 2
1.00
+30°
MARE SEREN 6 VS MARE SEREN 2
1.00
-44°
1.00
-34°
MARE SEREN 7 VS MARE SEREN 2
1.00
-45°
MARE SEREN 8 VS MARE SEREN 2
+40°
1.00
-35°
1.00
MARE SEREN 9 VS MARE SEREN 2
+41°
1.00
D(λ,α)
.40
.48
.56
.64
.72
.80
WAVELENGTH (μ)
MARE SEREN 10 VS MARE SEREN 2
1.00
+52°
MARE SEREN 11 VS MARE SEREN 2
1.00
+52°
MARE SEREN 13 VS MARE SEREN 2
1.00
-52°
MARE SEREN 14 VS MARE SEREN 2
1.00
+30°
1.00
-45°
MARE TRANQ 1 VS MARE SEREN 2
1.00
-2°
1.00
+9°
1.00
+10°
1.00
+12°
1.00
-12°
1.00
-16°
1.00
-20°
1.00
+20°
1.00
+31°
1.00
.40
.48
.56
.64
.72
.80
WAVELENGTH (μ)

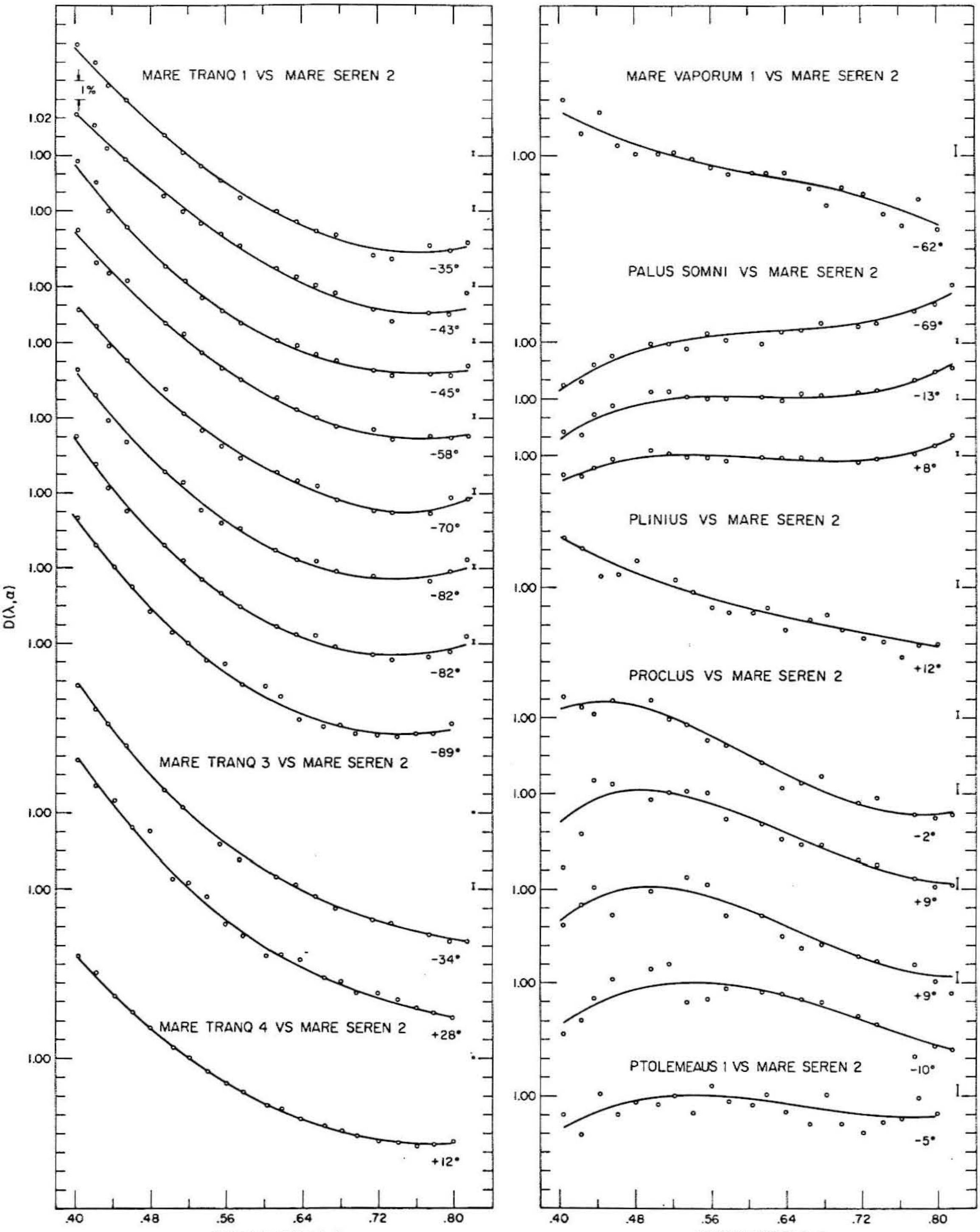
MARE TRANQ 1 VS MARE SEREN 2
1%
1.02
1.00
-35°
-43°
-45°
-58°
-70°
-82°
-82°
-89°
MARE TRANQ 3 VS MARE SEREN 2
-34°
+28°
MARE TRANQ 4 VS MARE SEREN 2
+12°
D(λ, a)
.40
.48
.56
.64
.72
.80
WAVELENGTH (μ)
MARE VAPORUM 1 VS MARE SEREN 2
-62°
PALUS SOMNI VS MARE SEREN 2
-69°
-13°
+8°
PLINIUS VS MARE SEREN 2
+12°
PROCLUS VS MARE SEREN 2
-2°
+9°
+9°
-10°
PTOLEMEAUS 1 VS MARE SEREN 2
-5°
WAVELENGTH (μ)

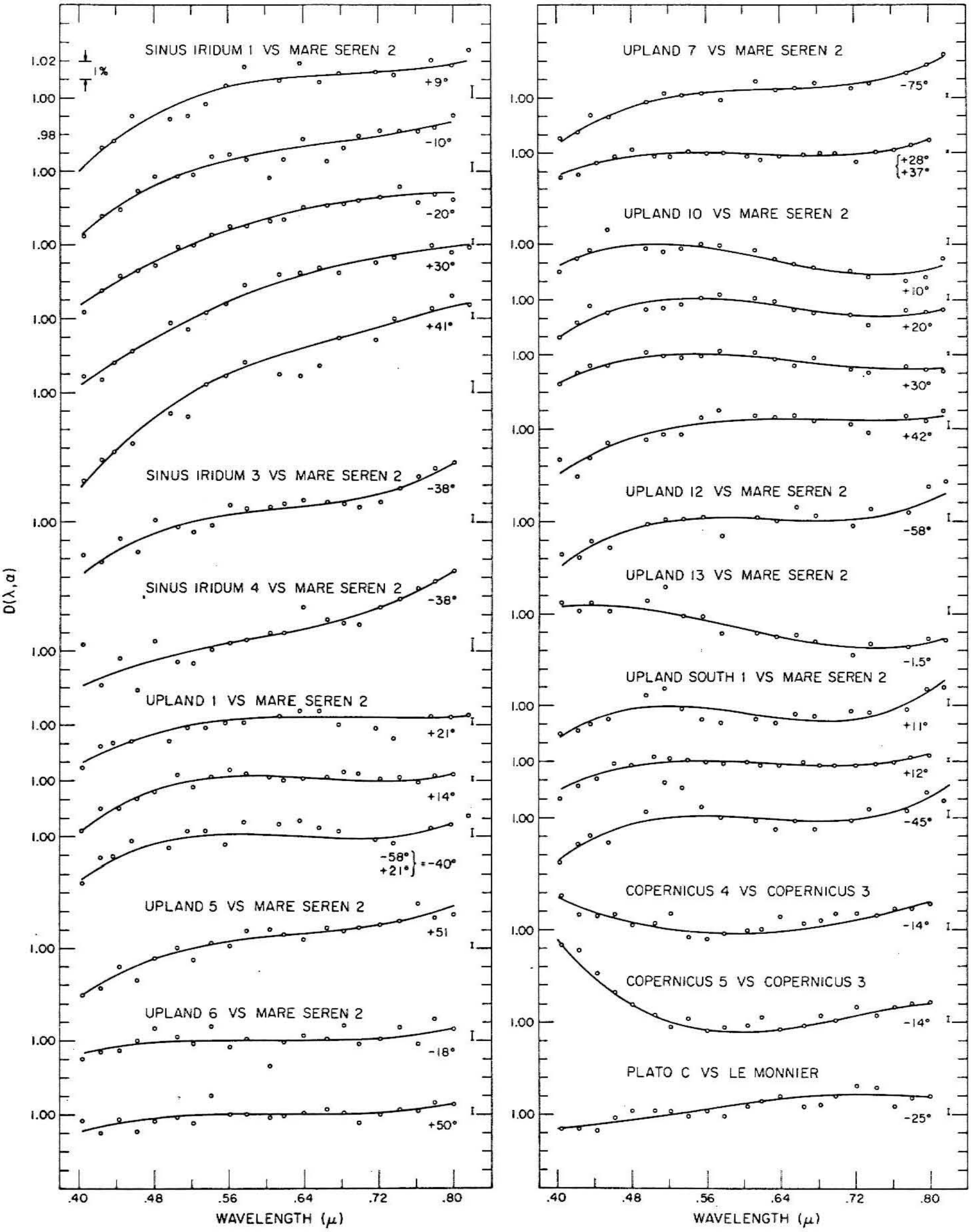
SINUS IRIDUM 1 VS MARE SEREN 2
1%
1.02
1.00
.98
+9°
-10°
-20°
+30°
+41°
SINUS IRIDUM 3 VS MARE SEREN 2
-38°
SINUS IRIDUM 4 VS MARE SEREN 2
-38°
UPLAND 1 VS MARE SEREN 2
+21°
+14°
-58°
+21°
= -40°
UPLAND 5 VS MARE SEREN 2
+51
UPLAND 6 VS MARE SEREN 2
-18°
+50°
D(λ, a)
.40
.48
.56
.64
.72
.80
WAVELENGTH (μ)
UPLAND 7 VS MARE SEREN 2
-75°
+28°
+37°
UPLAND 10 VS MARE SEREN 2
+10°
+20°
+30°
+42°
UPLAND 12 VS MARE SEREN 2
-58°
UPLAND 13 VS MARE SEREN 2
-1.5°
UPLAND SOUTH 1 VS MARE SEREN 2
+11°
+12°
-45°
COPERNICUS 4 VS COPERNICUS 3
-14°
COPERNICUS 5 VS COPERNICUS 3
-14°
PLATO C VS LE MONNIER
-25°
1.00
.40
.48
.56
.64
.72
.80
WAVELENGTH (μ)

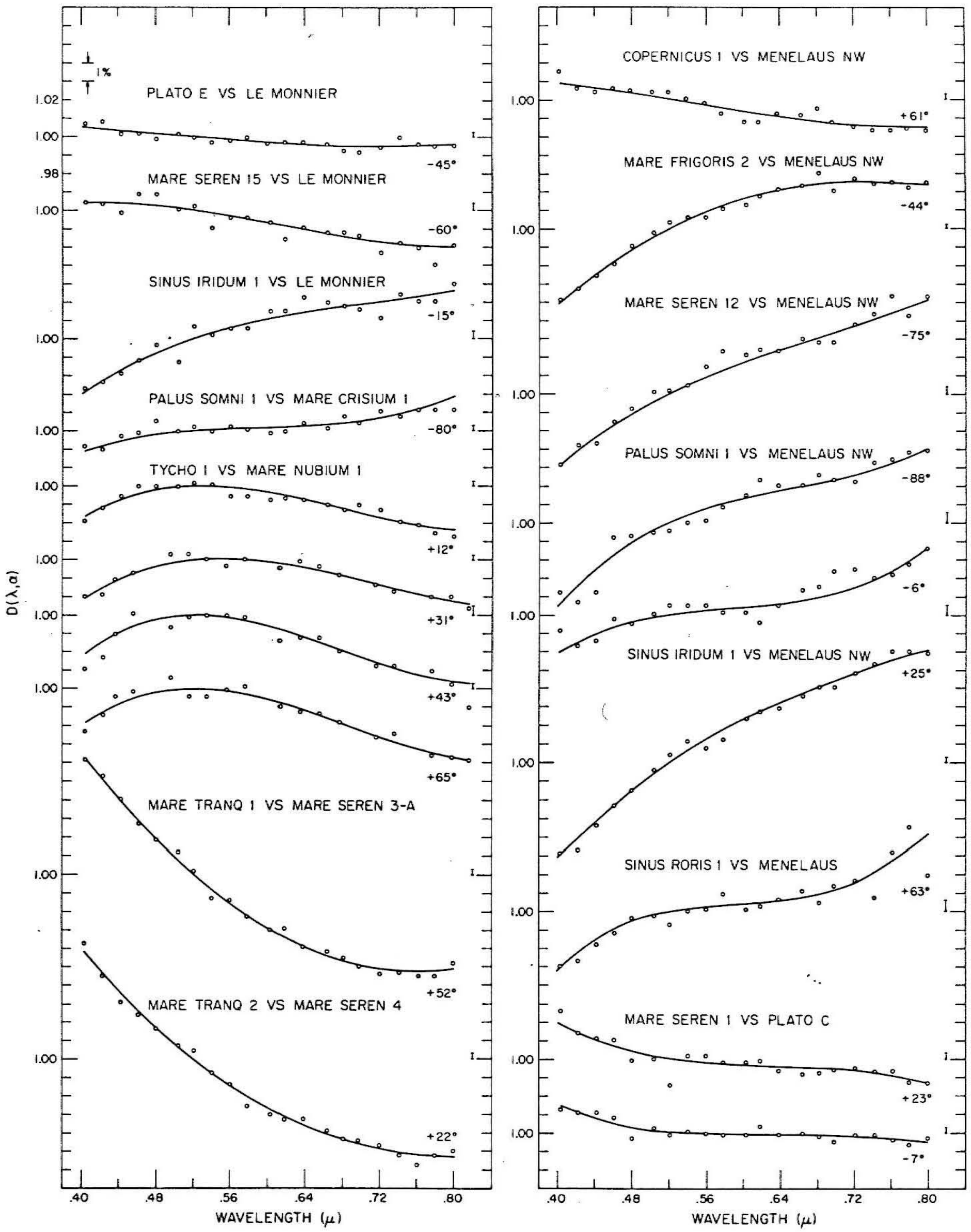
1%
PLATO E VS LE MONNIER
1.02
1.00
.98
-45°
MARE SEREN 15 VS LE MONNIER
1.00
-60°
SINUS IRIDUM 1 VS LE MONNIER
1.00
-15°
PALUS SOMNI 1 VS MARE CRISIUM 1
1.00
-80°
TYCHO 1 VS MARE NUBIUM 1
1.00
+12°
1.00
+31°
1.00
+43°
1.00
+65°
MARE TRANQ 1 VS MARE SEREN 3-A
1.00
+52°
MARE TRANQ 2 VS MARE SEREN 4
1.00
+22°
D(λ,α)
.40
.48
.56
.64
.72
.80
WAVELENGTH (μ)
COPERNICUS 1 VS MENELAUS NW
1.00
+61°
MARE FRIGORIS 2 VS MENELAUS NW
1.00
-44°
MARE SEREN 12 VS MENELAUS NW
1.00
-75°
PALUS SOMNI 1 VS MENELAUS NW
1.00
-88°
1.00
-6°
SINUS IRIDUM 1 VS MENELAUS NW
1.00
+25°
SINUS RORIS 1 VS MENELAUS
1.00
+63°
MARE SEREN 1 VS PLATO C
1.00
+23°
1.00
-7°
.40
.48
.56
.64
.72
.80
WAVELENGTH (μ)

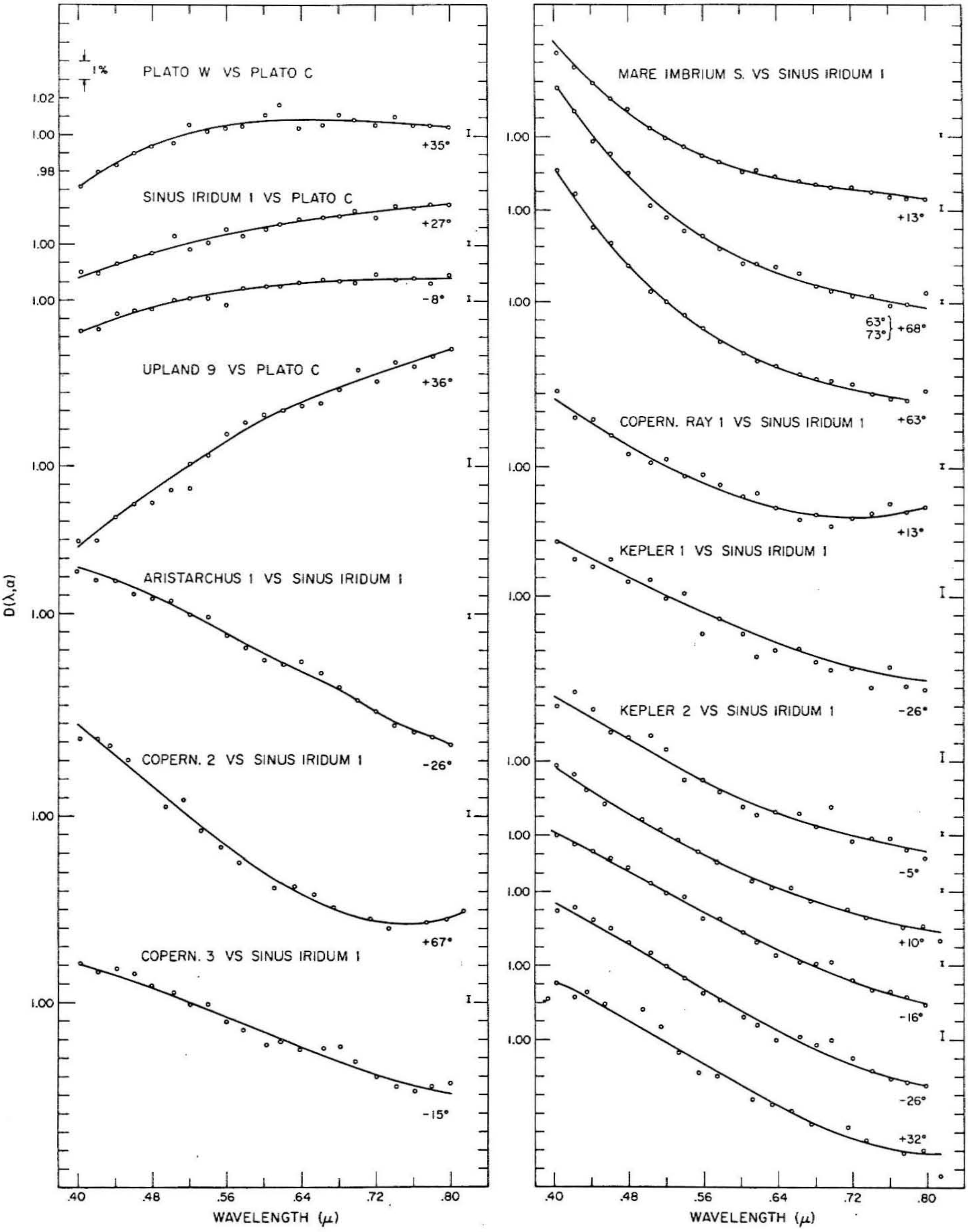
1%
PLATO W VS PLATO C
+35°
SINUS IRIDUM 1 VS PLATO C
+27°
-8°
UPLAND 9 VS PLATO C
+36°
ARISTARCHUS 1 VS SINUS IRIDUM 1
-26°
COPERN. 2 VS SINUS IRIDUM 1
+67°
COPERN. 3 VS SINUS IRIDUM 1
-15°
1.02
1.00
.98
D(λ,α)
.40
.48
.56
.64
.72
.80
WAVELENGTH (μ)
MARE IMBRIUM S. VS SINUS IRIDUM 1
+13°
63°
73°
+68°
+63°
COPERN. RAY 1 VS SINUS IRIDUM 1
+13°
KEPLER 1 VS SINUS IRIDUM 1
-26°
KEPLER 2 VS SINUS IRIDUM 1
-5°
+10°
-16°
-26°
+32°
1.00
.40
.48
.56
.64
.72
.80
WAVELENGTH (μ)

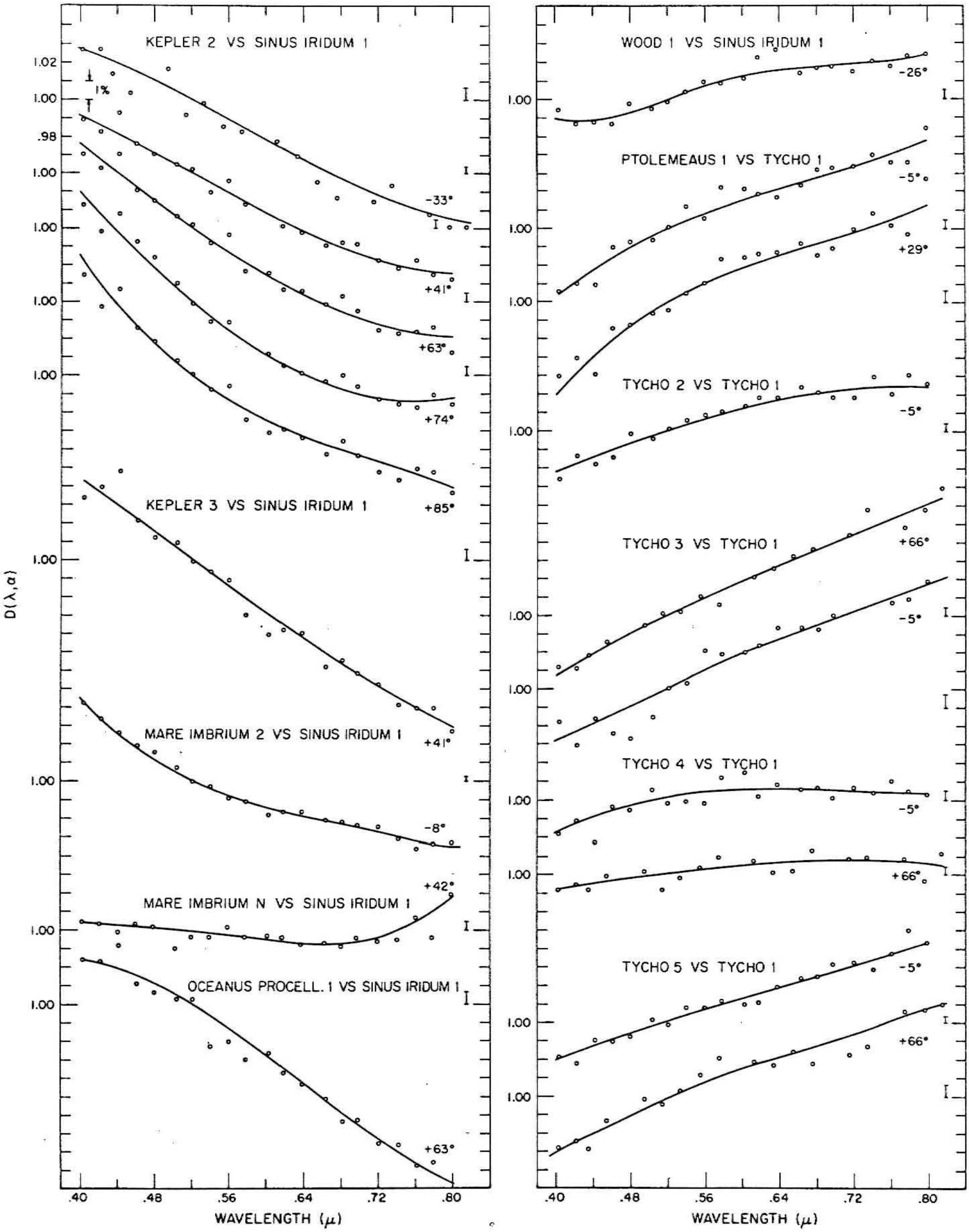
KEPLER 2 VS SINUS IRIDUM 1
1.02
1%
1.00
.98
-33°
1.00
+41°
1.00
+63°
1.00
+74°
1.00
+85°
KEPLER 3 VS SINUS IRIDUM 1
1.00
+41°
MARE IMBRIUM 2 VS SINUS IRIDUM 1
1.00
-8°
+42°
MARE IMBRIUM N VS SINUS IRIDUM 1
1.00
OCEANUS PROCELL. 1 VS SINUS IRIDUM 1
1.00
+63°
D(λ, α)
.40
.48
.56
.64
.72
.80
WAVELENGTH (μ)
WOOD 1 VS SINUS IRIDUM 1
-26°
1.00
PTOLEMEAUS 1 VS TYCHO 1
-5°
1.00
+29°
1.00
TYCHO 2 VS TYCHO 1
-5°
1.00
TYCHO 3 VS TYCHO 1
+66°
1.00
-5°
1.00
TYCHO 4 VS TYCHO 1
1.00
-5°
1.00
+66°
TYCHO 5 VS TYCHO 1
-5°
1.00
+66°
1.00
.40
.48
.56
.64
.72
.80
WAVELENGTH (μ)

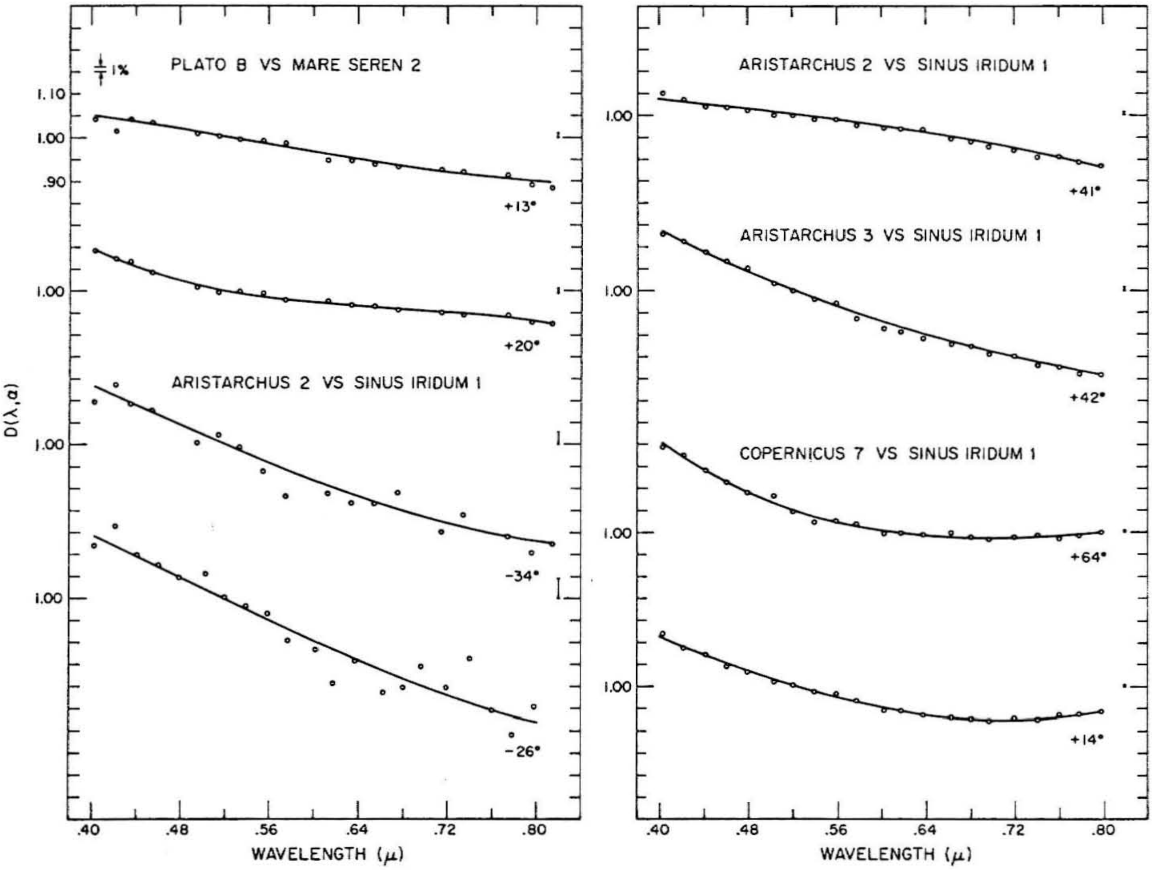
1%
PLATO B VS MARE SEREN 2
1.10
1.00
.90
+13°
1.00
+20°
ARISTARCHUS 2 VS SINUS IRIDUM 1
1.00
-34°
1.00
-26°
D(λ,α)
.40
.48
.56
.64
.72
.80
WAVELENGTH (μ)
ARISTARCHUS 2 VS SINUS IRIDUM 1
1.00
+41°
ARISTARCHUS 3 VS SINUS IRIDUM 1
1.00
+42°
COPERNICUS 7 VS SINUS IRIDUM 1
1.00
+64°
1.00
+14°
.40
.48
.56
.64
.72
.80
WAVELENGTH (μ)

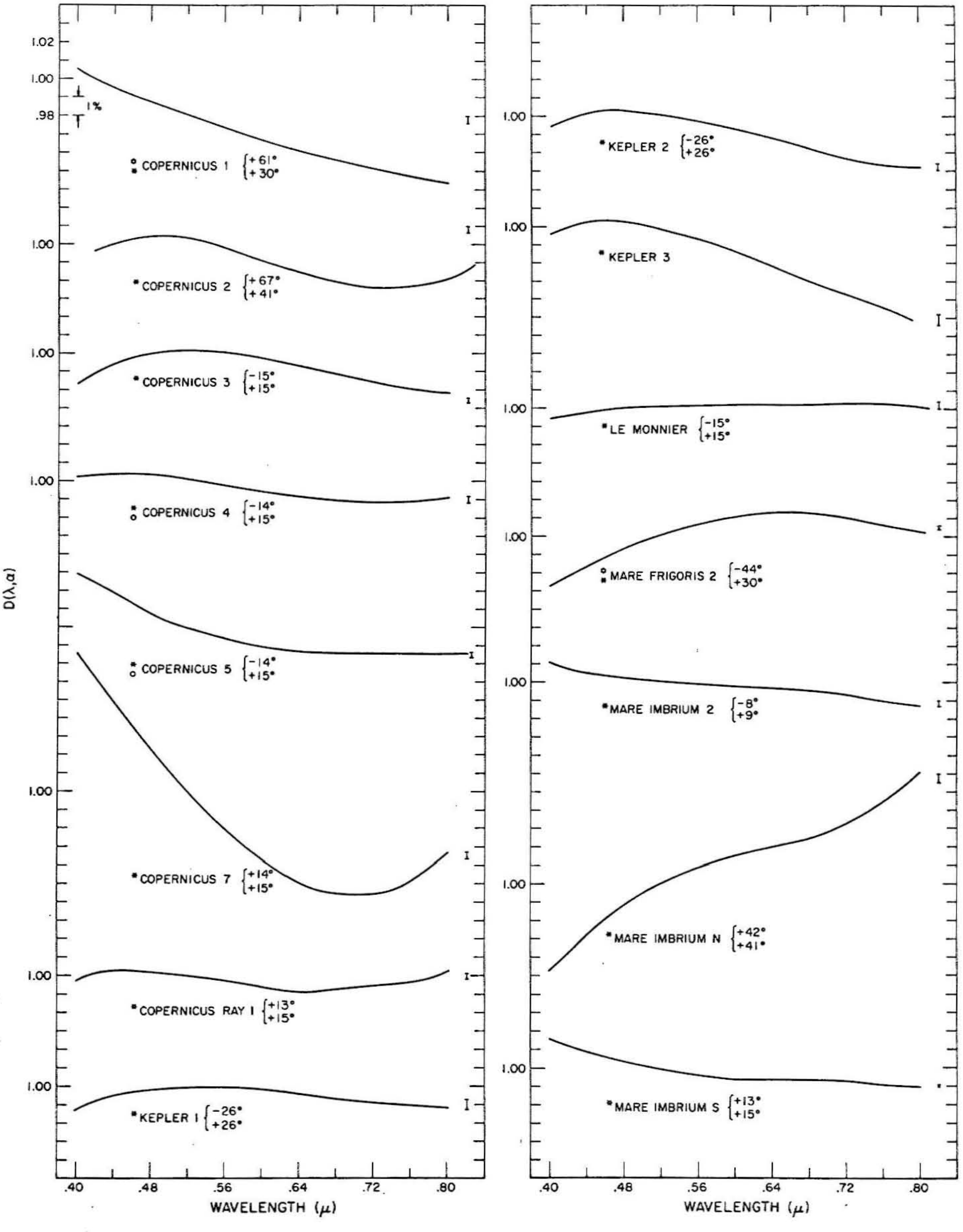
1.02
1.00
.98
1%
COPERNICUS 1 {+61° +30°
1.00
COPERNICUS 2 {+67° +41°
1.00
COPERNICUS 3 {-15° +15°
1.00
COPERNICUS 4 {-14° +15°
COPERNICUS 5 {-14° +15°
1.00
COPERNICUS 7 {+14° +15°
1.00
COPERNICUS RAY 1 {+13° +15°
1.00
KEPLER 1 {-26° +26°
D(λ,α)
.40
.48
.56
.64
.72
.80
WAVELENGTH (μ)
1.00
KEPLER 2 {-26° +26°
1.00
KEPLER 3
1.00
LE MONNIER {-15° +15°
1.00
MARE FRIGORIS 2 {-44° +30°
1.00
MARE IMBRIUM 2 {-8° +9°
1.00
MARE IMBRIUM N {+42° +41°
1.00
MARE IMBRIUM S {+13° +15°
.40
.48
.56
.64
.72
.80
WAVELENGTH (μ)

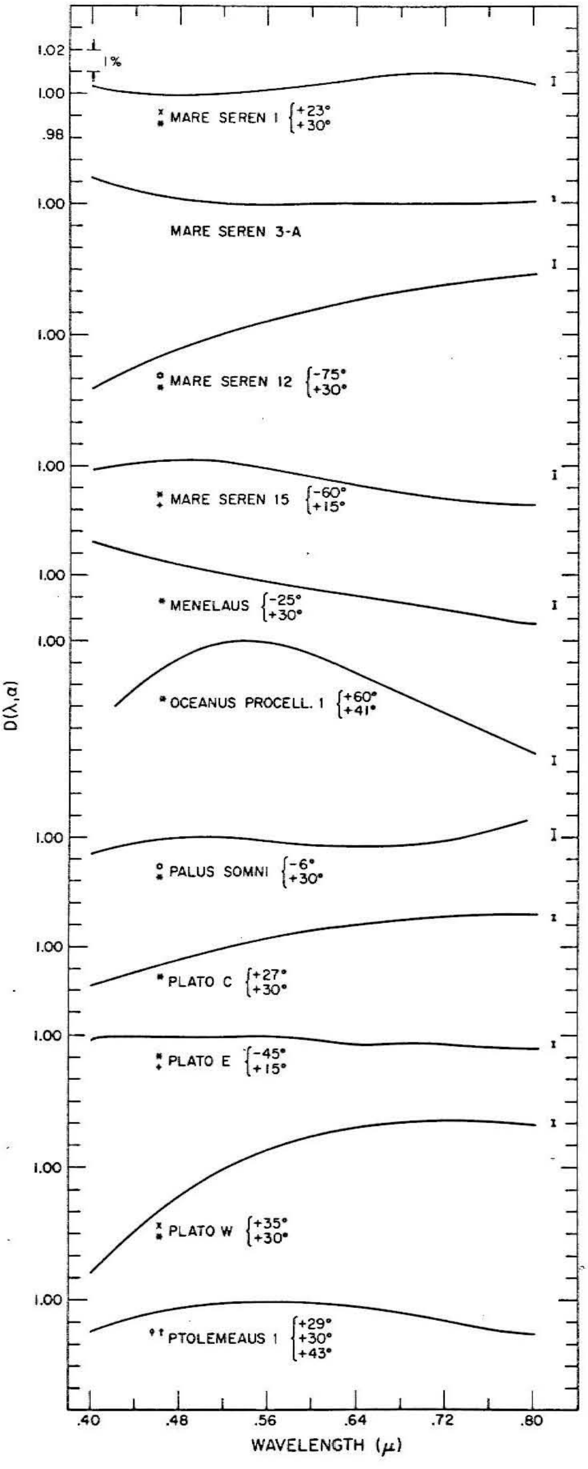
1.02
1.00
.98
1%
MARE SEREN 1 {+23°, +30°}
1.00
MARE SEREN 3-A
1.00
MARE SEREN 12 {-75°, +30°}
1.00
MARE SEREN 15 {-60°, +15°}
1.00
MENELAUS {-25°, +30°}
1.00
OCEANUS PROCELL. 1 {+60°, +41°}
D(λ,α)
1.00
PALUS SOMNI {-6°, +30°}
1.00
PLATO C {+27°, +30°}
1.00
PLATO E {-45°, +15°}
1.00
PLATO W {+35°, +30°}
1.00
PTOLEMEAUS 1 {+29°, +30°, +43°}
.40
.48
.56
.64
.72
.80
WAVELENGTH (μ)

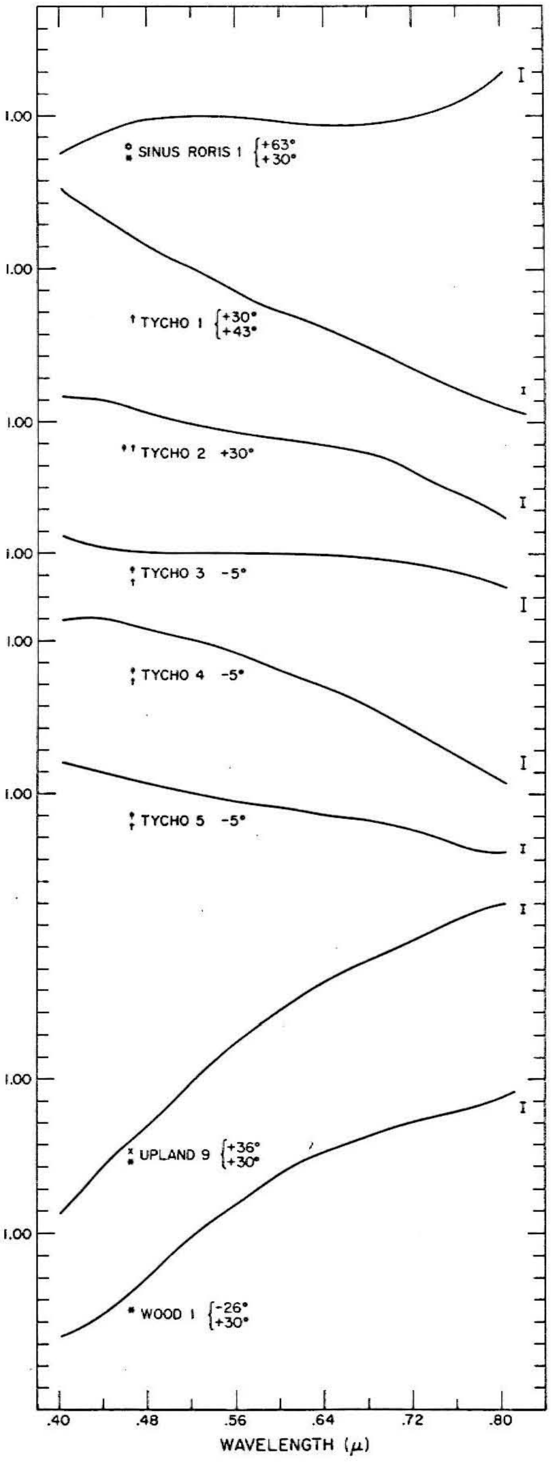
1.00
SINUS RORIS 1 {+63°, +30°}
1.00
TYCHO 1 {+30°, +43°}
1.00
TYCHO 2 +30°
1.00
TYCHO 3 -5°
1.00
TYCHO 4 -5°
1.00
TYCHO 5 -5°
1.00
UPLAND 9 {+36°, +30°}
1.00
WOOD 1 {-26°, +30°}
.40
.48
.56
.64
.72
.80
WAVELENGTH (μ)

TABLES

Table 1. -Filter characteristics for the two sets of interference filters used. Given are the effective wavelengths (λ_e), the passband ($\Delta\lambda$) computed as the half-width and the peak transmission (T).

Table 2. -Information on the observations made is given. The latitude (λ) and longitude (φ) of the lunar positions are given as computed from Supplement 2 of the Rectified Lunar Atlas by E.A.Whitaker, G.P.Kuiper, W.K. Hartman and L.H.Spradley which is distributed by the Aeronautical Chart and Information Center. The lunar phase angle (α) is also given.

Table 3. -A comparison of the results shown by several photographic imagery studies (Appendix I) with the results of the photoelectric study described herein. B = Bluer, R = Redder.

FIGURE CAPTIONS

Fig. 1. -Idealized absolute reflectivity curves for two lunar areas (top) with the resulting idealized relative reflectivity curve (bottom) for this lunar area-pair.

Fig. 2. -Deviations of Wildey and Pohn (1964) color measurements from the average color for all observations plotted against phase angle. Data for four lunar positions are shown. The line is the predicted absolute color-phase effect for the entire Moon based on measurements by Gehrels, et. al. (1964).

Fig. 3. -Lunar areas observed in this study are shown as dots on the reproduction of an ACIC lunar mosaic.

Fig. 4. -Frequency distribution of the red to blue (0.4μ - 0.8μ) ratio of the relative spectral curves measured in this study. The standard area would appear at 1.0 on this display.

Fig. 5. -Deviation of color measurements from a 3rd order polynomial fitted through the data. The points are connected only to illustrate the effects.

Fig. 6. -The actual data for two cases shown in Figure 7.

Fig. 7. -Shown are sequences of relative color curves obtained at several lunar areas. The phase angles at which the measurements were made are shown with each curve.

Figs. 8-10. -Red to blue ratios (0.4μ - 0.76μ) of spectral curves measured at different phase angles are plotted. The vertical error bars are the errors assigned to each curve as defined in the text.

Fig. 11. -Relative spectral curves for areas in Mare Serenitatis.

Fig. 12. -Relative spectral curve for areas in several maria.

Fig. 13. -Relative spectral curves for areas in and near Mare Imbrium.

Fig. 14. -Relative spectral curves for very low albedo mare areas.

Fig. 15. -Relative spectral curves for several areas in northwestern Mare Tranquillitatis. These curves are relative to Mare Tranquillitatis 1, which is given in Figure 14 relative to the standard area in Mare Serenitatis.

Fig. 16. -Relative spectral curves for upland regions.

Fig. 17. -Relative spectral curves for bright blue craters.

Fig. 18. -Relative spectral curves for the second class of bright craters, as discussed in the text.

Fig. 19. -Relative spectral curves for three areas on the floor of the crater Plato.

Fig. 20. -Relative spectral curves for areas associated with the crater Tycho.

Fig. 21. -Relative spectral curves for areas associated with the crater Kepler.

Fig. 22. -Relative spectral curves for areas associated with the crater Copernicus.

Fig. 23. -Relative spectral curves for two bright rays and near by mare areas.

Fig. 24. -Scatter diagram of measurements by this author and those made by several other authors. The measurements of each author are not normalized one to another so that the correlation line for, say, Coyne is not colinear with the line for, say, Gehrels, et. al. Each comparison must be performed separately.

Fig. 25. -The absolute spectral reflectivity curve for the central floor of the crater Plato normalized to 1.0 at 0.527 μ . The dashed line indicates the absolute spectral reflectivity curve of the standard area in Mare Serenitatis.

Figs. 26,27. -Laboratory reflection spectra for various rock powders as obtained by Adams and Filice (1967) and Adams (1968).

Fig. 28. -Color-phase relation as calculated from polarization data by Gehrels, et. al. (1964).

REFERENCES

Adams, J.B., Lunar Surface Composition and Particle Size: Implications from Laboratory and Lunar Spectral Reflectivity Data, J. Geophys. Res., 72, 5717-5720 (1967).

__________, Petrologic Significance of Absorption Bands in the Near Infrared and the Composition of the Lunar and Martian Surfaces, Science, in press (1968).

__________, Filice, A.L., Spectral Reflectance 0.4 to 2.0 of Silicate Rock Powders, J. Geophys. Res., 72, 5705-5715 (1967).

Barabashov, N.P., Spectrophotometric Investigations of the Lunar Surface, Astr. Zhurnal, 1, 44-57 (1924).

__________, On Color Contrasts of the Lunar Surface, Circ. Kharkov Astr. Obs., 12, 3 (1953).

__________, and Chekirda, A.T., On the Color of the Bright Rays of the Craters Tycho, Copernicus and Kepler, Circ. Astr. Obs. Kharkov State Univ., 13, 3-13 (1955).

__________, and Chekirda, A.T., On Color Contrasts of the Lunar Surface, Trans. Astro. Obs. Kharkov State Univ., 3 (1954).

__________, and Yezerskii, V.I., Spectrophotometrical Observations of Lunar Craters, Izvestiya, Com. Phys., of Planets, 3, 50-55 (1961).

__________, Yezerskii, V.I. and Fedorets, V.A., Color Contrasts of the Lunar Surface, Sov. Astr., 3, 484-489 (1959).

Coyne, G.V., Comparative Spectrophotometry of Selected Areas on the Lunar Surface, Doctoral Dissertation Georgetown University, (1962).

__________, Comparative Spectrophotometry of Selected Areas on the Lunar Surface, A.J., 68, 59-66 (1963).

__________, Differential Colors on the Moon, A.J., 70, 115-119 (1965).

Dubois, J., A Contribution to the Study of Lunar Luminescence, Publication de l'Observatoire de l'Universite de Bordeaux, Series A, 13, (1959).

Duke, M.B. and Silver, L.T., Petrology of Eucrites, Howardites and Mesosiderites, Geochem. Cosmochem. Acta. 31, 1637-1665 (1967).

Evsiukov, N.M., On Color Contrasts of the Lunar Surface, Astr. Zhurnal, 43, 5 (1966).

Fessenkoff, B., Determination of the Color of the Seas, A. N., (1929).

Fielder, G., The Color of Moonlight and the Composition of the Moon's Surface, Journal of the International Lunar Society, 1, 25-31 (1957).

Firsoff, V.A. Color on the Moon, Sky and Telescope, 17, 381 (1958).

Gehrels, T., Coffeen, T. and Owings, D. Wavelength dependence of Polarization. III. The Lunar Surface, A.J., 69, 10 826-852, (1964).

Gōetz, A.F.H., Infrared 8-13 Spectroscopy of the Moon and Some Cold Silicate Powders, Doctoral Dissertation, California Institute of Technology (1967).

Goetz, F.W., Photographic Photometry of the Lunar Surface, Tubingen: Veroff. Sternwarte Oestenberg Tubingen. 1, (1919).

Greenacre, J.A., A Recent Observation of Lunar Color Phenomena, Sky and Telescope, 26, 316 (1963).

Hapke, B., "Optical Properties of the Moon's Surface" in The Nature of the Lunar Surface Layer, W.N. Hess, D.H. Menzel and J.A. O'Keefe, eds., Johns Hopkins Press, Baltimore (1966)

Hargreaves, F.J. An Attempt to Determine the Color of the Lunar Surface by Direct Color Photography, Journal of the British Astronomical Assoc., 34, 243-245 (1924).

Hovis, W. A., Jr., and Callahan, W.R., Infrared Reflectance Spectra of Igneous Rocks, Tuffs, and Red Sandstone from 0.5 to 22 Microns, J. Opt. Soc. Am., 56, 639-643 (1966)

Keenan, P.C., The Measurement of Lunar Color Differences, P.A.S.P., 43, 203-214 (1931).

Kozlova, K.I. and Glagolevskii, Y.V., Electrophotometric Color Excesses and Color Indices of 14 Lunar Craters Near Full Moon, Astron. Cir. ALMA-ATA, Astrobot. Sec., 209, 13-14 (1961).

Kozyrev, N.A., Observation of a Volcanic Process on the Moon, Sky and Telescope, 18, 184-186 (1959).

Kuiper, G.P., Interpretation of Ranger VII Records, Communication No. 58, Lunar and Planetary Lab., University of Arizona, 4, 18-20 (1966).

Markov, A.V., The Reflective Abilities and Color Indices of Earth and Lunar Details by the Photoelectric Method, Izvestia, AN Kax. USSR, 90, 1-2 (1950).

McCord, T.B., Observational Study of Lunar Visible Emission, J. Geophys. Res., 72, 2087-2097 (1967).

__________, A Double Beam Astronomical Photometer, Applied Optics, in press (1968).

Miethe, A., and Seegert, B., On Qualitative Differences of Light Reflected by Various Parts of the Lunar Surface, A.N. 188, 9, 239, 371 (1911).

__________, and Seegert, B., Qualitative Differences in the Light Reflected from Various Parts of the Moon, A.N. 198, 4736 (1914).

Murray, B., and Liu, S., Photoelectric Study of a Suspected Color Variation in Mare Serenitatis, First Report on Grant NsG 56-60 NASA to California Institute of Technology, 14-16 (1961).

Nash, D. B., Proton Irradiation Darkening of Rock Powders: Contamination and Temperature Effects, and Applications to Solar-Wind Darkening of the Moon, J. Geophys. Res., 72, 3087-3089 (1967).

Ney, E.P., Woolf, N.J., and Collins, R.J., Mechanisms for Lunar Luminescence, J. Geophys. Res., 71, 1787-1793 (1966).

Petrova, N. N., A Spectrophotometric Study of the Lunar Surface, Sov. Astron. AJ, 1, (1966).

Petrushevski, A. N. 91, 207-208 (1878).

Polozhentzeve, T.A. Relative Spectrophotometry of Lunar Details, Izvestya Astron. Obs. Pulkove, 21, 180-184 (1958).

__________, Status of the Alphonsus Crater Prior to November 3/4 1958 Eruption, Bull. Comm. on Planetary Phys. Acad. Scienc. SSSR. Kharkov Univ. (1961)

Rackham, T. W., Photographic Colorimetry of the Moon in Narrow Passbands, Icarus, 3, 45-51 (1964).

Radlova, L.N., Visual Colorimetry of the Moon, Uchenyye Zapiski Leningrad State Univ., 12, (1941).

__________, Photographic Colorimetry of the Moon, Astron, J. (USSR), 20, (1943).

__________, The Color of the Rays on the Lunar Surface, Astr. Zhurnal, 37, 990-992 (1961).

Rosenberg, J., Photometric Measurements of the Lunar Surface and the Area Photometer of the Osterberg Observatory, Tubingen, A.N., 214 (1921).

Scott, N.W., Color on the Moon, Nature, 204, 1075-1076 (1964).

__________ Personal Communication, (1967).

Sergeeve, A.N., Spectrophotometry of Lunar Formations, Izvestya, Com. Phys. and Planets, June, (1959).

Sharanov, V.V., On the Problem of Color Differences Upon the Lunar Surface, Astron. Circ. USSR. 157, 9-12 (1955).

__________, Studies of Colorimetry of the Moon, II, A New Study of the Potsdam Spectrophotometry, Bull. Leningrad State Univ., 1, (1956).

__________, Visual Colorimetry of the Lunar Surface, Sov. Astron. A.J. 6, (1962).

Sytinskaya, N.N., Combined Catalog of Absolute Values of the Visual Reflectivity of 104 Lunar Features, Astr. Zhurnal, 30, 295 (1953).

Teifel, V.G., Spectrophotometry of the Lunar Surface III, Different Spectral Pecularities in Lunar Formations, Tr. Sektora Astrobot. AN Kaz. SSR., 8, (1960a).

__________, Spectrophotometry of the Lunar Surface, II, Catalogue of Color Indexes of Lunar Objects, Tr. Sektora Astrobot. AN Kaz, SSR, 8, (1960b).

__________, Spectrocolorimetric Pecularities of the System of the Lunar Crater Aristarchus, Ast. Circ. of USSR. 17, 215 (1960c).

__________, Color Features of the Lunar Surface as Determined by Observations at Full Moon, Izvestia, Phys. Planets, 3 (1961).

Tihov, G.S., RAK, 136-141 (1924).

Turkevich, A.L., Franzgrote, E.J., and Patterson, J.H., Chemical Analysis of the Moon at the Surveyor V Landing Site, Science, 158, 635-637 (1967).

Van den Bergh, S., The Color of the Moon, AlJ., 67, 147-150 (1962).

Vigroux, E., Spectrophotometric Comparison of the Light Scattered from Some Lunar Features, Journal des Observateurs, 39, 134 (1956).

Wegner, Gl, Colorimetric Measurements of Lunar Features, P.A.S.P., 364 (1960).

Wildey, R.L., and Pohn, H.A., Detailed Photoelectric Photometry of the Moon, A.J., 69, 8, 619, 634 (1964).

Wilsing, J., and Scheiner, J., Spectrophotometric Measurements on Rocks, on the Moon, Mars, and Jupiter, Publ. Astrophys. Obs. Potsdam 24, 4 (1921).

Wood, R. W., Selective Absorption of Light on the Moon's Surface and Lunar Petrography, Ap. J., 36, 74 (1912).

__________, Petrography of the Moon, Journal of the British Astronomical Association, 24 370 (1914).

Wright, W.H., The Moon as Photographed by Light of Different Colors, P.A.S.P., 41, 125-132, 241 (1929).

Yezerskii, V.I., and Fedorets, V.A., On Color Contrasts of the Lunar Surface, Circ. Kharkov Astron. Obs., 15, 17-20 (1956).